ANL/NE-13/8 Rev. 2

Argonne NATIONAL LABORATORY

VARI3D & PERSENT: Perturbation and Sensitivity Analysis

Nuclear Engineering Division

ANL/NE-13/8 Rev. 2

VARI3D & PERSENT: Perturbation and Sensitivity Analysis

prepared by
M. A. Smith, C. Adams, W. S. Yang, and E. E. Lewis
Nuclear Engineering Division, Argonne National Laboratory

August 1, 2018

SUMMARY

The nodal diffusion method is one of the most widely used approaches in modern reactor analysis. In the nodal diffusion method, a coarse multi-group set of "homogenized" parameters is constructed such that the complex geometry of a reactor core along with the energy dependence of neutron and gamma ray cross sections in a nuclear reactor are conserved in the simpler geometry. The homogenization is typically done on a fuel assembly level as is the case in the DIF3D code developed at Argonne National Laboratory. The nodal methodology is used primarily to predict fuel cycle behavior of nuclear systems of which there is a substantial amount of validation in the literature. Another use of the nodal method is to obtain reactivity coefficients and kinetics parameters for use in a safety analysis of a given nuclear reactor. While there are many ways to obtain reactivity worth and kinetics parameters, the work presented in this manuscript is unique as it provides the user with the ability to compute reactivity worths, kinetics parameters, and cross section sensitivities with a Cartesian and hexagonal geometry based transport code.

This manuscript serves as a single manual for two separate codes: VARI3D and PERSENT. The VARI3D code (VARIational 3D) is based upon the classic finite difference diffusion theory solver available in DIF3D. The PERSENT code (PERturbation and SENitivity for Transport) is based upon the variational nodal method employed in DIF3D termed VARIANT. The VARIANT solver was added to DIF3D in 1995 and has seen continued development and use for the last 18 years. Because VARI3D primarily uses deprecated coding practices, rather than incorporating the perturbation and sensitivity treatments for transport within VARI3D, a new coding development was built using modern Fortran coding. The primary purpose of this manual is to describe the theory behind PERSENT (and by convenience, that of VARI3D) and discuss the input and output of PERSENT along with giving potential users an idea of how to use it. While this manuscript does describe the input and output of VARI3D, the PERSENT code is intended to be the replacement capability of VARI3D as PERSENT can generate nearly identical (if not superior) diffusion theory results.

In this manuscript, the relevant aspects of generalized perturbation theory that apply to both VARI3D and PERSENT are covered. The input and output of VARI3D is displayed by excerpting several of the example problems. Similarly, the input and output of PERSENT is displayed along with tips on how best to use the code. Note that the input and output of the inhomogeneous solver wrapped around DIF3D (DIF3D_IFS) is also discussed as it is needed to carry out some of the sensitivities in PERSENT such as reaction rate ratios.

This manuscript describes several perturbation and sensitivity problems and the results computed using PERSENT. From these sections, potential users should find that PERSENT provides not only the typical tables of numbers desired in perturbation and sensitivity analysis work, but also can visually plot the result for a more thorough understanding of the space and energy distribution (Section 5). Overall, PERSENT is observed to produce accurate reactivity worths and sensitivities for the displayed set of test problems and clearly demonstrates the need to have a transport based sensitivity capability as evident from the thousands of percent errors observed in the 21 group hexagonal fast reactor problem (covered in Section 7). The uncertainty calculation capability is described in Section 3 and demonstrated in Section 7.

TABLE OF CONTENTS

LIST OF FIGURES

LIST OF TABLES

1 Introduction

One of the most well used methods currently employed for reactor analysis is the diffusion approximation. This approximation is typically employed at the whole-core level using homogenized assembly cross sections in a nodal framework as is the case in the DIF3D code [1-6] developed at Argonne National Laboratory. Perturbation theory methods have been developed for a wide range of applications in reactor analysis [7-12] many of which are still widely used for reactivity and sensitivity coefficient calculations. The reactivity change (i.e., change in the eigenvalue of the neutron transport equation) due to perturbations introduced in the system can be expressed by a conventional perturbation equation which requires a combination of the unperturbed or perturbed forward flux and the unperturbed or perturbed adjoint flux. The solution to the perturbation equation provides the contribution of a given perturbation to the reactivity change for the entire phase space of the transport equation (space, angle, and energy). The perturbation theory capability is primarily used to get coefficients for point kinetics safety analysis or the more simplified asymptotic analysis.

The response parameter can be expanded to include quantities other than just the eigenvalue response (reactivity coefficient) such as reaction rate and reaction rate ratios. In this case, the "perturbation theory" terminology is referred to as "generalized perturbation theory" (GPT) [13-15]. GPT methods are used to calculate the sensitivity coefficients of a response parameter with respect to input parameters (e.g., isotopic cross sections). The sensitivity coefficients are used to estimate the uncertainty in a given response parameter due to uncertain cross section data. It can also be used to reduce the response parameter uncertainty given existing integral experiment data [16,17]. A general usage uncertainty calculation capability was added to the PERSENT (PERturbation and SENsitivity for Transport) code for importing a co-variance matrix and computing the uncertainty.

VARI3D [18] is a GPT code that computes reactivity coefficients and sensitivities to reaction rate, reaction rate ratio, and reactivity worth based upon changes in microscopic cross section data and material density changes. VARI3D is based upon the finite difference diffusion theory option of DIF3D [1] and has most frequently been used to compute the reactivity coefficient distributions and kinetics parameters employed in safety analyses. All of the geometry options are available for reactivity coefficients, but the sensitivity calculations are limited to the R-Z geometry. This last limitation is the primary motivation for developing the PERSENT code as existing 3D sensitivity tools are only based upon diffusion theory. The PERSENT code allows users to perform perturbation theory and sensitivity calculations using the nodal transport based solver VARIANT [2-4] within DIF3D which was chosen noting the recent upgrades [5,6]. It is important to note that this is not the first attempt at building a perturbation theory code around the VARIANT methodology [19]. Unfortunately, that work only considered conventional perturbation theory formulation and was never made into a production capable code (a PhD thesis). The work on PERSENT is thus a completely new development with respect to coding. The following sections detail the perturbation and sensitivity theory which is implemented in both VARI3D and PERSENT. The later sections detail the input and output options of both codes.

2 Perturbation Theory Methodology

VARI3D is based upon the diffusion equation while PERSENT is based upon the second-order even-parity transport equation. Both use the conventional multi-group approximation and rely upon the DIF3D solver as the flux solver. VARI3D uses the finite difference diffusion option of DIF3D termed DIF3D-FDD. PERSENT uses the VARIANT nodal transport option of DIF3D which combines spherical harmonic angular trial functions with orthogonal polynomial spatial trial functions within each "node" (mesh). External to this work, DIF3D was configured to provide forward and adjoint solutions to the steady state neutron transport equation in either an eigenvalue or fixed source (inhomogeneous) solution for both DIF3D-FDD and DIF3D-VARIANT. The creation of the PERSENT code relies heavily upon the changes made to incorporate general order space-angle trial functions [5,6]. Additional changes were made to allow a transport-based fixed source to be incorporated along with changes to allow the anisotropic scattering order to be increased to an order consistent with the spherical harmonics approximation.

2.1 Multigroup Transport Equation

The steady-state neutron transport equation can be written as

$$\nabla\cdot\hat{\Omega}\psi(r,E,\hat{\Omega})+\Sigma_t(r,E)\psi(r,E,\hat{\Omega})=S(r,E,\hat{\Omega}), \tag{2.1}$$

where $\psi(r,E,\hat{\Omega})$ is the neutron flux, $\Sigma_t(r,E)$ is the total cross section, and $S(r,E,\hat{\Omega})$ is the source which includes all scattering, fission, and fixed sources. The multi-group approximation reduces equation 2.1 into a series of equations

$$\nabla\cdot\hat{\Omega}\psi_g(r,\hat{\Omega})+\Sigma_{t,g}(r)\psi_g(r,\hat{\Omega})=S_g(r,\hat{\Omega}), \tag{2.2}$$

which are coupled together via the source which is expanded as

$$\begin{aligned}S_g(r,\hat{\Omega})=&\sum_{g'}\int d\Omega'\Sigma_{t,g'\to g}(r,\hat{\Omega}'\to\hat{\Omega})\psi_{g'}(r,\hat{\Omega}')\\&+\lambda\sum_{g'}\chi_{g,g'}(r)\cdot\nu\Sigma_{f,g'}(r)\int d\Omega'\psi_{g'}(r,\hat{\Omega}')+Q_g(r,\hat{\Omega})\end{aligned}. \tag{2.3}$$

Note that for calculations without a fixed source, $Q_g(r,\hat{\Omega})$, equation 2.2 becomes a eigenvalue problem (λ). When a fixed source is present, $\lambda=1$ or some other fixed input quantity.

Because of the complexity of having to deal with the even-parity method, we start with a pseudo-discretization of the first order equations 2.2 and 2.3. Using conventional matrix notation, we can write equations 2.2 and 2.3 as the series of coupled equations

$$A_g\psi_g=S_g=\sum_{g'}\left\{W_{g,g'}+\lambda\cdot F_{g,g'}\right\}\psi_{g'}+Q_g. \tag{2.4}$$

Assembling with respect to energy, equation 2.4 can be written as

$$\left\{A-W-\lambda\cdot F\right\}\psi=B(\lambda)\psi=Q. \tag{2.5}$$

For the even-parity method in DIF3D-VARIANT, we obtain an equation similar to equation 2.4, but it is only in terms of the even-parity flux which allows equation 2.5 to be written as

$$B(\lambda)\psi^{+}=Q^{+}. \tag{2.6}$$

Because the diffusion theory approximation is the lowest order spherical harmonics approximation (i.e. P_1), the DIF3D-FDD theory is identical to DIF3D-VARIANT and thus equation 2.6 applies. We use equation 2.6 for the remaining derivation of the perturbation and sensitivity analysis and assume all equations are for a single mesh. Further, equations 2.5 and 2.6 are qualitatively similar and to avoid confusion with the even-parity and adjoint notation, we use equation 2.5 with the understanding that the flux from here on refers to the even-parity flux in DIF3D-VARIANT or the scalar flux in DIF3D-FDD.

2.2 Perturbation Theory for Reactivity Coefficients

For reactivity coefficients, the parameter value of interest is the eigenvalue and thus the fixed source appearing in equation 2.6 is zero leading to the eigenvalue problem

$$B(\lambda)\psi = 0. \tag{2.7}$$

Equation 2.7 has an associated adjoint equation

$$B^*(\lambda^*)\psi^* = 0. \tag{2.8}$$

It has been proven that the multi-group diffusion equation has a unique and physically realistic solution for spatially continuous and discrete formulations [20,21]. Thus, for the fundamental mode eigenvalue, we know that $\lambda = \lambda^*$.

With respect to the reactivity coefficient, we seek the response to the reactivity between a reference system λ and some perturbed state $\hat{\lambda}$

$$\rho = \left(1-\frac{1}{\hat{k}}\right)-\left(1-\frac{1}{k}\right) = (1-\hat{\lambda})-(1-\lambda) = -\Delta\lambda. \tag{2.9}$$

Focusing on the perturbed system we define $B(\lambda)$ to be perturbed by $\Delta B(\lambda)$ such that we have a new system $\hat{B}(\lambda) = B(\lambda)+\Delta B(\lambda)$. The corresponding forward and adjoint equations (and their solutions) for this perturbed system are given as

$$\hat{B}(\hat{\lambda})\hat{\psi} = 0 \qquad \& \qquad \hat{B}^*(\hat{\lambda}^*)\hat{\psi}^* = 0, \tag{2.10}$$

noting the additional definitions of $\hat{\lambda} = \lambda + \Delta\lambda$ and $\hat{\psi} = \psi + \Delta\psi$.

Focusing on the eigenvalue perturbation (i.e. the parameter we are interested in) and noting that $B(\lambda) = A - W - \lambda \cdot F$, we can expand the forward equation into

$$\begin{aligned}\hat{B}(\hat{\lambda})\hat{\psi} = 0 &= B(\hat{\lambda})\hat{\psi} + \Delta B(\hat{\lambda})\hat{\psi} = B(\lambda+\Delta\lambda)\hat{\psi} + \Delta B(\lambda+\Delta\lambda)\hat{\psi} \\ &= 0 = B(\lambda)\hat{\psi} - \Delta\lambda \cdot F\hat{\psi} + \Delta B(\hat{\lambda})\hat{\psi}\end{aligned} \tag{2.11}$$

We can take the inner product of equation 2.11 with its adjoint ψ^* defined by equation 2.8 to write

$$\left\langle \psi^*, \Delta B(\hat{\lambda})\hat{\psi} \right\rangle = \Delta\lambda \cdot \left\langle \psi^*, F\hat{\psi} \right\rangle - \cancel{\left\langle \psi^*, B(\lambda)\hat{\psi} \right\rangle}. \tag{2.12}$$

Note the deleted term (strike through) which is due to the definition of equation 2.8. We can solve equation 2.12 for $\Delta\lambda$ to get

$$\Delta\lambda = \frac{\left\langle \psi^*, \Delta B\left(\hat{\lambda}\right)\hat{\psi}\right\rangle}{\left\langle \psi^*, F\hat{\psi}\right\rangle} = \frac{\left\langle \psi^*, \hat{B}\left(\hat{\lambda}\right)\hat{\psi}\right\rangle - \left\langle \psi^*, B\left(\hat{\lambda}\right)\hat{\psi}\right\rangle}{\left\langle \psi^*, F\hat{\psi}\right\rangle} . \tag{2.13}$$

In conclusion, the reactivity coefficient equation is thus

$$\rho = \frac{\left\langle \psi^*, B\left(\hat{\lambda}\right)\hat{\psi}\right\rangle - \left\langle \psi^*, \hat{B}\left(\hat{\lambda}\right)\hat{\psi}\right\rangle}{\left\langle \psi^*, F\hat{\psi}\right\rangle} = \frac{\left\langle \psi^*, B\left(\hat{\lambda}\right)\hat{\psi}\right\rangle}{\left\langle \psi^*, F\hat{\psi}\right\rangle} . \tag{2.14}$$

The equation for first order perturbation theory is obtained by expanding equation 2.11

$$\begin{aligned} 0 &= -\Delta\lambda \cdot F\hat{\psi} + B(\lambda)\hat{\psi} + \Delta B\left(\hat{\lambda}\right)\hat{\psi} \\ &= -\Delta\lambda \cdot F\hat{\psi} + B(\lambda)\hat{\psi} + \{\Delta B(\lambda) - \Delta\lambda \cdot \Delta F\}\hat{\psi} \\ &= -\Delta\lambda \cdot F\psi + B(\lambda)\hat{\psi} - \Delta\lambda \cdot F\Delta\psi + \Delta B(\lambda)\psi - \Delta\lambda\Delta F\psi + \Delta B(\lambda)\Delta\psi - \Delta\lambda \cdot \Delta F\Delta\psi \\ &= -\Delta\lambda \cdot F\psi + B(\lambda)\hat{\psi} + \Delta B(\lambda)\psi + \cancel{\{-\Delta\lambda \cdot F\Delta\psi - \Delta\lambda\Delta F\psi + \Delta B(\lambda)\Delta\psi - \Delta\lambda\Delta F\Delta\psi\}} \end{aligned} \tag{2.15}$$

As seen, all $\Delta\psi$ terms are eliminated, and after applying the inner product with the adjoint yields, noting again the usage of equation 2.8 to remove zero terms, we obtain the first order perturbation equation

$$\rho_0 = -\Delta\lambda = -\frac{\left\langle \psi^*, \Delta B(\lambda)\psi\right\rangle}{\left\langle \psi^*, \hat{F}\psi\right\rangle} = \frac{\left\langle \psi^*, B(\lambda)\psi\right\rangle - \left\langle \psi^*, \hat{B}(\lambda)\psi\right\rangle}{\left\langle \psi^*, \hat{F}\psi\right\rangle} = -\frac{\left\langle \psi^*, \hat{B}(\lambda)\psi\right\rangle}{\left\langle \psi^*, \hat{F}\psi\right\rangle} . \tag{2.16}$$

This equation is only first order accurate with respect to ψ. The conventional approach is to further reduce this to

$$\rho_0 \approx \frac{\left\langle \psi^*, B(\lambda)\psi\right\rangle - \left\langle \psi^*, \hat{B}(\lambda)\psi\right\rangle}{\left\langle \psi^*, F\psi\right\rangle} = -\frac{\left\langle \psi^*, \hat{B}(\lambda)\psi\right\rangle}{\left\langle \psi^*, F\psi\right\rangle} , \tag{2.17}$$

to get the standard first order scheme which is implemented in PERSENT as FIRST_ORDER_PT whereas the implementation of equation 2.16 is termed NS_FIRST_ORDER (Non Standard).

Note that first order perturbation theory is predominately used in diffusion theory and that experience with its use in transport is minimal. The primary reason for its need is to minimize the computational effort involved in obtaining reactivity coefficients for a safety analysis. In general, the magnitude of the perturbation (i.e. $\hat{\lambda}$) depends upon the magnitude of the geometric or compositional perturbation. This relation is non-linear and thus the reactivity coefficient defined by equation 2.14 is not usable in a simple linear fashion (typical approach for point kinetics models). One should construct a reactivity response curve consisting of multiple points computed along the proposed perturbation path noting that most perturbations consider single variable perturbations only. In fact, one could go further and construct a multi-dimensional table of reactivity data considering the simultaneous perturbation of several variables (e.g. fuel density, coolant density, structural temperature, …). Thus, the reactivity coefficients of interest are always tied to the underlying safety analysis being performed.

2.3 First Order Perturbation Theory Treatment in PERSENT

Most of the perturbations in fast reactor systems are modeled with a variety of point kinetics schemes and consider small changes (i.e. less than <<10%) around the nominal condition. In these safety analysis models, what one typically desires is a simple linear reactivity coefficient that corresponds with a "small" perturbation with a definitive upper bound (say at most a 1% change in sodium density). Such reactivity coefficients are ideally conservative for most safety analysis cases given the lack of detailed multi-variable reactivity coefficient tables. In the literature, the reactivity coefficients are typically referred to as first order perturbation theory reactivity coefficients, but in reality, they are equivalent to exact perturbation theory given the assumption about a small perturbation is met.

In the VARI3D software, a first order reactivity coefficient option was added to specifically compute the instantaneous reactivity coefficients for the diffusion system it solves. To be brief, the perturbation in the diffusion coefficient is made to be linear with respect to changes in absorption and a few other correction factors are computed based upon the balance. This allows the user to obtain the instantaneous reactivity coefficient for any provided input perturbation. Such an approach may be feasible for diffusion theory, but in PERSENT we are focused on transport and thus take a slightly different approach.

To demonstrate the issue we have in transport, we first show that equation 2.17 holds true for small perturbations by using PERSENT on two perturbations of a reactor core test problem in Table 2.1 and Table 2.2. In Table 2.1, we modify the sodium density in the outer core region by the absolute amount specified (0.01 means the sodium atom density is adjusted by 0.01 atoms/barn-cm) while in Table 2.2, we modify the Pu-239 density in the same manner. In both tables, we provide the diffusion theory and transport theory exact perturbation worths of each change where we progressively reduce the total amount of the density change. *The reported values are worth/kg change which causes all perturbations to have a similar magnitude.* The column EPT corresponds to exact perturbation theory, FO corresponds to applying equation 2.17, the first order perturbation theory relation without concern for the perturbation magnitude, while FOI corresponds to the desired first order perturbation theory reactivity coefficient scaled to the correct magnitude of the users perturbation.

Table 2.1. Example Evaluation of First Order Perturbation for a Na Density Change

Density Change	EPT Diffusion	FO Diffusion	FOI Diffusion	EPT Transport	FO Transport	FOI Transport
0.01	0.0328	-0.0606	0.0337	-0.0366	-0.1366	-0.0439
0.001	0.0336	0.0229	0.0337	-0.0431	-0.0546	-0.0439
0.0001	0.0337	0.0326	0.0337	-0.0438	-0.0450	-0.0439
0.00001	0.0337	0.0336	0.0337	-0.0439	-0.0440	-0.0439
0.000001	0.0337	0.0337	0.0337	-0.0439	-0.0439	-0.0439

Focusing on Table 2.1, the first sodium density change (amounts to a 10% change in total sodium density), one can see that the FO perturbation is considerably in error compared with the exact perturbation theory result in both diffusion and transport. The coefficient for transport is also observed to be of a different sign and magnitude from that of the diffusion theory result. As the total sodium density perturbation is reduced, the first order and exact

perturbation results become identical in both diffusion and transport calculation options. The same behavior is observed with the Pu density results in Table 2.2, although the first order perturbation is generally accurate even at larger perturbations (the 0.001 density change amounts to a 10% change in the atom density). Because the physical changes impact the transport equation in different ways, the density impacts have two different outcomes for the two different isotopic perturbations and thus the above results are expected.

Table 2.2. Example Evaluation of First Order Perturbation for a Pu Density Change

Density Change	EPT Diffusion	FO Diffusion	FOI Diffusion	EPT Transport	FO Transport	FOI Transport
0.001	86.2	85.8	85.8	86.2	85.3	85.4
0.0001	85.8	85.8	85.8	85.4	85.4	85.4
0.00001	85.8	85.8	85.8	85.4	85.4	85.4
0.000001	85.8	85.8	85.8	85.4	85.4	85.4
0.0000001	85.9	85.9	85.9	85.5	85.5	85.5

In principle, what one can learn from Table 2.1 and Table 2.2, and a broader set of problems, is that the first order approximation can be a very accurate and thus is a cheap way to compute a reactivity coefficient when the perturbation itself is small. The negative feature is that an accurate first order reactivity coefficient is only obtained when the perturbation is "small enough" which can be a difficult thing to guarantee in many reactor systems and perturbations. Because the first order methodology itself is inappropriate to use to construct a reactivity coefficient response curve in most safety calculations (i.e. one should use exact perturbation theory), we eliminate it as a specific option in PERSENT to avoid users from generating it which has occurred in the past for VARI3D. The PERSENT implementation of FIRST_ORDER_PT is entirely focused on achieving the first order reactivity coefficient for a small perturbation. In this sense, we modify the user's perturbation such that it is always small and yields the FOI coefficient as seen in Table 2.1 and Table 2.2.

How to accomplish this in diffusion theory has been well studied. To achieve it in even-parity transport theory is a bit more complicated. To deal with it in PERSENT, we rely upon a physical observation of the perturbation which is defined to be "small" based upon the actual reactivity worth:

$$worth = \frac{1}{k_{base}} - \frac{1}{k_{pert}}. \tag{2.18}$$

By analysis, the change in the base eigenvalue is

$$k_{pert} = k_{base} + \delta$$

$$worth = \frac{1}{k_{pert}}\left(\frac{k_{base}+\delta}{k_{base}} - 1\right) \approx \frac{\delta}{k_{base}^2}. \tag{2.19}$$

One finds the approximation in equation 2.19 is very accurate for a critical system when $\delta \le 0.00001$. Not surprisingly, the first order perturbation approximation in equation 2.17 is very accurate for changes to the base eigenvalue of this magnitude or less. From Table 2.1 and Table 2.2 it should be apparent that larger perturbations can yield similarly accurate results.

As a consequence of this observation, we choose to develop a methodology in PERSENT to adjust the user perturbation to a smaller perturbation where equation 2.17 will always produce the correct GPT result. To accomplish this, we weight the transport equation

$$\hat{\Omega}\cdot\nabla\psi\left(\vec{r},\hat{\Omega},E\right)+\Sigma_t\left(\vec{r}\right)\psi\left(\vec{r},\hat{\Omega},E\right)=$$
$$\int d\Omega'\int dE'\Sigma_s\left(\vec{r},\hat{\Omega}'\to\hat{\Omega},E'\to E\right)\psi\left(\vec{r},\hat{\Omega},E\right) \quad , \tag{2.20}$$
$$+\frac{1}{k}\int d\Omega'\int dE'\chi\left(E,E'\right)\nu\left(E'\right)\Sigma_f\left(\vec{r},\hat{\Omega}',E'\right)\psi\left(\vec{r},\hat{\Omega},E\right)$$

with its adjoint and integrate over all variables to obtain:

$$k=\frac{Fission}{Absorption+Leakage}$$
$$Fission=\int d\Omega\int dE\ \left\{\psi^\dagger\left(\vec{r},\hat{\Omega},E\right)\int d\Omega'\int dE'\chi\left(E,E'\right)\nu\left(E'\right)\Sigma_f\left(\vec{r},\hat{\Omega}',E'\right)\psi\left(\vec{r},\hat{\Omega},E\right)\right\}$$
$$Absorption=\int d\Omega\int dE\ \left\{\begin{bmatrix}\psi^\dagger\left(\vec{r},\hat{\Omega},E\right)\cdot\\ \Sigma_t\left(\vec{r}\right)\psi\left(\vec{r},\hat{\Omega},E\right)\\ -\int d\Omega'\int dE'\Sigma_s\left(\vec{r},\hat{\Omega}'\to\hat{\Omega},E'\to E\right)\psi\left(\vec{r},\hat{\Omega},E\right)\end{bmatrix}\right\} \quad , \tag{2.21}$$
$$Leakage=\int d\Omega\int dE\ \left\{\psi^\dagger\left(\vec{r},\hat{\Omega},E\right)\hat{\Omega}\cdot\nabla\psi\left(\vec{r},\hat{\Omega},E\right)\right\}$$

In this simplistic form, one can see the integral type of expression for the eigenvalue appears. In PERSENT, we compute the forward flux weighted integrals of the changes in fission production, absorption, and the total cross section that occur due to the perturbation to get:

$$\delta_{Fission}=\left|\sum_i^{NumRegions}\sum_g^{NumGroups}\left(\nu\Sigma_{f,g,i}^{base}-\nu\Sigma_{f,g,i}^{perturbed}\right)\cdot\phi_{g,i}\cdot V_i\right|$$
$$\delta_{Absorption}=\left|\sum_i^{NumRegions}\sum_g^{NumGroups}\left(\Sigma_{a,g,i}^{base}-\Sigma_{a,g,i}^{perturbed}\right)\cdot\phi_{g,i}\cdot V_i\right|$$
$$\delta_{Leakage}=\left|\sum_i^{NumRegions}\sum_g^{NumGroups}\left(\Sigma_{t,g,i}^{base}-\Sigma_{t,g,i}^{perturbed}\right)\cdot\phi_{g,i}\cdot V_i\right| \tag{2.22}$$
$$Absorption=\left|\sum_i^{NumRegions}\sum_g^{NumGroups}\Sigma_{a,g,i}^{base}\cdot\phi_{g,i}\cdot V_i\right|$$
$$Fission=\left|\sum_i^{NumRegions}\sum_g^{NumGroups}\nu\Sigma_{f,g,i}^{base}\cdot\phi_{g,i}\cdot V_i\right|$$

Take note that the term $\delta_{Leakage}$ is particularly inaccurate but extremely cheap to compute.

With these quantities, we created a simplistic expression to evaluate:

$$\delta k\sim\left|\frac{Fission+\delta_{Fission}}{Absorption+\delta_{Absorption}+\delta_{Leakage}}-\frac{Fission}{Absorption}\right| \tag{2.23}$$

The accuracy of this equation is not really important of course because our ultimate goal is to only understand what significant digit the user provided perturbation impacts without having to compute the exact perturbation result. In this sense, we check the magnitude of this function relative to $\delta \le 0.00001$ and simply scale the user cross section perturbation by the resulting factor needed to place:

$$f \cdot \delta k \simeq 0.000001$$
$$\sigma^{*}_{perturbed} = \sigma_{base} + f \cdot \sigma_{perturbed} \tag{2.24}$$

The computed first order perturbation using this new cross section set is then scaled back up by using the inverse of the scaling factor in equation 2.24. By taking this approach, we guarantee whatever perturbation the user provides is within the accuracy range of the first order approximation as evident from the FOI results in Table 2.1 and Table 2.2 and thus the desired first order perturbation coefficient. As mentioned, the option FIRST_ORDER_PT imposes this approximation when it is used and there is no option to disable it. If one wants to test the accuracy of the first order approximation we suggest using NS_FIRST_ORDER as for small perturbations it will yield identical results or can be rescaled using the computed denominator from FIRST_ORDER_PT that is provided in the output.

2.4 Prompt Neutron Lifetime and Delayed Neutron Fraction

In addition to the preceding equations used to obtain reactivity coefficients, we also need to evaluate the prompt neutron lifetime, Λ, and the delayed neutron fraction, β. In this case, the derivation is well defined in the literature noting that both terms result from varying the amplitude of a given steady state solution of the transport equation. As such, the base of both terms is taken from the time dependent form:

$$\frac{1}{\nu(E)}\frac{\partial \psi(r,E,\hat{\Omega},t)}{\partial t} + \nabla \cdot \hat{\Omega}\psi(r,E,\hat{\Omega},t) + \Sigma_t(r,E)\psi(r,E,\hat{\Omega},t) = S(r,E,\hat{\Omega},t)\,. \tag{2.25}$$

Skipping a bulk of the details, we obtain its discrete form at the end of the time step:

$$\left\{\frac{1}{\nu}H + A - W - \lambda_0 \cdot F\right\}\psi - \sum_{m=1}^{\substack{Delay\\Families}} F_m C_m = Q\,, \tag{2.26}$$

where H is an identity-like matrix for VARIANT and C_m is the precursor concentration with F_m being the related fission source matrix for the precursor (similar structure to F). The relations used for defining the kinetics parameters are

$$\Lambda = \frac{1}{\lambda}\frac{\left\langle \psi^{*}, v^{-1}H\psi \right\rangle}{\left\langle \psi^{*}, F\psi \right\rangle} \qquad \& \qquad \beta = \frac{\sum_{i}^{isotopes} N_i \sum_{m}^{\substack{delay\\families}} \left\langle \psi^{*}, F_{i,m}\psi \right\rangle}{\left\langle \psi^{*}, F\psi \right\rangle}, \tag{2.27}$$

where one can see how they fit into equation 2.26. Note that β can be broken into its isotopic components relatively easily (common approach) and that $F_{i,m}$ is the isotopic fission source operator for a given family. Also note that the definition of Λ without the eigenvalue λ is termed the neutron generation time or $\Lambda_G = \Lambda \cdot \lambda$.

2.5 Point Kinetics Data

One typically wants a spatial and isotopic breakdown of β, but sometimes one also desires the overall domain averaged quantities. Computing a single set of β for the domain is quite straightforward, but the associated decay constants for the different families are not. To construct effective decay constants one must use some form of averaging. The standard point kinetics equations are given as

$$\frac{dp(t)}{dt} = \frac{\rho(t)-\beta}{\Lambda_G} p(t) + \sum_{i,m} \lambda_{i,m} c_{i,m}(t) \tag{2.28}$$

$$\frac{dc_{i,m}(t)}{dt} = -\lambda_{i,m} c_{i,m}(t) + \frac{\beta_{i,m}}{\Lambda_G} p(t). \tag{2.29}$$

In equations 2.28 and 2.29, one can see the precursor concentration for a given family (m) is unique to each unique isotope (i). For any given reactor domain, we can compute the $\beta_{i,m}$ for each family of each unique isotope in the domain (i.e. U235, U238, Pu239, etc.) by simply summing over all geometric regions and energy groups. For each of these unique isotopes we have a decay constant $\lambda_{i,m}$ for each family. Note that in a rigorous kinetics formulation, the precursor concentrations are unique at each point in space and thus with equations 2.28 and 2.29 we have already used spatially integrated quantities.

The formal point kinetics system we typically use has the isotope independent form:

$$\frac{dp(t)}{dt} = \frac{\rho(t)-\beta}{\Lambda_G} p(t) + \sum_{m} \bar{\lambda}_m C_m(t) \tag{2.30}$$

$$\frac{dC_m(t)}{dt} = -\bar{\lambda}_m C_m(t) + \frac{\bar{\beta}_m}{\Lambda_G} p(t). \tag{2.31}$$

The computation of $\bar{\beta}_m$ is straightforward

$$\bar{\beta}_m = \sum_i \beta_{i,m}. \tag{2.32}$$

The effective decay constants require a bit more algebra using the equivalence of the initial condition of equations 2.29 and 2.31.

$$\frac{dc_{i,m}(0)}{dt} = 0 = -\lambda_{i,m} c_{i,m}(0) + \frac{\beta_{i,m}}{\Lambda_G} p(0) \rightarrow c_{i,m}(0) = \frac{\beta_{i,m}}{\Lambda_G \lambda_{i,m}} p(t). \tag{2.33}$$

$$\frac{dC_m(0)}{dt} = 0 = -\bar{\lambda}_m C_m(0) + \frac{\bar{\beta}_m}{\Lambda_G} p(0) \rightarrow C_m(0) = \frac{\bar{\beta}_m}{\Lambda_G \bar{\lambda}_m} p(0). \tag{2.34}$$

Imposing $C_m(0) = \sum_i c_{i,m}(0)$ enforces conservation of energy (neutrons) and thus from equations 2.33 and 2.34 we find

$$C_m(0) = \frac{\bar{\beta}_m}{\Lambda_G \bar{\lambda}_m} p(0) = \sum_i \frac{\beta_{i,m}}{\Lambda_G \lambda_{i,m}} p(0) = \frac{p(0)}{\Lambda_G} \sum_i \frac{\beta_{i,m}}{\lambda_{i,m}} \rightarrow \bar{\lambda}_m = \frac{\bar{\beta}_m}{\sum_i \beta_{i,m} / \lambda_{i,m}}. \tag{2.35}$$

In PERSENT, the Λ and β operation is merged into a single function call where Λ, β, $\bar{\beta}_m$, and $\bar{\lambda}_m$ are the minimal output provided. Using additional input flags, the calculated $\lambda_{i,m}$ and $\beta_{i,m}$ values are provided along with space-energy details for Λ and β.

2.6 Even-parity Operator Specific Issues

When using the first order transport equation, there are no real issues with operator applications shown in the preceding perturbation equations as one simply applies the perturbed part of the operator to a component of the flux vector. The most complicated it can get is when scattering cross sections are modified and require matrix-vector operations applied to multiple source energy groups.

In the even-parity method, the odd-parity flux is substituted into the even-parity transport equation which adds some complexity to the operator application. In order to solve for the even-parity flux, one must know the odd-parity source. In order to solve for the odd-parity flux which makes up the odd-parity source, one must have solved for the even-parity flux. This obviously implies a chicken-egg scenario which does not cast well to a simple matrix-vector product like the preceding equations infer. In the initial PERSENT code, we solved this issue by iteratively updating the odd-parity components which infers the coefficient matrix A_g is non-linear (or iterative) rather than definitive: $A_g \cdot \psi_g \rightarrow A_g\left(\psi_g\right)\cdot\psi_g$.

This non-linear aspect makes the operator application terribly complex and expensive in the sensitivity computation due to a general inability to evaluate the derivative. To show how complicated this can become, we expand our approximation into a two group system and examine how odd-parity scattering cross sections greatly complicate the entire operator application process. To start, we take the discrete first order transport and separate it into the even- and odd-parity terminology.

$$\nabla\cdot\hat{\Omega}\psi^{+}(r,E,\hat{\Omega})+\Sigma_t(r,E)\psi^{-}(r,E,\hat{\Omega})=S^{-}(r,E,\hat{\Omega}) \tag{2.36}$$

$$\nabla\cdot\hat{\Omega}\psi^{-}(r,E,\hat{\Omega})+\Sigma_t(r,E)\psi^{+}(r,E,\hat{\Omega})=S^{+}(r,E,\hat{\Omega}) \tag{2.37}$$

We can cast these into a discrete form for both spatial polynomials and spherical harmonics consistent with VARIANT over each mesh (node) and define

$$\left(V_k\otimes U_k\right)\psi_g^{+}+\Sigma_{t,g}\left(I^{-}\otimes F\right)\psi_g^{-}=\left(\Sigma_{s,g,g}^{-}\otimes F\right)\psi_g^{-}+S_g^{-} \tag{2.38}$$

$$-\left(V_k^T\otimes U_k^T\right)\psi_g^{-}+\left(E_\gamma\otimes D_\gamma\right)\psi_{g,\gamma}^{-}+\Sigma_{t,g}\left(I^{+}\otimes F\right)\psi_g^{+}=\left(\Sigma_{s,g,g}^{+}\otimes F\right)\psi_g^{+}+S_g^{+} \tag{2.39}$$

The definition of these matrices are consistent with those used in the VARIANT manual [29]. ψ_g^{+} represents the even-parity flux while ψ_g^{-} is the odd-parity flux. Note that we have separated out the within group scattering terms as is typically done in VARIANT.

The next step in VARIANT requires equation 2.38 to be solved for the odd parity flux and substituted into equation 2.39.

$$\psi_g^{-}=\left[\left(\Sigma_{t,g}I^{-}-\Sigma_{s,g,g}^{-}\right)\otimes F\right]^{-1}\left[-\left(V_k\otimes U_k\right)\psi_g^{+}+S_g^{-}\right] \tag{2.40}$$

$$\left(H_{K,L}\otimes P_{K,L}\right)\psi_g^+-\left(Y_{k,g}\otimes Z_k\right)S_g^-+\left(E_\gamma\otimes D_\gamma\right)\psi_{g,\gamma}^-+\Sigma_{t,g}\left(I^+\otimes F\right)\psi_g^+=\left(\Sigma_{s,g,g}^+\otimes F\right)\psi_g^++S_g^+$$

$$A\psi_g^+=S_g^++\left(Y_{k,g}\otimes Z_k\right)S_g^--\left(E_\gamma\otimes D_\gamma\right)\psi_{g,\gamma}^-$$

$$A=H_{K,L}\otimes P_{K,L}+\Sigma_{t,g}I^+\otimes F-\Sigma_{s,g,g}^+\otimes F \tag{2.41}$$

$$P_{K,L}=U_K^TF^{-1}U_L \qquad Z_k=U_k^TF^{-1}$$

$$H_{K,L}=V_K^T\left(\Sigma_{t,g}I^--\Sigma_{s,g,g}^-\right)^{-1}V_L \quad Y_{k,g}=V_K^T\left(\Sigma_{t,g}I^--\Sigma_{s,g,g}^-\right)^{-1}$$

In these equations we depart somewhat from VARIANT in that we merge the cross sections with the angular matrices to make our notation more convenient and compact. To complete the system, we must define expressions for the sources

$$S_g^+=\sum_{g',g\neq g'}\left(\Sigma_{s,g'\to g}^+\otimes F\right)\psi_{g'}^++q_{g'}^+ \tag{2.42}$$

$$S_g^-=\sum_{g',g\neq g'}\left(\Sigma_{s,g'\to g}^-\otimes F\right)\psi_{g'}^-+q_{g'}^- \tag{2.43}$$

In these last two equations we allow a fixed source or fission source consideration with the arbitrarily defined $q_{g'}^{\pm}$. This is of course where the non-linearity of the operator comes in as in order to define either the even- or odd-parity source for a given group, we must have both the even- and odd-parity flux solution, either of which requires us to have the solution for the other first.

To understand the problem, we expand equations 2.40 through 2.43 in a two group form with anisotropic up-scattering which we partition into a single system as

$$\begin{bmatrix}A_1 & 0\\ 0 & A_2\end{bmatrix}\begin{bmatrix}\psi_1^+\\ \psi_2^+\end{bmatrix}=\begin{bmatrix}S_1^+\\ S_2^+\end{bmatrix}+\begin{bmatrix}Y_{k,1}\otimes Z_k & 0\\ 0 & Y_{k,2}\otimes Z_k\end{bmatrix}\begin{bmatrix}S_1^-\\ S_2^-\end{bmatrix}-\left(E_\gamma\otimes D_\gamma\right)\begin{bmatrix}\psi_{1,\gamma}^-\\ \psi_{2,\gamma}^-\end{bmatrix} \tag{2.44}$$

We can do the same with the sources in equation 2.42 and equation 2.43 to define

$$\begin{bmatrix}S_1^{\pm}\\ S_2^{\pm}\end{bmatrix}=\begin{bmatrix}0 & \left(\Sigma_{s,2\to1}^{\pm}\otimes F\right)\\ \left(\Sigma_{s,1\to2}^{\pm}\otimes F\right) & 0\end{bmatrix}\begin{bmatrix}\psi_1^{\pm}\\ \psi_2^{\pm}\end{bmatrix}+\begin{bmatrix}q_1^{\pm}\\ q_2^{\pm}\end{bmatrix} \tag{2.45}$$

We can substitute this into equation 2.44 to obtain

$$\begin{bmatrix}A_1 & -\Sigma_{s,2\to1}^+\otimes F\\ -\Sigma_{s,1\to2}^+\otimes F & A_2\end{bmatrix}\begin{bmatrix}\psi_1^+\\ \psi_2^+\end{bmatrix}=\begin{bmatrix}\left(Y_{k,1}\Sigma_{s,2\to1}^-\otimes Z_kF\right)\psi_2^-\\ \left(Y_{k,2}\Sigma_{s,1\to2}^-\otimes Z_kF\right)\psi_1^-\end{bmatrix}+\begin{bmatrix}\left(Y_{k,1}\otimes Z_k\right)q_1^-\\ \left(Y_{k,2}\otimes Z_k\right)q_2^-\end{bmatrix}+\begin{bmatrix}q_1^+\\ q_2^+\end{bmatrix}-\left(E_\gamma\otimes D_\gamma\right)\begin{bmatrix}\psi_{1,\gamma}^-\\ \psi_{2,\gamma}^-\end{bmatrix} \tag{2.46}$$

The final equation we need to complete this system is the odd-parity flux from equation 2.40 which we can write as:

$$\begin{bmatrix}\psi_1^- \\ \psi_2^-\end{bmatrix} = -\begin{bmatrix}\left(\Sigma_{t,1}I^- - \Sigma_{s,1,1}^- \otimes F\right)^{-1}\left(V_k \otimes U_k\right) & 0 \\ 0 & \left(\Sigma_{t,2}I^- - \Sigma_{s,2,2}^- \otimes F\right)^{-1}\left(V_k \otimes U_k\right)\end{bmatrix}\begin{bmatrix}\psi_1^+ \\ \psi_2^+\end{bmatrix}$$
$$+\begin{bmatrix}0 & \left(\Sigma_{t,1}I^- - \Sigma_{s,1,1}^- \otimes F\right)^{-1}\left(\Sigma_{s,2\to1}^- \otimes F\right) \\ \left(\Sigma_{t,2}I^- - \Sigma_{s,2,2}^- \otimes F\right)^{-1}\left(\Sigma_{s,1\to2}^- \otimes F\right) & 0\end{bmatrix}\begin{bmatrix}\psi_1^- \\ \psi_2^-\end{bmatrix} \qquad (2.47)$$
$$+\begin{bmatrix}\left(\Sigma_{t,1}I^- - \Sigma_{s,1,1}^- \otimes F\right)^{-1} & 0 \\ 0 & \left(\Sigma_{t,2}I^- - \Sigma_{s,2,2}^- \otimes F\right)^{-1}\end{bmatrix}\begin{bmatrix}q_1^\pm \\ q_2^\pm\end{bmatrix}$$

Practically speaking, in large energy group calculations, it is not possible to include the scattering terms in the left hand side matrix as seen in equation 2.46. Instead, Gauss-Seidel iteration is used to converge this system. Equation 2.46 forms the basis of the operator that we must apply. However, because it contains references to odd-parity moments which requires the solution of equation 2.47, this indicates the operator requires multiple evaluations.

After some study, the bulk of the work actually involves iteratively applying equation 2.47 to "converge" the odd-parity group sources. From there, they can be substituted into equation 2.44. Such an approach is perfectly fine for the perturbation aspects given the number of times the operator is to be applied. For sensitivity calculations, this is a complete disaster as we cannot realistically identify an easy way to linearize the operator which is the easiest way to minimize computational effort. To avert this, we must completely eliminate the odd-parity moments which begins at equations 2.38 and 2.39. In the following we rearrange the equations with the intention of partitioning them with respect to energy

$$\left(V_k \otimes U_k\right)\psi_g^+ + \Sigma_{t,g}\left(I^- \otimes F\right)\psi_g^- = \sum_{g'}\left(\Sigma_{s,g'\to g}^- \otimes F\right)\psi_{g'}^- + q_{g'}^- \qquad (2.48)$$

$$-\left(V_k^T \otimes U_k^T\right)\psi_g^- + \left(E_\gamma \otimes D_\gamma\right)\psi_{g,\gamma}^- + \Sigma_{t,g}\left(I^+ \otimes F\right)\psi_g^+ = \sum_{g'}\left(\Sigma_{s,g'\to g}^+ \otimes F\right)\psi_{g'}^+ + q_{g'}^+ \qquad (2.49)$$

We begin by defining multi-group cross section angle-energy matrices

$$\underline{\underline{\Sigma}}_t^\pm = \begin{bmatrix}\Sigma_{t,1}I^\pm & 0 & 0 \\ 0 & \ddots & 0 \\ 0 & 0 & \Sigma_{t,g}I^\pm\end{bmatrix} \quad \underline{\underline{\Sigma}}_s^\pm = \begin{bmatrix}\Sigma_{s,1\to1}^\pm & \cdots & \Sigma_{s,g'\to1}^\pm \\ \vdots & \ddots & \vdots \\ \Sigma_{s,1\to g}^\pm & \cdots & \Sigma_{s,g\to g}^\pm\end{bmatrix}, \qquad (2.50)$$

odd-parity angle-energy matrices

$$\underline{\underline{V}}_k = \begin{bmatrix}V_k & 0 & 0 \\ 0 & V_k & 0 \\ 0 & 0 & V_k\end{bmatrix} \quad \underline{\underline{E}}_\gamma = \begin{bmatrix}E_\gamma & 0 & 0 \\ 0 & E_\gamma & 0 \\ 0 & 0 & E_\gamma\end{bmatrix}, \qquad (2.51)$$

and the assembled flux and source vectors

$$\underline{\psi}^+ = \begin{bmatrix}\psi_1^+ \\ \vdots \\ \psi_g^+\end{bmatrix} \quad \underline{\psi}^- = \begin{bmatrix}\psi_1^- \\ \vdots \\ \psi_g^-\end{bmatrix} \quad \underline{q}^\pm = \begin{bmatrix}q_1^\pm \\ \vdots \\ q_g^\pm\end{bmatrix} \quad \underline{\psi}_\gamma^- = \begin{bmatrix}\psi_{1,\gamma}^- \\ \vdots \\ \psi_{g,\gamma}^-\end{bmatrix}. \qquad (2.52)$$

Substituting this into equation 2.48, we can write the odd-parity equation as

$$\left(\underline{\underline{V}}_k \otimes U_k\right)\underline{\psi}^+ + \left(\underline{\underline{\Sigma}}_t^- \otimes F\right)\underline{\psi}^- = \left(\underline{\underline{\Sigma}}_s^- \otimes F\right)\underline{\psi}^- + \underline{q}^- . \tag{2.53}$$

We can solve equation 2.53 for the odd-parity flux to get

$$\begin{aligned}\underline{\psi}^- &= \left(\left(\underline{\underline{\Sigma}}_t^- - \underline{\underline{\Sigma}}_s^-\right)\otimes F\right)^{-1}\left\{-\left(\underline{\underline{V}}_k \otimes U_k\right)\underline{\psi}^+ + \underline{q}^-\right\} \\ &= \left(\underline{\underline{\Sigma}}_\tau \otimes F^{-1}\right)\left\{-\left(\underline{\underline{V}}_k \otimes U_k\right)\underline{\psi}^+ + \underline{q}^-\right\} \quad .\end{aligned} \tag{2.54}$$

$$\underline{\underline{\Sigma}}_\tau = \left(\underline{\underline{\Sigma}}_t^- - \underline{\underline{\Sigma}}_s^-\right)^{-1}$$

We substitute equations 2.50 to 2.52 into equation 2.49 to write the even-parity equation as

$$-\left(\underline{\underline{V}}_k^T \otimes U_k^T\right)\underline{\psi}^- + \left(\underline{\underline{E}}_\gamma \otimes D_\gamma\right)\underline{\psi}_\gamma^- + \left(\underline{\underline{\Sigma}}_t^+ \otimes F\right)\underline{\psi}^+ = \left(\underline{\underline{\Sigma}}_s^+ \otimes F\right)\underline{\psi}^+ + \underline{q}^+ . \tag{2.55}$$

We can substitute equation 2.54 into equation 2.55 to obtain the final even-parity only form of the transport equation

$$\begin{aligned}&\left(\underline{\underline{V}}_k^T \otimes U_k^T\right)\left(\underline{\underline{\Sigma}}_\tau \otimes F^{-1}\right)\left(\underline{\underline{V}}_j \otimes U_j\right)\underline{\psi}^+ + \left(\underline{\underline{\Sigma}}_t^+ \otimes F\right)\underline{\psi}^+ = \\ &\left(\underline{\underline{\Sigma}}_s^+ \otimes F\right)\underline{\psi}^+ + \underline{q}^+ + \left(\underline{\underline{V}}_k^T \otimes U_k^T\right)\left(\underline{\underline{\Sigma}}_\tau \otimes F^{-1}\right)\underline{q}^- - \left(\underline{\underline{E}}_\gamma \otimes D_\gamma\right)\underline{\psi}_\gamma^-\end{aligned} \tag{2.56}$$

The problem with using this form is the appearance of the additional cross section matrix in equation 2.54 which is not consistent with the VARIANT implementation [2,29]. This matrix is effectively full with respect to energy on each non-zero angular moment and, in general, it completely connects all of the even-parity flux moments together.

Given the above approach, the entire operator application in PERSENT was rebuilt from the original version to take this matrix approach which is used as if it is a full matrix application in the odd-parity space. For the upcoming cross section sensitivity, we need to be able to take the derivative of the operator with respect to the cross section input. The formulation matrices to work with are given as:

$$\begin{aligned}\underline{\underline{A}} &= \left(\underline{\underline{V}}_k^T \otimes U_k^T\right)\left(\underline{\underline{\Sigma}}_\tau \otimes F^{-1}\right)\left(\underline{\underline{V}}_j \otimes U_j\right) + \left(\underline{\underline{\Sigma}}_t^+ \otimes F\right) - \left(\underline{\underline{\Sigma}}_s^+ \otimes F\right) \\ \underline{\underline{B}}(\lambda) &= \underline{\underline{A}} - \lambda\left(\underline{\underline{\Sigma}}_{fission}^+ \otimes F\right)\end{aligned} \quad . \tag{2.57}$$

It is very important to note that we do not include the boundary condition term in equation 2.57. This is correct as when the above system is summed over all nodes (meshes), the boundary terms that are used to connect the nodes together cancel out. Thus to define the perturbation or sensitivity operations, we only need to apply the node wise operations and sum over all nodes in the domain. For fixed source problems, the fission source term vanishes and the fixed source terms from equation 2.56 must be maintained. We find the eigenvalue can be defined as

$$k = \frac{\underline{\psi}^{+,*}\left(\underline{\underline{\Sigma}}_{fission}^+ \otimes F\right)\underline{\psi}^+}{\underline{\psi}^{+,*}\underline{\underline{A}}\underline{\psi}^+} . \tag{2.58}$$

The derivative of interest in an eigenvalue sensitivity can be written as:

$$\frac{\partial k}{\partial \sigma_x} = \frac{\partial}{\partial \sigma_x} \frac{\underline{\psi}^{+,*} \left(\underline{\underline{\Sigma}}^{+}_{fission} \otimes F \right) \underline{\psi}^{+}}{\underline{\psi}^{+,*} \underline{\underline{A}} \underline{\psi}^{+}}$$

$$= \frac{1}{\underline{\psi}^{+,*} \underline{\underline{A}} \underline{\psi}^{+}} \underline{\psi}^{+,*} \left(\frac{\partial \underline{\underline{\Sigma}}^{+}_{fission}}{\partial \sigma_x} \otimes F \right) \underline{\psi}^{+} - \frac{\underline{\psi}^{+,*} \left(\underline{\underline{\Sigma}}^{+}_{fission} \otimes F \right) \underline{\psi}^{+}}{\left(\underline{\psi}^{+,*} \underline{\underline{A}} \underline{\psi}^{+} \right)^2} \underline{\psi}^{+,*} \frac{\partial \underline{\underline{A}}}{\partial \sigma_x} \underline{\psi}^{+} \quad . \qquad (2.59)$$

$$\frac{\partial \underline{\underline{A}}}{\partial \sigma_x} = -\left(\underline{\underline{V}}^{T}_{k} \otimes U^{T}_{k} \right) \left(\underline{\underline{\Sigma}}_{\tau} \frac{\partial \left(\underline{\underline{\Sigma}}^{-}_{t} - \underline{\underline{\Sigma}}^{-}_{s} \right)}{\partial \sigma_x} \underline{\underline{\Sigma}}_{\tau} \otimes F^{-1} \right) \left(\underline{\underline{V}}_{j} \otimes U_j \right) + \left(\frac{\partial \underline{\underline{\Sigma}}^{+}_{t}}{\partial \sigma_x} \otimes F \right) - \left(\frac{\partial \underline{\underline{\Sigma}}^{+}_{s}}{\partial \sigma_x} \otimes F \right)$$

In equation 2.59, one can see that the derivative of the new cross section matrix from equation 2.54 produces three matrix operations where there was only one before. The details from here on how to minimize the computational effort involved in evaluating the matrix vector products are beyond the point of this discussion. Instead, the purpose of showing the derivative was to demonstrate that with the new approach, we do not need to store the even- or odd-parity sources in equations 2.42 or 2.43 so long as we can compute the inverse cross section matrix in equation 2.54.

3 Sensitivity Functional

To do the sensitivity analysis, we first select a part of the input $\alpha(r)$ which is inferred to be a given component of the cross section data (type, energy group, angular moment) at a given position in the domain. Focusing on some response parameter R, such as the fission rate in a particular position in the domain, we can define the sensitivity of that response parameter with respect to the variation in the input parameter as

$$s_\alpha(x) = \frac{\alpha(x)}{R}\frac{\partial R}{\partial \alpha(x)}. \tag{3.1}$$

The simplest procedure for evaluating the derivative in the definition of the sensitivity function is the "brute force" approach where direct recalculations with perturbed parameters are used to obtain finite-difference approximations of the derivative. The perturbed system equations have to be solved for each input parameter change, and hence this approach is not very useful when evaluating the effects of several alterations in the input parameters on a few response parameters. This difficulty can be overcome by employing the adjoint sensitivity formalism, in which the sensitivity function is evaluated without solving the perturbed system equations by employing adjoint variables. There are several alternative theoretical approaches to the adjoint-based sensitivity analysis. The prominent methods are the variational method, [9,11,18,19], the perturbation method [10,13,14], and the differential method [22,23]. The variational method is implemented in PERSENT as it only requires the use of a single method to obtain the sensitivities for all of the response parameters of interest.

To begin, we define a functional $G(\alpha,\psi,\psi^*,\Gamma,\Gamma^*)$ for a given response $R(\alpha,\psi,\psi^*)$ where we have dropped the x dependence of $\alpha(x)$ for convenience and introduce the Lagrange multipliers Γ and Γ^*.

$$G(\alpha,\psi,\psi^*,\Gamma,\Gamma^*) = R(\alpha,\psi,\psi^*) - \left\langle \Gamma^*, B(\alpha,\lambda)\psi \right\rangle - \left\langle \Gamma, B^*(\alpha,\lambda)\psi^* \right\rangle \tag{3.2}$$

The following equations show some example response functions of interest

$$R(\alpha,\psi,\psi^*) = \int dE \int d\Omega \int dV \sigma_{fission}^{U-235}\psi(\vec{r},E,\Omega) \tag{3.3}$$

$$R(\alpha,\psi,\psi^*) = \frac{\int dE \int d\Omega \int dV \sigma_{capture}^{U238}\psi(\vec{r},E,\Omega)}{\int dE \int d\Omega \int dV \sigma_{fission}^{Pu239}\psi(\vec{r},E,\Omega)} \tag{3.4}$$

$$R(\alpha,\hat{\psi},\psi^*) = \frac{\left\langle \psi^*, B(\alpha,\hat{\lambda})\hat{\psi} \right\rangle - \left\langle \psi^*, \hat{B}(\alpha,\hat{\lambda})\hat{\psi} \right\rangle}{\left\langle \psi^*, F\hat{\psi} \right\rangle}. \tag{3.5}$$

As will be shown later, the response function in equation 3.3 is not usable with equation 3.2 unless it is an inhomogeneous problem and not a homogeneous eigenvalue one. The response in equation 3.5 requires a slight alteration of the functional in equation 3.2 due to the dependence on $\hat{\psi}$, and we note that both equation 3.3 and 3.4 may or may not be dependent upon the input parameter α. Also note that the functional reduces to the simple definition of the responses in equations 3.3 through 3.5 in the unperturbed case where $B(\alpha,\lambda)\psi = 0$ and $B^*(\alpha,\lambda)\psi^* = 0$.

Focusing on the functional in equation 3.2, we take the variation with respect to α and find

$$\begin{aligned}\delta G = &\frac{\partial R(\alpha,\psi,\psi^*)}{\partial \alpha}\delta\alpha + \frac{\partial R(\alpha,\psi,\psi^*)}{\partial \psi}\delta\psi + \frac{\partial R(\alpha,\psi,\psi^*)}{\partial \psi^*}\delta\psi^* \\ &-\left\langle \Gamma^*, B(\alpha,\lambda)\delta\psi\right\rangle - \left\langle \delta\Gamma^*, B(\alpha,\lambda)\psi\right\rangle + \left\langle \Gamma^*, \delta\lambda F\psi\right\rangle - \left\langle \Gamma^*, \delta B(\alpha,\lambda)\psi\right\rangle \\ &-\left\langle \Gamma, B^*(\alpha,\lambda)\delta\psi^*\right\rangle - \left\langle \delta\Gamma, B^*(\alpha,\lambda)\psi^*\right\rangle + \left\langle \Gamma, \delta\lambda^* F^*\psi^*\right\rangle - \left\langle \Gamma, \delta B^*(\alpha,\lambda)\psi^*\right\rangle\end{aligned} \tag{3.6}$$

with its associated derivative with respect to α given as

$$\begin{aligned}\frac{\partial G}{\partial \alpha} = &\frac{\partial R(\alpha,\psi,\psi^*)}{\partial \alpha} + \frac{\partial R(\alpha,\psi,\psi^*)}{\partial \psi}\frac{\partial \psi}{\partial \alpha} + \frac{\partial R(\alpha,\psi,\psi^*)}{\partial \psi^*}\frac{\partial \psi^*}{\partial \alpha} \\ &-\left\langle \frac{\partial \Gamma^*}{\partial \alpha}, \cancel{B(\alpha,\lambda)\psi}\right\rangle - \left\langle \Gamma^*, \frac{\partial B(\alpha,\lambda)}{\partial \alpha}\psi\right\rangle + \left\langle \Gamma^*, \frac{\partial \lambda}{\partial \alpha}F\psi\right\rangle - \left\langle B^*(\alpha,\lambda)\Gamma^*, \frac{\partial \psi}{\partial \alpha}\right\rangle \\ &-\left\langle \frac{\partial \Gamma}{\partial \alpha}, \cancel{B^*(\alpha,\lambda)\psi^*}\right\rangle - \left\langle \Gamma, \frac{\partial B^*(\alpha,\lambda)}{\partial \alpha}\psi^*\right\rangle + \left\langle \Gamma, \frac{\partial \lambda^*}{\partial \alpha}F^*\psi^*\right\rangle - \left\langle B(\alpha,\lambda)\Gamma, \frac{\partial \psi^*}{\partial \alpha}\right\rangle.\end{aligned} \tag{3.7}$$

Requiring equation 3.6 to be stationary with respect to Γ requires

$$B^*(\alpha,\lambda)\psi^* = 0, \tag{3.8}$$

which was defined to be true. A similar result occurs when requiring equation 3.6 to be stationary with respect to Γ^* hence the elimination of the two terms in equation 3.7. Requiring equation 3.6 to be stationary with respect to the variations of flux vectors ψ and ψ^* (i.e. $\delta\psi$ and $\delta\psi^*$) yields the relations

$$\frac{\partial R(\alpha,\psi,\psi^*)}{\partial \psi} - B^*(\alpha,\lambda)\Gamma^* = 0 \tag{3.9}$$

$$\frac{\partial R(\alpha,\psi,\psi^*)}{\partial \psi^*} - B(\alpha,\lambda)\Gamma = 0 \tag{3.10}$$

where the relation $B^*(\alpha,\lambda) = B^T(\alpha,\lambda)$ was used to switch the application of the operator in the inner products of equation 3.6. Note that the inner product was removed by choosing to constrain the resulting system over the entire dependent variable range. Assuming $\frac{\partial R(\alpha,\psi,\psi^*)}{\partial \psi}$ and $\frac{\partial R(\alpha,\psi,\psi^*)}{\partial \psi^*}$ are non-zero, equations 3.9 and 3.10 will have non-zero solutions for Γ^* and Γ for specific restrictions on S and S^*.

$$B^*(\alpha,\lambda)\Gamma^* = S^* = \frac{\partial R(\alpha,\psi,\psi^*)}{\partial \psi} \tag{3.11}$$

$$B(\alpha,\lambda)\Gamma = S = \frac{\partial R(\alpha,\psi,\psi^*)}{\partial \psi^*} \tag{3.12}$$

Note that $B(\alpha,\lambda)$ and $B^*(\alpha,\lambda)$ are evaluated using the unperturbed configuration (with respect to α). Requiring equation 3.6 to be stationary with respect to λ requires

$$\left\langle \Gamma^*, F\psi \right\rangle = \left\langle F^*\Gamma^*, \psi \right\rangle = 0 \tag{3.13}$$

$$\left\langle \Gamma, F^*\psi^* \right\rangle = \left\langle F\,\Gamma, \psi^* \right\rangle = 0 \tag{3.14}$$

These additional equations impose an additional constraint of orthogonality on Γ and Γ^* for the singular inhomogeneous equations (3.11) and (3.12) to yield unique solutions. With equations (3.11) to (3.14), equation 3.7 reduces to

$$\frac{\partial G}{\partial \alpha} = \frac{\partial R(\alpha,\psi,\psi^*)}{\partial \alpha} - \left\langle \Gamma^*, \frac{\partial B(\alpha,\lambda)}{\partial \alpha}\psi \right\rangle - \left\langle \Gamma, \frac{\partial B^*(\alpha,\lambda)}{\partial \alpha}\psi^* \right\rangle. \tag{3.15}$$

Merging equation 3.15 with equation 3.1 we obtain the final form of the sensitivity function to be evaluated:

$$s_\alpha(x) = \frac{\alpha(x)}{R}\left[\frac{\partial R(\alpha,\psi,\psi^*)}{\partial \alpha} - \left\langle \Gamma^*, \frac{\partial B(\alpha,\lambda)}{\partial \alpha}\psi \right\rangle - \left\langle \Gamma, \frac{\partial B^*(\alpha,\lambda)}{\partial \alpha}\psi^* \right\rangle \right]. \tag{3.16}$$

3.1 Solution of the Inhomogeneous Lagrange Multipliers

Obtaining solutions to equations 3.11 through 3.14 requires additional discussion. We start with equations 3.12 and 3.14 and the homogeneous solution ψ^* to

$$B^*(\lambda)\psi^* = 0 = \left(A^* - \lambda F^*\right)\psi^*. \tag{3.17}$$

According to the Fredholm alternative theorem, equation (3.12) has a solution if and only if its source is orthogonal to the fundamental mode adjoint flux, that is $\left\langle \psi^*, S \right\rangle = 0$. Similarly, equation (3.11) has a solution if and only if its source is orthogonal to the flux, $\left\langle \psi, S^* \right\rangle = 0$. As a consequence, to obtain meaningful Lagrange multipliers, we must verify that $\left\langle \psi^*, S \right\rangle = 0$ and $\left\langle \psi, S^* \right\rangle = 0$ for the response of interest.

For now, we will assume these statements are true and continue the derivation by noting that there are an infinite number of possibilities for Γ as $B(\alpha,\lambda)$ is singular. We can write all of the possible solutions to equations 3.11 and 3.12 as

$$\Gamma = \tilde{\Gamma} + a\psi \quad \& \quad \Gamma^* = \tilde{\Gamma}^* + a^*\psi^* \tag{3.18}$$

where the constants a^* and a are used to isolate a particular solution to equations 3.11 and 3.12. Plugging these expressions into equation 3.13 and 3.14 we find

$$\left\langle \tilde{\Gamma}^*, F\psi \right\rangle = 0 = \left\langle \Gamma^* - a^*\psi^*, F\psi \right\rangle = \left\langle \Gamma^*, F\psi \right\rangle - a^*\left\langle \psi^*, F\psi \right\rangle \tag{3.19}$$

$$\left\langle \tilde{\Gamma}, F^*\psi^* \right\rangle = 0 = \left\langle \Gamma - a\psi, F^*\psi^* \right\rangle = \left\langle \Gamma, F^*\psi^* \right\rangle - a\left\langle \psi, F^*\psi^* \right\rangle \tag{3.20}$$

Solving for the two constants we find

$$a^* = \frac{\left\langle \Gamma^*, F\psi \right\rangle}{\left\langle \psi^*, F\psi \right\rangle} \quad \& \quad a = \frac{\left\langle \Gamma, F^*\psi^* \right\rangle}{\left\langle \psi, F^*\psi^* \right\rangle} = \frac{\left\langle \psi^*, F\Gamma \right\rangle}{\left\langle \psi^*, F\psi \right\rangle}. \tag{3.21}$$

Given that $\langle \psi^*, F\psi \rangle$ is non-zero, one finds that the constraints of equations 3.13 and 3.14 actually specify the unique solution we are interested in:

$$\tilde{\Gamma} = \Gamma - a\psi \quad \& \quad \tilde{\Gamma}^* = \Gamma^* - a^*\psi^*. \tag{3.22}$$

Updating the sensitivity expression we can write

$$s_\alpha = \frac{\alpha}{R}\left[\frac{\partial R(\alpha,\psi,\psi^*)}{\partial\alpha} - \left\langle \tilde{\Gamma}^*, \frac{\partial B(\alpha,\lambda)}{\partial\alpha}\psi \right\rangle - \left\langle \tilde{\Gamma}, \frac{\partial B^*(\alpha,\lambda)}{\partial\alpha}\psi^* \right\rangle\right]. \tag{3.23}$$

In the previous version of PERSENT, we utilized finite difference relationships to evaluate the operator derivative:

$$\frac{\partial B(\alpha,\lambda)}{\partial\alpha} = \frac{B(\alpha + c\cdot\alpha,\lambda) - B(\alpha,\lambda)}{c\cdot\alpha} \tag{3.24}$$

and the derivative of the response itself

$$\frac{\partial R(\alpha,\psi,\psi^*)}{\partial\alpha} = \frac{R(\alpha + c\cdot\alpha,\psi,\psi^*) - R(\alpha,\psi,\psi^*)}{c\cdot\alpha}. \tag{3.25}$$

This approach is eliminated with the formulation changes in equation 2.36 to 2.59 and we simply apply the operator similarly to that shown in equations 2.59.

Another problem resolved in the previous version of PERSENT was how to handle the perturbation of multiple isotopes at the same time. In most multi-group methods, the broad group isotropic cross sections for each homogenized assembly are different due to the different compositions and thus different self-shielding. As a simple example, we consider a one-group, two-region problem with isotopes PU239A and PU239B that have different microscopic broad group capture cross sections σ_γ^{PU239A} and σ_γ^{PU239B} due to different self-shielding. The preceding system of equations requires $\alpha = \sigma_\gamma^{PU239}$, but in PERSENT, the user is allowed to specify a single adjustment for the two isotopes which can be difficult to follow if the targeted cross section is significantly different (say 150%). To counter this we can consider the following options:

(1) $\alpha = \sigma_\gamma^{PU239A}$

(2) $\alpha = \sigma_\gamma^{PU239B}$

(3) $\alpha = \sigma_\gamma^{PU239A} + \sigma_\gamma^{PU239B}$

(4) $\alpha = \dfrac{N^{PU239A}\sigma_\gamma^{PU239A} + N^{PU239B}\sigma_\gamma^{PU239B}}{N^{PU239A} + N^{PU239B}}$

With a single operator approach, when using the first two options, one should normalize the adjustment in all other PU isotopes by the ratio of the capture in the specified one, e.g.

$\sigma_\gamma^{PU239B} \rightarrow \sigma_\gamma^{PU239B} + c\frac{\sigma_\gamma^{PU239B}}{\sigma_\gamma^{PU239A}}$. The third option is the most practical approach if the two isotopes have nearly identical cross sections noting that options 1 and 2 yield an identical result if they are. The fourth option is likely the best if the user specifies a change in two different evaluated sets of isotope data such as σ_γ^{PU239A} and σ_γ^{PU238B}, however, it is not clear how to choose the value of *c* in this option.

In the previous version of PERSENT, we implemented option three. In that approach we assumed the base isotopes of interest are effectively the same. Focusing on a finite difference modification of the sensitivity function we can write

$$s_\alpha = \frac{\alpha}{R}\frac{\partial R}{\partial \alpha} \approx \frac{\alpha}{R}\frac{R(\alpha + c\cdot\alpha) - R(\alpha)}{c\cdot\alpha} = \frac{R(\alpha + c\cdot\alpha) - R(\alpha)}{c\cdot R}. \quad (3.26)$$

One can quite easily see that $R(\alpha + c\cdot\alpha)$ implies $\sigma_\gamma^{PU239A} \rightarrow \sigma_\gamma^{PU239A} + c\cdot\sigma_\gamma^{PU239A}$ and $\sigma_\gamma^{PU239B} \rightarrow \sigma_\gamma^{PU239B} + c\cdot\sigma_\gamma^{PU239B}$. The other finite difference relations in equations 3.24 and 3.25 have similar forms to equation 3.26. With an explicit derivative now being used in the operator application, we have effectively eliminated options 3 and 4 from being possible.

The derivative of any part of the operator with respect to a given cross section produces a simple delta at the point in the cross section matrix corresponding to the isotope that is flagged as "Pu-239." The α multiplier that appears in equation 3.23 is never computed as the cross section scaling is simply passed into the operator itself. This approach is identical to taking option 1 or 2 separately and adding them together correctly. In effect, by having the ability to apply the derivative properly, the updated version of PERSENT computes the sensitivity of a given isotope as the additive sum of taking the derivative with respect to each specific isotope of that type which is the desired sensitivity result.

To accomplish this, all of the routines in PERSENT had to be rewritten based upon a single isotopic classification setup. This setup is carried out in every PERSENT calculation when a sensitivity is being performed or the kinetics parameters are to be calculated. The entire ISOTXS file is processed to identify each isotope in terms of its origin, typically an ENDF specific assigned label such as PU239_7. All operator applications that require a focused isotopic observation are then setup to focus all work to only consider the impact due to that specific isotope type. In this way, the user only needs to specify a single isotope in the isotope sets for sensitivity operations and PERSENT will automatically treat all similar isotopes in the same manner. The only exception to this rule is cross section perturbations where a specific isotope in the ISOTXS is specified and modified uniquely.

To allow the user to maintain the previous functionality, the input option "TARGET_UNIQUE" was added. Any isotope added to this list will be computed uniquely as implied with option 1 above. By rule, the existing functionality assumes that the regional dependence of the sensitivity vector is of little interest given its inclusion into the uncertainty quantification as a single isotope. By using the new input option, the user can isolate the region dependence of every isotope, i.e. Pu239A, Pu239B, Pu239C,… which will not only appear in the sensitivity vector output, but also in any uncertainty quantification subroutines. There is at

present no ability to recast a sensitivity file from one set of sensitivity vectors to another form (i.e. merge or separate isotopes) as it can be handled properly by just executing the sensitivity calculation again.

3.2 Evaluation of a Reaction Rate Sensitivity

A reaction rate can be generically written as

$$R = \int_{Interest} dV \int d\Omega \int dE\, \Sigma_x(r,E)\psi(r,\Omega,E). \tag{3.27}$$

With regard to a scattering cross section, we can write

$$R = \int_{Interest} dV \int d\Omega' \int dE'\, \Sigma_x(r,\Omega'\to\Omega,E'\to E)\psi(r,\Omega',E'). \tag{3.28}$$

Of the possible options, we consider the reaction rates of the type

$$R = \sum_g \sum_{n\in interest} \Sigma_{x,n,g} \int_n dV \int d\Omega\, \psi_{n,g}(r,\Omega) = \underline{\Sigma}_{x,n}^T \underline{\psi}, \tag{3.29}$$

where Σ_x can refer to (n,γ), (n,fission), and other such reactions. We introduce the vector notation $\underline{\psi}$ which is all space-angle-energy flux moments from all nodes assembled into a single vector. $\underline{\Sigma}_{x,n}$ is used to define the integral quantity of equation 3.27 noting that it has the same vector definition as $\underline{\psi}$ but contains zeros for all nodes that are not of interest. For scattering type reactions, we use

$$R_{g,L} = \sum_{g'} \sum_{n\in interest} \int_n dV\, \Sigma_{x,n,g'\to g} \sum_{m=-L}^{L} \int d\Omega Y_L^m(\Omega)\psi_{n,g'}(r,\Omega) = \underline{\Sigma}_{x,L,g,n}^T \underline{\psi} = \underline{\psi}^T \underline{\Sigma}_{x,L,g,n}, \tag{3.30}$$

where $Y_L^m(\Omega)$ are orthonormal angular trial functions (spherical harmonics). Focusing on the use of equation 3.27 in the sensitivity functional, we need to solve equation 3.11 which takes the following general form:

$$B^*(\alpha,\lambda)\Gamma^* = S^* = \frac{\partial R(\alpha,\psi,\psi^*)}{\partial \psi} = \frac{\partial\left(\underline{\psi}^T \underline{\Sigma}_{x,n}\right)}{\partial \underline{\psi}} = \underline{\Sigma}_{x,n}. \tag{3.31}$$

The orthogonality condition states that $\langle \psi, S^* \rangle = 0 \neq \underline{\psi}^T \underline{\Sigma}_{x,n}$ which is almost certainly not true unless the flux solution is zero in the response region of interest (the sensitivity is zero) or the response itself is zero. In summary, the sensitivity functional is invalid for computing sensitivities to this type of parameter. However, if we change from an eigenvalue problem to a inhomogeneous problem, $B(\alpha,\lambda)\to B(\alpha) = A(\alpha) - W(\alpha)$, the operator on the left hand side is not singular and thus equations (3.11) and (3.12) have a solution for any source distribution. In this case, equation 3.31 is solvable where Γ^* is required to define equation 3.22.

3.3 Evaluation of a Reaction Rate Ratio Sensitivity

The sensitivity of a reaction rate ratio is based upon the localized measurement of a reaction rate ratio

$$R = \frac{\int_{interest} dV \int d\Omega \int dE\, \Sigma_x(r,\Omega,E)\psi(r,\Omega,E)}{\int_{interest} dV \int d\Omega \int dE\, \Sigma_y(r,\Omega,E)\psi(r,\Omega,E)} = \frac{\underline{\Sigma}_{x,n}^T \underline{\psi}}{\underline{\Sigma}_{y,n}^T \underline{\psi}} = \frac{\underline{\psi}^T \underline{\Sigma}_{x,n}}{\underline{\psi}^T \underline{\Sigma}_{y,n}}. \tag{3.32}$$

In this case, the node of interest must contain both the numerator and denominator reaction rates. Focusing on the sensitivity functional for a two node (of interest) example, we can write

$$R = \frac{\underline{\psi}^T \underline{\Sigma}_{c,1} + \underline{\psi}^T \underline{\Sigma}_{c,2}}{\underline{\psi}^T \underline{\Sigma}_{f,1} + \underline{\psi}^T \underline{\Sigma}_{f,2}}. \tag{3.33}$$

with the derivative expressed as

$$\begin{aligned} \frac{\partial R(\alpha,\psi,\psi^*)}{\partial \psi} &= \frac{\frac{\partial}{\partial \underline{\psi}}\left(\underline{\psi}^T \underline{\Sigma}_{c,1} + \underline{\psi}^T \underline{\Sigma}_{c,2}\right)}{\left(\underline{\psi}^T \underline{\Sigma}_{f,1} + \underline{\psi}^T \underline{\Sigma}_{f,2}\right)} - \frac{\left(\underline{\psi}^T \underline{\Sigma}_{c,1} + \underline{\psi}^T \underline{\Sigma}_{c,2}\right)\frac{\partial}{\partial \underline{\psi}}\left(\underline{\psi}^T \underline{\Sigma}_{f,1} + \underline{\psi}^T \underline{\Sigma}_{f,2}\right)}{\left(\underline{\psi}^T \underline{\Sigma}_{f,1} + \underline{\psi}^T \underline{\Sigma}_{f,2}\right)^2} \\ &= \frac{\left(\underline{\Sigma}_{c,1} + \underline{\Sigma}_{c,2}\right)}{\left(\underline{\psi}^T \underline{\Sigma}_{f,1} + \underline{\psi}^T \underline{\Sigma}_{f,2}\right)} - \frac{\left(\underline{\psi}^T \underline{\Sigma}_{c,1} + \underline{\psi}^T \underline{\Sigma}_{c,2}\right)\left(\underline{\Sigma}_{f,1} + \underline{\Sigma}_{f,2}\right)}{\left(\underline{\psi}^T \underline{\Sigma}_{f,1} + \underline{\psi}^T \underline{\Sigma}_{f,2}\right)^2}. \end{aligned} \tag{3.34}$$

In this case, equation 3.32 is not further reducible. Checking the orthogonality restriction $\langle \psi, S^* \rangle = 0$, one finds

$$\langle \psi, S^* \rangle = \frac{\left(\underline{\psi}^T \underline{\Sigma}_{c,1} + \underline{\psi}^T \underline{\Sigma}_{c,2}\right)}{\left(\underline{\psi}^T \underline{\Sigma}_{f,1} + \underline{\psi}^T \underline{\Sigma}_{f,2}\right)} - \frac{\left(\underline{\psi}^T \underline{\Sigma}_{c,1} + \underline{\psi}^T \underline{\Sigma}_{c,2}\right)\left(\underline{\psi}^T \underline{\Sigma}_{f,1} + \underline{\psi}^T \underline{\Sigma}_{f,2}\right)}{\left(\underline{\psi}^T \underline{\Sigma}_{f,1} + \underline{\psi}^T \underline{\Sigma}_{f,2}\right)^2} = 0. \tag{3.35}$$

As can be seen, the functional is valid for this response because the orthogonality condition is met. Noting that the vector notation is just a choice to represent equation 3.29, one finds that the by-node definition of the vector $\underline{\Sigma}_{x,n}$ is a constant which fills the flat (angle and space) moment on a group-wise basis (i.e. each multi-group constant) while a scattering operation provides a single group constant (all other groups are zero) which is also flat by space, but selects a given Legendre moment (i.e. L) in angle. With regard to equation 3.33, the quantity $\underline{\psi}^T \underline{\Sigma}_{c,1} + \underline{\psi}^T \underline{\Sigma}_{c,2}$ is meant to be a complete evaluation of the numerator in equation 3.30 while $\underline{\Sigma}_{f,1} + \underline{\Sigma}_{f,2}$ infers the actual vector definition (sum of two cross section moments).

Equation 3.32 is a rather specific case, but technically equation 3.27 can include a conglomeration of different reactions in the numerator and denominator. After some algebra, one finds that the constraints in equations 3.11 and 3.12 on the sensitivity functional are always satisfied, or, in more general terms, the orthogonality rule is always valid so long as the numerator and denominator are linear with respect to ψ and all contributing terms contain ψ in some form. To complete the derivation, we display the derivative with respect to α,

$$\frac{\partial R(\alpha,\psi,\psi^*)}{\partial \alpha} = \frac{\frac{\partial}{\partial \alpha}\left\{\underline{\psi}^T \underline{\Sigma}_{c,1} + \underline{\psi}^T \underline{\Sigma}_{c,2}\right\}}{\underline{\psi}^T \underline{\Sigma}_{f,1} + \underline{\psi}^T \underline{\Sigma}_{f,2}} - \left(\frac{\underline{\psi}^T \underline{\Sigma}_{c,1} + \underline{\psi}^T \underline{\Sigma}_{c,2}}{\underline{\psi}^T \underline{\Sigma}_{f,1} + \underline{\psi}^T \underline{\Sigma}_{f,2}}\right)\frac{\frac{\partial}{\partial \alpha}\left\{\underline{\psi}^T \underline{\Sigma}_{f,1} + \underline{\psi}^T \underline{\Sigma}_{f,2}\right\}}{\underline{\psi}^T \underline{\Sigma}_{f,1} + \underline{\psi}^T \underline{\Sigma}_{f,2}}. \tag{3.36}$$

The previous approach of using the finite difference formula was removed in the updated PERSENT code and the above derivatives for the reaction rate were implemented as a new subroutine.

We also consider the cumulative ratio response of

$$R = \frac{\underline{\psi}^T \underline{\Sigma}_{c,1}}{\underline{\psi}^T \underline{\Sigma}_{f,1}} + \frac{\underline{\psi}^T \underline{\Sigma}_{c,2}}{\underline{\psi}^T \underline{\Sigma}_{f,2}}, \tag{3.37}$$

which has the derivative

$$\frac{\partial R(\alpha,\psi,\psi^*)}{\partial \psi} = \frac{\frac{\partial}{\partial \underline{\psi}}\left\{\underline{\psi}^T\underline{\Sigma}_{c,1}\right\}}{\underline{\psi}^T\underline{\Sigma}_{f,1}} - \frac{\underline{\psi}^T\underline{\Sigma}_{c,1}}{\underline{\psi}^T\underline{\Sigma}_{f,1}}\frac{\frac{\partial}{\partial \underline{\psi}}\left\{\underline{\psi}^T\underline{\Sigma}_{f,1}\right\}}{\underline{\psi}^T\underline{\Sigma}_{f,1}} + \frac{\frac{\partial}{\partial \underline{\psi}}\underline{\psi}^T\underline{\Sigma}_{c,2}}{\underline{\psi}^T\underline{\Sigma}_{f,2}} - \frac{\underline{\psi}^T\underline{\Sigma}_{c,2}}{\underline{\psi}^T\underline{\Sigma}_{f,2}}\frac{\frac{\partial}{\partial \underline{\psi}}\left\{\underline{\psi}^T\underline{\Sigma}_{f,2}\right\}}{\underline{\psi}^T\underline{\Sigma}_{f,2}}$$
$$= \frac{\underline{\Sigma}_{c,1}}{\underline{\psi}^T\underline{\Sigma}_{f,1}} - \frac{\underline{\psi}^T\underline{\Sigma}_{c,1}}{\underline{\psi}^T\underline{\Sigma}_{f,1}}\frac{\underline{\Sigma}_{f,1}}{\underline{\psi}^T\underline{\Sigma}_{f,1}} + \frac{\underline{\Sigma}_{c,2}}{\underline{\psi}^T\underline{\Sigma}_{f,2}} - \frac{\underline{\psi}^T\underline{\Sigma}_{c,2}}{\underline{\psi}^T\underline{\Sigma}_{f,2}}\frac{\underline{\Sigma}_{f,2}}{\underline{\psi}^T\underline{\Sigma}_{f,2}} \quad . \tag{3.38}$$

In this case one finds that equation 3.38 cannot be simplified further. Checking the orthogonality restriction $\langle \psi, S^* \rangle = 0$, one finds the orthogonality condition is met:

$$\langle \psi, S^* \rangle = \frac{\underline{\psi}^T\underline{\Sigma}_{c,1}}{\underline{\psi}^T\underline{\Sigma}_{f,1}} - \frac{\underline{\psi}^T\underline{\Sigma}_{c,1}}{\underline{\psi}^T\underline{\Sigma}_{f,1}}\frac{\underline{\psi}^T\underline{\Sigma}_{f,1}}{\underline{\psi}^T\underline{\Sigma}_{f,1}} + \frac{\underline{\psi}^T\underline{\Sigma}_{c,2}}{\underline{\psi}^T\underline{\Sigma}_{f,2}} - \frac{\underline{\psi}^T\underline{\Sigma}_{c,2}}{\underline{\psi}^T\underline{\Sigma}_{f,2}}\frac{\underline{\psi}^T\underline{\Sigma}_{f,2}}{\underline{\psi}^T\underline{\Sigma}_{f,2}} = 0 . \tag{3.39}$$

Because equation 3.33 is the typical usage, equation 3.37 is not implemented in the current code.

3.4 Evaluation of the Power Fraction

The sensitivity of a power fraction is based upon the relative measurement of power generation

$$R = \frac{\int_{\text{interest}} dV \int d\Omega \int dE\, PC(r,\Omega,E)\psi(r,\Omega,E)}{\int dV \int d\Omega \int dE\, PC(r,\Omega,E)\psi(r,\Omega,E)} = \frac{\underline{P}_n^T\underline{\psi}}{\underline{P}^T\underline{\psi}} = \frac{\underline{\psi}^T\underline{P}_n}{\underline{\psi}^T\underline{P}}, \tag{3.40}$$

where $PC(r,\Omega,E)$ is the power conversion cross section which includes contributions from capture and fission. This evaluation has a similar setup to the reaction rate ratio and the derivative is expressed as

$$\frac{\partial R(\alpha,\psi,\psi^*)}{\partial \psi} = \frac{\frac{\partial}{\partial \underline{\psi}}\left(\underline{\psi}^T\underline{P}_n\right)}{\underline{\psi}^T\underline{P}} - \frac{\left(\underline{\psi}^T\underline{P}_n\right)\frac{\partial}{\partial \underline{\psi}}\left(\underline{\psi}^T\underline{P}\right)}{\left(\underline{\psi}^T\underline{P}\right)^2} = \frac{\underline{P}_n}{\underline{\psi}^T\underline{P}} - \frac{\left(\underline{\psi}^T\underline{P}_n\right)\underline{P}}{\left(\underline{\psi}^T\underline{P}\right)^2} . \tag{3.41}$$

Given that equation 3.41 is effectively the reaction rate ratio, we know that it already satisfies the orthogonality condition.

3.5 Evaluation of a Reactivity Worth Sensitivity

Consistent with the previous sensitivity examples, we are also interested in the sensitivity of a reactivity worth defined as

$$R = \frac{\left\langle \psi^*, B\left(\hat{\lambda}\right)\hat{\psi}\right\rangle - \left\langle \psi^*, \hat{B}\left(\hat{\lambda}\right)\hat{\psi}\right\rangle}{\left\langle \psi^*, F\,\hat{\psi}\right\rangle} = \frac{\underline{\psi}^{*T}\underline{\underline{B}}\underline{\hat{\psi}} - \underline{\psi}^{*T}\underline{\underline{\hat{B}}}\underline{\hat{\psi}}}{\underline{\psi}^{*T}\underline{\underline{F}}\underline{\hat{\psi}}}, \tag{3.42}$$

where the notation $\underline{\underline{F}}$ refers to a matrix. This response is not consistent with the functional defined in equation 3.2 as the perturbed flux $\hat{\psi}$ and eigenvalue $\hat{\lambda}$ now appear in the system. While under certain conditions we could make use of the same functional, the functional does not include all four states of the perturbed and base system and thus would prevent several reactivity coefficients of interest from being studied. Instead we recognize that equation 3.42 can be written as

$$R = \lambda - \hat{\lambda}, \tag{3.43}$$

which infers that the sensitivities of λ and $\hat{\lambda}$ can be linearly combined:

$$\frac{\partial R}{\partial \alpha} = \frac{\partial \lambda}{\partial \alpha} - \frac{\partial \hat{\lambda}}{\partial \alpha}. \tag{3.44}$$

At issue is that we do not yet have a functional representation for either λ or $\hat{\lambda}$ that includes the cross section. This new representation is obtained by combining equation 2.7 and 2.8 to get:

$$B(\lambda)\psi = 0 \quad \rightarrow \quad A\psi = \lambda F\psi \quad \rightarrow \quad \psi^{*T} A\psi = \lambda \psi^{*T} F\psi \quad \rightarrow \quad \lambda = \frac{\underline{\psi}^{*T} \underline{\underline{A}} \underline{\psi}}{\underline{\psi}^{*T} \underline{\underline{F}} \underline{\psi}}. \tag{3.45}$$

This equation is only valid because of the equivalence in the eigenvalue between the forward and adjoint flux solutions. Note that the perturbed system has an equivalent form using the perturbed operators. Taking equation 3.45 as the basic response of interest, we see that it is perfectly suitable to the functional in equation 3.2 and infers we need two inhomogeneous flux solutions for both the perturbed and base configurations thus a total of eight flux vectors to evaluate the entire system.

We must first verify that the response obeys the limits of the functional beginning with the derivatives in equations 3.11 and 3.12. Starting with equation 3.11 we have

$$\begin{aligned}
&\frac{\partial R}{\partial \underline{\psi}} = \frac{\frac{\partial}{\partial \underline{\psi}}\left\{\underline{\psi}^{*T} \underline{\underline{A}} \underline{\psi}\right\}}{\underline{\psi}^{*T} \underline{\underline{F}} \underline{\psi}} - \frac{\underline{\psi}^{*T} \underline{\underline{A}} \underline{\psi} \frac{\partial}{\partial \underline{\psi}}\left\{\underline{\psi}^{*T} \underline{\underline{F}} \underline{\psi}\right\}}{\underline{\psi}^{*T} \underline{\underline{F}} \underline{\psi} \cdot \underline{\psi}^{*T} \underline{\underline{F}} \underline{\psi}} = \frac{\underline{\psi}^{*T} \underline{\underline{A}}}{\underline{\psi}^{*T} \underline{\underline{F}} \underline{\psi}} - \frac{\underline{\psi}^{*T} \underline{\underline{A}} \underline{\psi} \cdot \underline{\psi}^{*T} \underline{\underline{F}}}{\underline{\psi}^{*T} \underline{\underline{F}} \underline{\psi} \cdot \underline{\psi}^{*T} \underline{\underline{F}} \underline{\psi}} = \underline{S}^{*T} \\
&\underline{S}^{*} = \frac{1}{\underline{\psi}^{*T} \underline{\underline{F}} \underline{\psi}} \underline{\underline{A}}^{*} \underline{\psi}^{*} - \frac{\lambda}{\underline{\psi}^{*T} \underline{\underline{F}} \underline{\psi}} \underline{\underline{F}}^{*} \underline{\psi}^{*} = 0 \\
&\frac{\partial R}{\partial \underline{\psi}^{*}} = \frac{\frac{\partial}{\partial \underline{\psi}^{*}}\left\{\underline{\psi}^{*T} \underline{\underline{A}} \underline{\psi}\right\}}{\underline{\psi}^{*T} \underline{\underline{F}} \underline{\psi}} - \frac{\underline{\psi}^{*T} \underline{\underline{A}} \underline{\psi} \frac{\partial}{\partial \underline{\psi}^{*}}\left\{\underline{\psi}^{*T} \underline{\underline{F}} \underline{\psi}\right\}}{\underline{\psi}^{*T} \underline{\underline{F}} \underline{\psi} \cdot \underline{\psi}^{*T} \underline{\underline{F}} \underline{\psi}} = \frac{\underline{\underline{A}} \underline{\psi}}{\underline{\psi}^{*T} \underline{\underline{F}} \underline{\psi}} - \frac{\underline{\psi}^{*T} \underline{\underline{A}} \underline{\psi} \cdot \underline{\underline{F}} \underline{\psi}}{\underline{\psi}^{*T} \underline{\underline{F}} \underline{\psi} \cdot \underline{\psi}^{*T} \underline{\underline{F}} \underline{\psi}} \\
&\underline{S} = \frac{1}{\underline{\psi}^{*T} \underline{\underline{F}} \underline{\psi}} \underline{\underline{A}} \underline{\psi} - \frac{\lambda}{\underline{\psi}^{*T} \underline{\underline{F}} \underline{\psi}} \underline{\underline{F}} \underline{\psi} = 0
\end{aligned}, \tag{3.46}$$

Given that the sources are zero, we are left with the direct term given as

$$s_{\alpha} = \frac{\alpha}{R} \frac{\partial R(\alpha, \psi, \psi^{*})}{\partial \alpha} = \frac{\alpha}{R} \left\{ \frac{\underline{\psi}^{*T} \frac{\partial \underline{\underline{A}}(\alpha)}{\partial \alpha} \underline{\psi}}{\underline{\psi}^{*T} \underline{\underline{F}} \underline{\psi}} - \frac{\underline{\psi}^{*T} \underline{\underline{A}} \underline{\psi} \cdot \underline{\psi}^{*T} \frac{\partial \underline{\underline{F}}(\alpha)}{\partial \alpha} \underline{\psi}}{\underline{\psi}^{*T} \underline{\underline{F}} \underline{\psi} \cdot \underline{\psi}^{*T} \underline{\underline{F}} \underline{\psi}} \right\}. \tag{3.47}$$

The finite difference relation is used to evaluate the remaining derivative such that we have

$$\begin{aligned}
s_{\alpha} &= \frac{1}{R} \frac{\underline{\psi}^{*T} \left\{ \underline{\underline{A}}(\alpha + c \cdot \alpha) - \underline{\underline{A}}(\alpha) \right\} \underline{\psi}}{c \cdot \underline{\psi}^{*T} \underline{\underline{F}} \underline{\psi}} - \lambda \frac{\underline{\psi}^{*T} \left\{ \underline{\underline{F}}(\alpha + c \cdot \alpha) - \underline{\underline{F}}(\alpha) \right\} \underline{\psi}}{c \cdot \underline{\psi}^{*T} \underline{\underline{F}} \underline{\psi}} \\
&= \frac{1}{c \cdot \lambda} \frac{\underline{\psi}^{*T} \left\{ \underline{\underline{B}}(\alpha + c \cdot \alpha, \lambda) - \underline{\underline{B}}(\alpha, \lambda) \right\} \underline{\psi}}{\underline{\psi}^{*T} \underline{\underline{F}} \underline{\psi}}
\end{aligned}. \tag{3.48}$$

It is important to note that since the response is the eigenvalue, we can reintroduce the original operator in equation 3.48. We neglect the first order reactivity worth evaluation given the problems noted earlier by assuming the user can reproduce the first order perturbation result using exact perturbation theory.

3.6 Evaluation of the Prompt Neutron Lifetime and Beta Effective Sensitivity

The prompt neutron lifetime and Beta effective computations are done almost identically to the preceding reactivity worth case in equation 3.45. We have two components to consider: the neutron generation lifetime Λ_G and prompt neutron lifetime Λ. Focusing on the former, we have the response defined as

$$R = \frac{\left\langle \psi^*, \nu^{-1} H\psi \right\rangle}{\left\langle \psi^*, F\psi \right\rangle} = \frac{\underline{\psi}^{*T} \underline{\underline{H}} \underline{\psi}}{\underline{\psi}^{*T} \underline{\underline{F}} \underline{\psi}}, \tag{3.49}$$

which has the derivatives

$$\frac{\partial R}{\partial \underline{\psi}} = \underline{S}^{*T} = \frac{\left\{\underline{\psi}^{*T} \underline{\underline{F}} \underline{\psi}\right\} \frac{\partial}{\partial \underline{\psi}} \left\{\underline{\psi}^{*T} \underline{\underline{H}} \underline{\psi}\right\} - \left\{\underline{\psi}^{*T} \underline{\underline{H}} \underline{\psi}\right\} \frac{\partial}{\partial \underline{\psi}} \left\{\underline{\psi}^{*T} \underline{\underline{F}} \underline{\psi}\right\}}{\left\{\underline{\psi}^{*T} \underline{\underline{F}} \underline{\psi}\right\}^2},$$

$$\underline{S}^* = \frac{\left\{\underline{\psi}^{*T} \underline{\underline{F}} \underline{\psi}\right\} \left\{\underline{\underline{H}}^T \underline{\psi}^*\right\} - \left\{\underline{\psi}^{*T} \underline{\underline{H}} \underline{\psi}\right\} \left\{\underline{\underline{F}}^T \underline{\psi}^*\right\}}{\left\{\underline{\psi}^{*T} \underline{\underline{F}} \underline{\psi}\right\}^2}, \tag{3.50}$$

$$\frac{\partial R}{\partial \underline{\psi}^*} = \underline{S} = \frac{\left\{\underline{\psi}^{*T} \underline{\underline{F}} \underline{\psi}\right\} \left\{\underline{\underline{H}} \underline{\psi}\right\} - \left\{\underline{\psi}^{*T} \underline{\underline{H}} \underline{\psi}\right\} \left\{\underline{\underline{F}} \underline{\psi}\right\}}{\left\{\underline{\psi}^{*T} \underline{\underline{F}} \underline{\psi}\right\}^2},$$

By inspection one can see this response meets the orthogonality conditions of the sensitivity functional. The response for the prompt neutron lifetime is

$$R = \Lambda = \frac{1}{\lambda} \frac{\left\langle \psi^*, \nu^{-1} H\psi \right\rangle}{\left\langle \psi^*, F\psi \right\rangle} = \frac{\left\langle \psi^*, F\psi \right\rangle}{\left\langle \psi^*, A\psi \right\rangle} \frac{\left\langle \psi^*, \nu^{-1} H\psi \right\rangle}{\left\langle \psi^*, F\psi \right\rangle} = \frac{\underline{\psi}^{*T} \underline{\underline{F}} \underline{\psi}}{\underline{\psi}^{*T} \underline{\underline{A}} \underline{\psi}} \frac{\underline{\psi}^{*T} \underline{\underline{H}} \underline{\psi}}{\underline{\psi}^{*T} \underline{\underline{F}} \underline{\psi}}. \tag{3.51}$$

From here one can see that the derivatives appearing in equation 3.50 will be fundamentally different than those for equation 3.51:

$$\frac{\partial R}{\partial \underline{\psi}} = \underline{S}^{*T} = \Lambda_G \frac{\partial}{\partial \underline{\psi}} \frac{\underline{\psi}^{*T} \underline{\underline{F}} \underline{\psi}}{\underline{\psi}^{*T} \underline{\underline{A}} \underline{\psi}} + \frac{1}{\lambda} \frac{\partial}{\partial \underline{\psi}} \frac{\underline{\psi}^{*T} \underline{\underline{H}} \underline{\psi}}{\underline{\psi}^{*T} \underline{\underline{F}} \underline{\psi}}$$

$$\underline{S}^* = \Lambda_G \left\{ \cancel{\frac{\underline{\underline{F}}^T \underline{\psi}^*}{\underline{\psi}^{*T} \underline{\underline{A}} \underline{\psi}} - \frac{1}{\lambda} \frac{\underline{\underline{A}}^T \underline{\psi}^*}{\underline{\psi}^{*T} \underline{\underline{A}} \underline{\psi}}} \right\} + \frac{1}{\lambda} \left\{ \frac{\underline{\underline{H}}^T \underline{\psi}^*}{\underline{\psi}^{*T} \underline{\underline{F}} \underline{\psi}} - \Lambda_G \frac{\underline{\underline{F}}^T \underline{\psi}^*}{\underline{\psi}^{*T} \underline{\underline{F}} \underline{\psi}} \right\} \quad . \tag{3.52}$$

$$\frac{\partial R}{\partial \underline{\psi}^*} = \underline{S} = \Lambda_G \left\{ \cancel{\frac{\underline{\underline{F}} \underline{\psi}}{\underline{\psi}^{*T} \underline{\underline{A}} \underline{\psi}} - \frac{1}{\lambda} \frac{\underline{\underline{A}} \underline{\psi}}{\underline{\psi}^{*T} \underline{\underline{A}} \underline{\psi}}} \right\} + \frac{1}{\lambda} \left\{ \frac{\underline{\underline{H}} \underline{\psi}}{\underline{\psi}^{*T} \underline{\underline{F}} \underline{\psi}} - \Lambda_G \frac{\underline{\underline{F}} \underline{\psi}}{\underline{\psi}^{*T} \underline{\underline{F}} \underline{\psi}} \right\}$$

Note that the two terms highlighted for elimination in equation 3.52 are by definition zero and would not contribute to the fixed sources. Given that the only remaining difference is the scaling by eigenvalue, we do not need to perform fixed source computations for both Λ and Λ_G in order to get the complete sensitivity. Further inspection shows that the sensitivity of Λ can be determined as

$$s_\alpha^\Lambda = \frac{\alpha}{\Lambda}\frac{\partial R^\Lambda}{\partial \alpha} = \frac{\alpha}{\Lambda}\Lambda_G \frac{\partial}{\partial \alpha}\frac{\underline{\psi}^{*T}\underline{\underline{F}}\underline{\psi}}{\underline{\psi}^{*T}\underline{\underline{A}}\underline{\psi}} + \frac{1}{\lambda}\frac{\alpha}{\Lambda}\frac{\partial}{\partial \alpha}\frac{\underline{\psi}^{*T}\underline{\underline{H}}\underline{\psi}}{\underline{\psi}^{*T}\underline{\underline{F}}\underline{\psi}}$$

$$= \alpha\lambda\left\{\frac{\underline{\psi}^{*T}\frac{\partial \underline{\underline{F}}}{\partial \alpha}\underline{\psi}}{\underline{\psi}^{*T}\underline{\underline{A}}\underline{\psi}} - \frac{1}{\lambda}\frac{\underline{\psi}^{*T}\frac{\partial \underline{\underline{A}}}{\partial \alpha}\underline{\psi}}{\underline{\psi}^{*T}\underline{\underline{A}}\underline{\psi}}\right\} + \frac{\alpha}{\Lambda_G}\left\{\frac{\underline{\psi}^{*T}\frac{\partial \underline{\underline{H}}}{\partial \alpha}\underline{\psi}}{\underline{\psi}^{*T}\underline{\underline{F}}\underline{\psi}} - \Lambda_G\frac{\underline{\psi}^{*T}\frac{\partial \underline{\underline{F}}}{\partial \alpha}\underline{\psi}}{\underline{\psi}^{*T}\underline{\underline{F}}\underline{\psi}}\right\} \tag{3.53}$$

$$s_\alpha^\Lambda = \alpha\left\{\lambda\frac{\underline{\psi}^{*T}\frac{\partial \underline{\underline{F}}}{\partial \alpha}\underline{\psi}}{\lambda\underline{\psi}^{*T}\underline{\underline{F}}\underline{\psi}} - \frac{\underline{\psi}^{*T}\frac{\partial \underline{\underline{A}}}{\partial \alpha}\underline{\psi}}{\lambda\underline{\psi}^{*T}\underline{\underline{F}}\underline{\psi}}\right\} + s_\alpha^{\Lambda_G} = -s_\alpha^\lambda + s_\alpha^{\Lambda_G}.$$

where the eigenvalue sensitivity shown earlier in equation 3.47 now appears linearly with the sensitivity of Λ_G. We leave the solution of equation 3.53 for the user to compute and did not make it part of the computation in PERSENT.

The response for Beta is slightly more difficult, noting that it is typically broken down into delay family (m) and isotope (i) as shown earlier in equation 2.27.

$$R_{i,m} = \frac{N_i\left\langle \psi^*, F_{i,m}\psi\right\rangle}{\left\langle \psi^*, F\psi\right\rangle} = \frac{\underline{\psi}^{*T}\underline{\underline{F}}_{i,m}\underline{\psi}}{\underline{\psi}^{*T}\underline{\underline{F}}\underline{\psi}} \tag{3.54}$$

Taking the derivatives, we have

$$\underline{S}^* = \frac{\left\{\underline{\psi}^{*T}\underline{\underline{F}}\underline{\psi}\right\}\left\{\underline{\underline{F}}_{i,m}^T\underline{\psi}^*\right\} - \left\{\underline{\psi}^{*T}\underline{\underline{F}}_{i,m}\underline{\psi}\right\}\left\{\underline{\underline{F}}^T\underline{\psi}^*\right\}}{\left\{\underline{\psi}^{*T}\underline{\underline{F}}\underline{\psi}\right\}^2}$$

$$\underline{S} = \frac{\left\{\underline{\psi}^{*T}\underline{\underline{F}}\underline{\psi}\right\}\left\{\underline{\underline{F}}_{i,m}\underline{\psi}\right\} - \left\{\underline{\psi}^{*T}\underline{\underline{F}}_{i,m}\underline{\psi}\right\}\left\{\underline{\underline{F}}\underline{\psi}\right\}}{\left\{\underline{\psi}^{*T}\underline{\underline{F}}\underline{\psi}\right\}^2}, \tag{3.55}$$

both of which meet the orthogonality rule. At issue of course is that this infers that an inhomogeneous flux calculation must be performed for each family of each isotope which is impractical. Noting the denominator in equation 3.55 is constant for all families of all isotopes, we can choose to compute the sensitivity to the component sums (such as all U-235 in the geometry) which implies a sum

$$R_{^{235}U} = \sum_{i\in{}^{235}U}\sum_m \frac{N_i\left\langle \psi^*, F_{i,m}\psi\right\rangle}{\left\langle \psi^*, F\psi\right\rangle} = \sum_{i\in{}^{235}U}\sum_m \frac{\underline{\psi}^{*T}\underline{\underline{F}}_{i,m}\underline{\psi}}{\underline{\psi}^{*T}\underline{\underline{F}}\underline{\psi}}. \tag{3.56}$$

Even with this reduced form, there are about 20 actinides of interest in the domain and thus we would still need to perform 40 inhomogeneous flux calculations. The standard approach in VARI3D is to define an approximate form where the breakdown by isotope and family is only done using the direct term

$$s_{\alpha,i,m}(x) \approx \frac{\alpha(x)}{R_{i,m}}\frac{\partial R_{i,m}(\alpha,\psi,\psi^*)}{\partial \alpha}. \tag{3.57}$$

This is primarily done because Beta effective is the only useable (measurable) quantity which defines the response

$$R_{^{235}U} = \frac{\sum_i \sum_m N_i \left\langle \psi^*, F_{i,m}\psi \right\rangle}{\left\langle \psi^*, F\psi \right\rangle} = \frac{\sum_i \sum_m \underline{\psi}^{*T} \underline{\underline{F}}_{i,m} \underline{\psi}}{\underline{\psi}^{*T} \underline{\underline{F}} \underline{\psi}}. \quad (3.58)$$

The derivative appearing in equation 3.57 becomes the functional result for the response defined by equation 3.54 and thus a sum of the derivatives with respect to isotope and family to construct the full sensitivity. The source in equation 3.55 is taken to be the sum over all isotopes and families which contributes the relative fraction to any given delay family of a given isotope.

3.7 Other Sensitivity Options

VARI3D, being an older tool, also includes sensitivity options for a specific breeding ratio (i.e. a depletion-related quantity), adjoint reaction rate ratio, inverse reaction rate (inhomogeneous problems only), and a bilinear weighted reaction rate ratio. While all of these are possible with PERSENT, they were not added at this time due to the lack of practical need (i.e. there are no meaningful uses proposed). If needed, contact nera-software@anl.gov for support on any of these options noting that a generic breeding ratio option would require significant changes to the existing input structure.

3.8 Alternative Sensitivity Evaluation for Reactivity Worth

Because of the expense associated with the inhomogeneous systems above, any alternative idea should be considered if viable and more efficient. In the case of reactivity worth and reaction rate ratios, the equivalent generalized perturbation theory (EGPT) methodology has been devised [15,24]. The basic idea is that for reactivity worth, the fixed source appearing in the inhomogeneous problem can be approximately eliminated by using the perturbed forward and adjoint flux solutions. EGPT is mostly found by redefining the previous functional into one on the relative reactivity worth

$$\rho = \frac{\underline{\psi}^{*T} \underline{\underline{B}}\left(\hat{\lambda}\right) \hat{\underline{\psi}} - \underline{\psi}^{*T} \hat{\underline{\underline{B}}}\left(\hat{\lambda}\right) \hat{\underline{\psi}}}{\underline{\psi}^{*T} \underline{\underline{F}} \hat{\underline{\psi}}} = \rho_0 (1+f) = \frac{\underline{\psi}^{*T} \underline{\underline{B}}(\lambda) \underline{\psi} - \underline{\psi}^{*T} \hat{\underline{\underline{B}}}(\lambda) \underline{\psi}}{\underline{\psi}^{*T} \underline{\underline{F}} \underline{\psi}} (1+f). \quad (3.59)$$

where ρ_0 is the first order perturbation theory result and f is a correction factor. This leads to considerable changes in the results. For example, the Γ^* equation is modified:

$$\hat{B}^*(\alpha,\lambda)\Gamma^* = S^* = \frac{\partial R(\alpha,\psi,\psi^*)}{\partial \psi}. \quad (3.60)$$

The remaining parts of the derivation are beyond the scope of this manuscript. The reported equation to implement in EGPT is given in [15] as

$$s_\alpha(x) = \frac{\alpha(x)}{\rho}\left[\frac{\underline{\psi}^{*T} \underline{\underline{F}} \hat{\underline{\psi}}}{\underline{\psi}^{*T} \hat{\underline{\underline{F}}} \hat{\underline{\psi}} \cdot \underline{\psi}^{*T} \underline{\underline{F}} \underline{\psi}} \cdot \underline{\psi}^{*T} \frac{\partial \underline{\underline{B}}(\alpha,\lambda)}{\partial \alpha} \underline{\psi} - \frac{1}{\hat{\underline{\psi}}^{*T} \hat{\underline{\underline{F}}} \hat{\underline{\psi}}} \hat{\underline{\psi}}^{*T} \frac{\partial \hat{\underline{\underline{B}}}\left(\alpha,\hat{\lambda}\right)}{\partial \alpha} \hat{\underline{\psi}}\right] \quad (3.61)$$

which has a "first order" approximation of

$$s_\alpha(x) = \frac{\alpha(x)}{\rho}\left[\frac{1}{\underline{\psi}^{*T} \underline{\underline{F}} \underline{\psi}} \cdot \underline{\psi}^{*T} \frac{\partial \underline{\underline{B}}(\alpha,\lambda)}{\partial \alpha} \underline{\psi} - \frac{1}{\hat{\underline{\psi}}^{*T} \hat{\underline{\underline{F}}} \hat{\underline{\psi}}} \hat{\underline{\psi}}^{*T} \frac{\partial \hat{\underline{\underline{B}}}\left(\alpha,\hat{\lambda}\right)}{\partial \alpha} \hat{\underline{\psi}}\right]. \quad (3.62)$$

Reference 15 further infers that equation 3.62 "can be interpreted as" the common finite difference relationship for the sensitivity:

$$s_\alpha(x) \sim \frac{\alpha}{\rho(\alpha)}\left\{\frac{\rho(\alpha+c\cdot\alpha)-\rho(\alpha)}{c\cdot\alpha}\right\} = \frac{\rho(\alpha+c\cdot\alpha)}{c\cdot\rho(\alpha)} - \frac{1}{c}. \tag{3.63}$$

Writing out the combination of two independent eigenvalue sensitivities, we can write the sensitivity of the reactivity worth as

$$s_\alpha = s_{\alpha,\lambda} - s_{\alpha,\hat{\lambda}} = \left\{ \frac{\alpha}{\lambda} \frac{\underline{\psi}^{*T} \frac{\partial \underline{\underline{B}}(\alpha,\lambda)}{\partial\alpha} \underline{\psi}}{\underline{\psi}^{*T} \underline{\underline{F}} \underline{\psi}} - \frac{\alpha}{\hat{\lambda}} \frac{\hat{\underline{\psi}}^{*T} \frac{\partial \hat{\underline{\underline{B}}}(\alpha,\hat{\lambda})}{\partial\alpha} \hat{\underline{\psi}}}{\hat{\underline{\psi}}^{*T} \hat{\underline{\underline{F}}} \hat{\underline{\psi}}} \right\}. \tag{3.64}$$

By inspection, one can see how to obtain the EGPT equivalent result using just the eigenvalue sensitivities. Because of problems with the preceding variational functional approach, we have only implemented the combined eigenvalue sensitivity approach for evaluating the reactivity worths. This is primarily based upon user feedback [27] which clearly indicated that independent eigenvalue sensitivities were the preferred approach.

3.9 Alternative Treatments for Fission Spectrum Sensitivity

Much like many older neutronics codes, the DIF3D code does not handle the fission source operator in the correct way, particularly the fission spectrum $\underline{\chi}$. If we look at the multi-group collapsing schemes, we find that all lattice codes start with a high number of energy groups where each isotope i has its own $\underline{\chi}_i$ to account for the different energy spectrum of the neutrons created by the fission process. Similarly, each isotope has an evaluated production $\underline{\nu}_i$ per fission and fission cross section $\underline{\sigma}_{f,i}$ along with other microscopic reaction cross sections. In conventional transport codes, we formulate everything in terms of macroscopic compositions because each region has a mixture of isotopes contained within it. For each unique mixture in the domain, we use the formulas:

$$\underline{\Sigma}_f = \sum_{i=1}^{Isotopes} N_i \underline{\sigma}_{f,i} \tag{3.65}$$

$$\nu_g \Sigma_{f,g} = \sum_{i=1}^{Isotopes} N_i \nu_{i,g} \sigma_{f,i,g} \tag{3.66}$$

$$\chi_{g,g'} \nu_{g'} \Sigma_{f,g'} = \sum_{i=1}^{Isotopes} N_i \chi_{i,g,g'} \nu_{i,g'} \sigma_{f,i,g'} \tag{3.67}$$

where N_i is the atom density of each isotope in the mixture. Use of these equations is required to ensure that the reaction rates are preserved on this level. Of these, equation 3.67 is the contentious one as almost all old codes like DIF3D assume the product can be separated into equation 3.66 and a "zone" $\underline{\chi}$ when solving the diffusion or transport equations. In most older codes, a zone $\underline{\chi}$ is defined using

$$\chi_{g,g'} = \frac{\sum_{i=1}^{Isotopes} \chi_{i,g,g'} \sum_{g"=1}^{G} N_i \nu_{i,g"} \sigma_{f,i,g"} \varphi_{g"}}{\sum_{i=1}^{Isotopes} \sum_{g"=1}^{G} N_i \nu_{i,g"} \sigma_{f,i,g"} \varphi_{g"}}, \tag{3.68}$$

where $\varphi_{g"}$ is the multigroup flux for this region from the lattice code. Equation 3.68 is then combined with equation 3.66 and has historically been found to be more than sufficient for most neutronics calculations. Of course the accuracy is only an illusion as it inherently relies upon the near consistency in the distribution of $\underline{\chi}_i$ among the various isotopes. This is rather easy to see by comparing the supposed equivalence between the two approaches

$$\frac{\sum_{i=1}^{Isotopes}\chi_{i,g,g'}\sum_{g"=1}^{G}N_i\nu_{i,g"}\sigma_{f,i,g"}\varphi_{g"}}{\sum_{i=1}^{Isotopes}\sum_{g"=1}^{G}N_i\nu_{i,g"}\sigma_{f,i,g"}\varphi_{g"}}\sum_{i=1}^{Isotopes}N_i\nu_{i,g'}\sigma_{f,i,g'}\approx\sum_{i=1}^{Isotopes}N_i\chi_{i,g,g'}\nu_{i,g'}\sigma_{f,i,g'}\,. \tag{3.69}$$

In DIF3D, and thus PERSENT, an additional approximation is made to equation 3.68 as the lattice fluxes are not available. This is particularly problematic to evaluating the $\underline{\chi}$ sensitivity as will be shown shortly. In DIF3D, equation 3.68 is replaced by

$$\chi_{g,g'}=\frac{\sum_{i=1}^{Isotopes}\chi_{i,g,g'}\sum_{g"=1}^{G}N_i\nu_{i,g"}\sigma_{f,i,g"}}{\sum_{i=1}^{Isotopes}\sum_{g"=1}^{G}N_i\nu_{i,g"}\sigma_{f,i,g"}}, \tag{3.70}$$

which can be considerably in error depending upon the spectrum of the reactor system of interest. To explain fully, we consider the two group, two isotope (U-235 and U-238) case of equation 3.70 written as

$$\chi_{g,g'}=\frac{N^{U235}\chi_{g,g'}^{U235}\left(\nu_1^{U235}\sigma_{f,1}^{U235}+\nu_2^{U235}\sigma_{f,2}^{U235}\right)+N^{U238}\chi_{g,g'}^{U238}\left(\nu_1^{U238}\sigma_{f,1}^{U238}+\nu_2^{U238}\sigma_{f,2}^{U238}\right)}{N^{U235}\left(\nu_1^{U235}\sigma_{f,1}^{U235}+\nu_2^{U235}\sigma_{f,2}^{U235}\right)+N^{U238}\left(\nu_1^{U238}\sigma_{f,1}^{U238}+\nu_2^{U238}\sigma_{f,2}^{U238}\right)}. \tag{3.71}$$

Expanding equations 3.66 and 3.67 we have

$$\begin{aligned}\nu_g\Sigma_{f,g}&=N^{U235}\nu_g^{U235}\sigma_{f,g}^{U235}+N^{U238}\nu_g^{U238}\sigma_{f,g}^{U238}\\ \chi_{g,g'}\nu_{g'}\Sigma_{f,g'}&=N^{U235}\chi_{g,g'}^{U235}\nu_{g'}^{U235}\sigma_{f,g'}^{U235}+N^{U238}\chi_{g,g'}^{U238}\nu_{g'}^{U238}\sigma_{f,g'}^{U238}\end{aligned}. \tag{3.72}$$

Knowing that equation 3.72 is the exact answer, it is rather easy to see that the alternate DIF3D form cannot be made consistent.

From here we look at the desired sensitivity of $\chi_{g,g'}^{U235}$ for this simple example which requires us to evaluate

$$\frac{\partial}{\partial\chi_{g,g'}^{U235}}\chi_{g,g'}\nu_{g'}\Sigma_{f,g'}=N^{U235}\nu_{g'}^{U235}\sigma_{f,g'}^{U235}\,. \tag{3.73}$$

The answer given in equation 3.73 is obviously the result of using the correct implementation of equation 3.67. Looking at the DIF3D implementation in equation 3.70, we obtain

$$\frac{\partial}{\partial\chi_{g,g'}^{U235}}\chi_{g,g'}\nu_{g'}\Sigma_{f,g'}=\frac{N^{U235}\chi_{g,g'}^{U235}\left(\nu_1^{U235}\sigma_{f,1}^{U235}+\nu_2^{U235}\sigma_{f,2}^{U235}\right)\left(N^{U235}\nu_{g'}^{U235}\sigma_{f,g'}^{U235}+N^{U238}\nu_{g'}^{U238}\sigma_{f,g'}^{U238}\right)}{N^{U235}\left(\nu_1^{U235}\sigma_{f,1}^{U235}+\nu_2^{U235}\sigma_{f,2}^{U235}\right)+N^{U238}\left(\nu_1^{U238}\sigma_{f,1}^{U238}+\nu_2^{U238}\sigma_{f,2}^{U238}\right)}. \tag{3.74}$$

This is clearly not the same as equation 3.73 and one can now see that the sensitivities computed using equation 3.70 will never be the correct ones. Moreover, there is no simple factor that can be provided by PERSENT to convert the computed results of equation 3.74 into the desired results of equation 3.73.

Based upon our numerical results on real reactor problems, differences of over an order of magnitude were observed between equations 3.67 and 3.70 for $\underline{\chi}$ sensitivities. From inspection of equation 3.70, it should be apparent that the basic issue is that the compositional chi approach is applied to the fission production contribution from all isotopes as opposed to just the isotope of interest. This means using a classic finite difference approach where the input to DIF3D is modified, assigned CHI_FD in PERSENT, will always produce incorrect sensitivities. To correct the issue requires us to compute the correct sensitivity by using equation 3.67 and thus equation 3.72 to get the equation 3.73 result. This poses an additional problem in that the total fission production source that DIF3D computes (i.e. the wrong one) and the one given by equation 3.67 (i.e. the right one) will not agree. This means the total contribution from all isotopes will not sum to unity, but to the ratio of the correct fission production operator divided by the DIF3D one. Thus the CHI labeled sensitivity in all sensitivity options of PERSENT is modified to make use of the following expression:

$$\frac{\partial}{\partial \chi_{i,g}} \left\langle \bar{\psi}^*, \bar{\chi}_C \cdot \sum_{i=1}^{Isotopes} N_i \cdot \bar{\nu\Sigma}_{f,i} \cdot \bar{\psi} \right\rangle \rightarrow \frac{\left\langle \bar{\psi}^*, \bar{\chi}_C \cdot \sum_{i=1}^{Isotopes} N_i \cdot \bar{\nu\Sigma}_{f,i} \cdot \bar{\psi} \right\rangle}{\left\langle \bar{\psi}^*, \sum_{i=1}^{Isotopes} N_i \cdot \bar{\chi}_i \cdot \bar{\nu\Sigma}_{f,i} \cdot \bar{\psi} \right\rangle} \frac{\partial}{\partial \chi_{i,g}} \left\langle \bar{\psi}^*, \sum_{i=1}^{Isotopes} N_i \cdot \bar{\chi}_i \cdot \bar{\nu\Sigma}_{f,i} \cdot \bar{\psi} \right\rangle . \quad (3.75)$$

In equation 3.75, $\bar{\chi}_C$ is the compositional one used in DIF3D defined by equation 3.70 and $\bar{\chi}_i$ is the isotopic one. This sensitivity in PERSENT is labeled (CHI) and is as close as one can get to the correct one as it takes the derivative of the correct operator and then normalizes it to be consistent with the actual fission source operator of DIF3D. While this sensitivity is also inaccurate, it is much more reasonable compared with codes that do not use the compositional fission spectrum approach.

3.10 Prompt Neutron Lifetime and Delayed Neutron Fraction Alterations

Similar to the modifications for the perturbation theory operations, we must also redefine the prompt neutron lifetime and delayed neutron fraction. The delayed neutron fraction is quite easy as it only depends upon the scalar flux and can be compactly written as

$$\beta = \frac{\sum_{i}^{isotopes} N_i \sum_{m}^{delay\ families} \left\langle \underline{\phi}^*, \underline{\underline{F}}_{i,m} \underline{\phi} \right\rangle}{\left\langle \underline{\phi}^*, \underline{\underline{F}} \underline{\phi} \right\rangle}, \quad (3.76)$$

The prompt neutron lifetime is considerably more complicated as we must first express equation 2.25 in terms of the even- and odd-parity flux vectors as

$$\begin{aligned}\frac{1}{v(E)}\frac{\partial \psi^{+}(r,E,\hat{\Omega},t)}{\partial t}+\nabla\cdot\hat{\Omega}\psi^{-}(r,E,\hat{\Omega},t)+\Sigma_t(r,E)\psi^{+}(r,E,\hat{\Omega},t)=S^{+}(r,E,\hat{\Omega},t)\\ \frac{1}{v(E)}\frac{\partial \psi^{-}(r,E,\hat{\Omega},t)}{\partial t}+\nabla\cdot\hat{\Omega}\psi^{+}(r,E,\hat{\Omega},t)+\Sigma_t(r,E)\psi^{-}(r,E,\hat{\Omega},t)=S^{-}(r,E,\hat{\Omega},t)\end{aligned}. \quad (3.77)$$

One should note the time derivative of the odd-parity flux further complicates the use of the new cross section matrix in equation 2.54. Whether one uses an explicit or implicit time formulation of equation 3.77, one finds that the $\frac{1}{v(E)}$ factor is always present in the odd-parity system. Looking back at equation 2.25, one should account for this aspect. Unlike the preceding perturbation theory component, for simplicity, we choose to retain the even- and odd-parity representations above thereby making the prompt neutron lifetime computed using

$$\Lambda=\frac{1}{\lambda}\frac{\left\langle \underline{\psi}^{+,*},\underline{\underline{v}}^{+}\otimes F\underline{\psi}^{+}\right\rangle+\left\langle \underline{\psi}^{-,*},\underline{\underline{v}}^{-}\otimes F\underline{\psi}^{-}\right\rangle}{\left\langle \underline{\psi}^{+,*},\underline{\underline{F}}\underline{\psi}^{+}\right\rangle}\approx\frac{1}{\lambda}\frac{\left\langle \underline{\phi}^{*},\underline{\underline{v}}\otimes F\underline{\phi}\right\rangle}{\left\langle \underline{\phi}^{*},\underline{\underline{F}}\underline{\phi}\right\rangle}, \quad (3.78)$$

where the new angle-energy matrix is given as

$$\underline{\underline{v}}^{\pm}=\begin{bmatrix} v_1^{-1}I^{\pm} & 0 & 0\\ 0 & \ddots & 0\\ 0 & 0 & v_g^{-1}I^{\pm}\end{bmatrix}. \quad (3.79)$$

Note that there is no connection between the even- and odd-parity moments as the angular functions are orthogonal to each other. The diffusion theory approximation is introduced above as one finds that Λ does not depend strongly on transport effects as there are not substantial streaming paths in real reactor systems. It is important to note that even in such a system, the diffusive component will still dominate the total value of Λ.

3.11 Uncertainty Computation Capabilities of PERSENT

PERSENT can be used to produce the various cross section sensitivities discussed in Section 3.2 through 3.8. To fully use them, we require the ability to introduce a covariance matrix and apply it to a selection of sensitivity vectors. To manage that in PERSENT, we defined new inputs consistent with the COMMARA matrix although we generalized them in the most recent version to handle any correlation between reaction and isotope that can be conceived within the PERSENT accepted set of reactions (see later sections on input).

Given a co-variance matrix D, one can construct a general calculation capability of

$$u=\sqrt{s_1^T\cdot D\cdot s_2}\,. \quad (3.80)$$

If one specifies the two sensitivity vectors s_1 and s_2 to be the same, one obtains the uncertainty for the given parameter (associated with the sensitivity vector) due to the cross section uncertainties as specified by the co-variance matrix. The option to apply equation 3.80 for two different sensitivity vectors on the same reactor (likely associated with two different parameters) is straightforward. This is commonly used in propagation of uncertainties. The option to apply equation 3.80 for sensitivity vectors from two different reactors is straightforward but requires the sensitivity vector from one problem to be stored in an ascii data file. This is most often done in representativity calculations.

In the output, PERSENT will optionally provide the row-wise collapse of equation 3.80 for a given group, isotope, and reaction, for the column-wise accumulation over group for a given isotope and reaction as is consistently done in other sensitivity codes. Or, in equation form it will print

$$u_{g,r,i,r',i'} = \sqrt{\sum_{g'} s_{1,g,r,i} \cdot D_{g,r,i,g',r',i'} \cdot s_{2,g',r',i'}}\,, \tag{3.81}$$

where g is group, i is isotope, and r is reaction. This represents the uncertainty contribution from one reaction of one isotope to a given group of a reaction for a given isotope. Because the fractional component of equation 3.80 can easily be negative, PERSENT will provide the output in imaginary number notation as appropriate. PERSENT will also optionally provide a row-wise collapse of equation 3.80 giving the isotope, reaction, and group uncertainty breakdown or

$$u_{g,r,i} = \sqrt{\sum_{g',r',i'} s_{1,g,r,i} \cdot D_{g,r,i,g',r',i'} \cdot s_{2,g',r',i'}}\,. \tag{3.82}$$

For debugging purpose, PERSENT optionally provides an isotope to isotope summary table which can be easily used to check the co-variance matrix data. This output is not standard in other sensitivity codes but given by PERSENT as

$$u_{i,i'} = \sqrt{\sum_{g,r,g',r'} s_{1,g,r,i} \cdot D_{g,r,i,g',r',i'} \cdot s_{2,g',r',i'}}\,. \tag{3.83}$$

As part of the standard output, PERSENT will give the reaction breakdown summary table defined by

$$u_{i,r'} = \sqrt{\sum_{g,r,g',i'} s_{1,g,r,i} \cdot D_{g,r,i,g',r',i'} \cdot s_{2,g',r',i'}}\,. \tag{3.84}$$

This output is quite standard for uncertainty assessments as is the final output of equation 3.80 itself.

The addition of the uncertainty quantification calculation within PERSENT completes the functionality needed for most sensitivity vector usages and eliminates the auxiliary executable that was provided in previous distributions. Internally, PERSENT loads the co-variance matrix as a unique operation and will automatically try to link both the reaction names and isotope names with the base ISOTXS file chosen. Additional warnings are given for those reactions and isotopes that are missing mapping information. The co-variance matrix is stored as a non-zero structure within PERSENT to minimize floating point operations and can trivially handle a completely full co-variance matrix although the creation of such a matrix is entirely unlikely.

4 VARI3D INPUT AND OUTPUT

The VARI3D code was written to compute reactivity coefficients and sensitivities, but it was never fully completed. As an example, the sensitivity calculation is only implemented for two-dimensional RZ geometries. The input for VARI3D is handled identically with other ARC tools, and thus the code itself is built in a similar fashion to the ARC tools. However, in many cases, the extensive use of F66 has made maintenance problematic and decreased the reliability of VARI3D compared with existing tools like DIF3D. The perturbation theory jargon used to describe the VARI3D input can be defined as:

1. Parameter: eigenvalue, reactivity worth, reaction rate, reaction rate ratio, etc.
2. Base Model or Base State: The input for a steady state neutronics calculation
3. Perturbed Model or State: The input for the perturbed steady state neutronics calculation
4. Sensitivity Model: The isotope/reaction you want to generate a sensitivity with respect to

The VARI3D input consists of three primary parts: A.VARI, A.PAR, and A.MODL. A.VARI is the control input while A.PAR is used to specify which type of parameter is being used. The A.MODL part of the input is mostly used to detail the perturbation to apply.

4.1 A.VARI Input

Starting with the control input, A.VARI specifies the general problem input and defines the sensitivities required. The input description is provided in the Documents/FileFormatDescriptions directory of the install package. A.VARI has five cards defined in Table 4.1.

Table 4.1. A.VARI Input Cards

Card #	General Description	Additional Info
1	Title	Put one in to prevent strange behavior on some platforms as it assumes one exists anyway
2	Storage and Debug	Put in 50,000,000 and don't use debugging
3	Special Options	Linearization of the diffusion operator is managed here along with style of output data
4	Sensitivity Specifications	Used to name the sensitivity, its targeted "parameter", and what model to use for defining the sensitivity. The edits are also controlled here
6	Flux and Adjoint Restart	Used to flag the restart status of the job

In Table 4.1, cards #3 and #4 are obviously the most important. As discussed in the theory section, in first order perturbation theory, it is common to linearize the diffusion coefficient when using diffusion theory. Card #3 allows for three options: 1) the generalized perturbation theory approach (default), 2) linear with respect to changes in the diffusion coefficient, and 3) linear with respect to changes in the transport cross section. Most users use the third option when they use first order perturbation theory.

Card #4 is used to define a sensitivity calculation. It is important to note that VARI3D is fundamentally built to only consider a single sensitivity per execution. However, one can

invoke multiple perturbation or sensitivity calculations in a single ARC path execution which is well demonstrated in the provided example problems. We dissect one such input later in this section for clarity. VARI3D supports four "models" for the "perturbed state" associated with the sensitivity: 1) perturbed state for the independent model change, 2) perturbed state for the dependent model change, 3) perturbed state of the numerator of a general reaction rate ratio, and 4) perturbed state of the denominator of a general reaction rate ratio. In this sense, VARI3D is far more general than the PERSENT code which is the primary focus of this manuscript. If no card #4 data is provided, VARI3D does the parameter calculation specified by the A.PAR input. If the sensitivity involves a GPT-based reactivity worth, sensitivity specifications for both the base and perturbed states must be provided.

4.2 A.PAR Input Details

The primary purpose of the A.PAR input is to define the parameter that VARI3D is to compute. Table 4.2 lists the parameters that are currently supported by VARI3D where the "type" number is the input id for each performance parameter in the input. Note that some of these parameters are only relevant in regard to sensitivities.

Table 4.2. VARI3D Supported List of Performance Parameters

Type	Performance Parameter
1	VARI3D definition of instantaneous breeding ratio
2	Reaction rate ratio
3	Power fraction
4	General adjoint reaction rate ratio
5	Linear reaction rate (fixed source problems only)
6	Inverse reaction rate (fixed source problems only)
10	First order perturbation theory reactivity worth
11	Generalized perturbation theory reactivity worth
12	Bilinear reaction rate ratio
13	Prompt generation time
14	Effective delayed neutron fraction

There are five card types supported by A.PAR which are summarized in Table 4.3. As can be seen, the parameter selections from Table 4.2 appear on card #1 in Table 4.3. Much like the sensitivity calculations, VARI3D can only perform one such calculation per call and thus the ARC batch job must be used to invoke multiple parameters to be computed with a single input file. With the exception of card #2, the remaining cards are rather straightforward to understand.

The second card in Table 4.3 is mostly associated with internal handling of the RTFLUX and ATFLUX files. As one would expect, one can attach the RTFLUX and ATFLUX files to a VARI3D input deck to improve the overall performance (i.e. perform the forward and adjoint flux calculations a priori). At issue of course is that one must be able to identify the files separately which is done with a version number that appears with each file. The enforcement of the version number can be done with the utility programs included with DIF3D. This execution option was added mostly due to the computational effort required to carry out the perturbation and sensitivity options which are no longer relevant today and thus we strongly

suggest that users not rely heavily on these input options. Note that we demonstrate how to handle the basic inclusion of pre-computed RTFLUX and ATFLUX files in the provided example problems.

Table 4.3. A.PAR Input Cards

Card #	General Description	Additional Info
1	Parameter and Edit Selections	Name and select the parameter to do and specify the edits to provide
2	External File Setup	Used to specify external binary files
3	Power Fraction Input	Specify the list of regions in the numerator
4	Reaction Rate Numerator Input	Specify the type of reaction and the regions in the numerator
5	Reaction Rate Denominator Input	Specify the type of reaction and the regions in the denominator

Table 4.4 shows the reaction rates that VARI3D supports for the reaction rate and reaction rate ratio calculations. Once again, we provide the input id associated with each reaction that appears on cards #4 and #5 in Table 4.3. Note that some of the quantities are only relevant for diffusion theory and that there is no concept of anisotropic scattering related reaction rates.

Table 4.4. Supported Reaction Rates in VARI3D

Type	Reaction	Type	Reaction
1	(n,fission)	22	Third dimension leakage
2	(n,gamma)	23	Transverse leakage (buckling term)
3	(n,alpha)	24	Total real leakage (sum of 20 to 22)
4	(n,proton)	25	Total leakage (sum of 20 to 23)
5	(n,deuteron)	30	Elastic scattering
6	(n,tritium)	31	Inelastic scattering
18	Total absorption (sum of 1 to 6)	32	(n,2n) scattering
19	Total capture (sum of 2 to 6)	33	Total scattering (sum of 30 to 32)
20	First dimension leakage	40	Fission production
21	Second dimension leakage	41	Power

4.3 A.MODL Input Details

The last part of the VARI3D input to consider is the model input which consists of the five input cards listed in Table 4.5. The input options are a little bit more difficult to understand in this case as multiple different schemes are handled with a single card. By far, cards #3 and #4 are most frequently used as one typically switches the compositions provided in the standard A.NIP3 input with other compositions also included in A.NIP3. Card #3 also provides the option of redefining an existing composition (i.e. changing the sodium density).

Table 4.5. A.MOD Input Cards

Card #	General Description	Additional Info
1	Model Name and Edit options	Assign a name to each model and specify the edits to display during the calculation
2	Isotopic cross section changes	Select isotope, reaction, and energy groups to modify by additive/multiplicative factor
3	Composition changes	Identify which compositions are to be swapped with other compositions already in the problem or define how a composition is modified
4	Region changes	Identify composition to region assignment changes. "Do not use this for sensitivities"
6	Compositional buckling changes	Define composition-wise buckling value changes.

As noted, VARI3D states that card #4 should not be used for sensitivities, but this card is also used to assign different compositions already provided in A.NIP3 input to existing regions which is effectively the same as replacing compositions. Card #2 is typically used for defining the sensitivity parameters, but it can also be used to define perturbations.

4.4 Breakdown of a VARI3D Perturbation Theory Input

For all of the input and output, we focus on the set of verification problems provided with VARI3D. Note that most of the input setup for VARI3D is based upon the ARC system and thus we suggest a review of section 3 in reference [1] should be done before attempting to read this section. In reference 1, concepts such as free form input and fixed form input along with job execution are discussed which are directly translatable to the VARI3D code.

The first example we discuss is a Doppler perturbation which is example problem #5 included with VARI3D. This problem is a hexagonal fast reactor model with inner, middle, and outer core regions, each having five axial (depletion) regions. Note that there are no blankets in this reactor as its focus was used to burn transuranic isotopes. This reactor has a high content of plutonium relevant to typical fast spectrum systems. We do not display the DIF3D input here as it is extensive and instead only focus on the relevant parts of the VARI3D input shown in Figure 4.1.

Starting with the A.VARI input, the card #2 input specifies (in sequential order as they appear on the line) that the memory space is 5100000 words with no bulk storage (default) and no debugging (5100000 0 0). The next three numbers (1 1 0) specify that the RTFLUX and ATFLUX files are desired to be saved followed by no desire to save the GEODST file. The purpose of these flags is due to the fact that VARI3D creates temporary versions of the files. The final number (1) specifies that extended edits are desired from VARI3D. The "3" on the card #3 input instructs VARI3D to use a diffusion coefficient that varies linearly with changes in the transport cross section which is consistent with most usages of first order perturbation theory.

Moving on to the A.PAR input, the card #1 input names the perturbation "DOPLER" where the follow up "10" indicates a first order perturbation theory option is desired. The "(0,

1,1)" input may appear as rather odd, but this is for free-format input which in this case reduces to "0 1 1" specifying output data that summed over group, but printed with respect region and reaction type. The final "1" indicates that the total parameter value is to be printed (default). The only really important data on the card #2 input is the specification of the MODEL input to use in this calculation named "DOPLER" which appears later in the A.MODL section. The ** input is the free form way of inserting a "blank" which translates to using the BASE model (one could have just put the word BASE in as an alternative). Note that the BASE input is not relevant to this particular reactivity coefficient (i.e. Doppler) and is ignored by VARI3D.

```
UNFORM=A.VARI
01          DOPPLER COEFF
02  5100000  0  0  1  1  0  1
03   3
UNFORM=A.PAR
01    DOPLER  10  (0,1,1)  1
02  (0,0)  DOPLER  **  1
UNFORM=A.MODL
01    DOPLER BASE       1
04    IC21DM IC21D
04    IC21EM IC21E
04    IC21FM IC21F
04    IC21GM IC21G
04    IC21HM IC21H
04    IC22DM IC22D
04    IC22EM IC22E
04    IC22FM IC22F
...
```

Figure 4.1. VARI3D Specific Input from Example Problem #5

Finishing with A.MODL, the card #1 input names the model as "DOPLER" and indicates that the "BASE" geometry configuration is the starting point. One can use a previously defined MODEL in a sequence of calculations if so desired. The additional "1" on the line indicates that the model information is to be printed by VARI3D. The card #4 input specifies the reassignment of composition data to regions in the geometry. In the first case, it assigns the composition IC21DM to region IC21D. To model most perturbations, users will typically define an alternative set of compositions that contain alternative isotopes. In this case, the IC21DM compositions have identical isotopic atom density representations of IC21D, but the isotopic cross section data used in IC21DM corresponds to higher temperature evaluations.

Figure 4.2 shows part of the output generated by running this example problem. The last "boxed" part is the most important as it is the total parameter result for the reactivity coefficient. In this case, the reactivity worth was computed as -0.00350 which is clearly linked to the magnitude of the temperature change in the cross section evaluation. The sum of the denominator (fission source norm) is provided along with the eigenvalues from the forward and adjoint flux calculations (in first order perturbation they are identical). Moving up in the figure, we see the breakdown of the reactivity worth for the areas defined in this particular job. In this case, the total values (TOTAL) are given for areas TCORE, ICORE, MCORE, and OCORE noting that the first is obviously the entire core while the remaining values specify a non-overlapping part of the total (inner, middle, and outer core). At the top of the figure one sees the reaction component breakdown of the reactivity worth for each area. The standard output

provides capture, fission, production, out scatter, in scatter, and leakage. The complete area edit output along with the region wise break down were excluded from Figure 4.2 for brevity.

```
PARAMETER = DOPLER

                  REACTN        REACTN        REACTN        REACTN      …
                     1             2             3             4        …
                   CAPT          FISS         NU-F S        OUT-SC      …
AREA
1  TCORE      -3.9893E-03   -1.4823E-04    6.8259E-04    2.0178E-04    …
2  ICORE      -1.0968E-03   -3.1452E-05    1.5181E-04    2.7237E-05    …
3  MCORE      -2.1948E-03   -7.4759E-05    3.5352E-04    1.3393E-04    …
4  OCORE      -6.9776E-04   -4.2023E-05    1.7726E-04    4.0609E-05    …

PARAMETER = DOPLER

  SENS. BY GROUP TOTAL
AREA
1  TCORE      -3.5030E-03
2  ICORE      -9.9242E-04
3  MCORE      -1.9386E-03
4  OCORE      -5.7190E-04

                * * * * * * * * * * * * * * * * * * * * * *
                *                                         *
                *  PARAMETER NAME     =        DOPLER     *
                *  PARAMETER NUMBER   =             1     *
                *  TOTAL VALUE        =  -3.50296588E-03  *
                *  DENOMINATOR VALUE  =   3.10602266E+19  *
                *  RTFLUX EIGENVALUE  =   9.99686003E-01  *
                *  ATFLUX EIGENVALUE  =   9.99686003E-01  *
                *                                         *
                * * * * * * * * * * * * * * * * * * * * * *
```

Figure 4.2. VARI3D Example Output from Example Problem #5

4.5 Breakdown of a VARI3D Sensitivity Input

Much like the preceding perturbation theory input, we also display a sensitivity input taken from example benchmark #4 case #10 in Figure 4.3. The geometry in this case is a RZ representation of the ZPR6-7 critical assembly the details of which can be found elsewhere [28]. The specific reactivity worth of interest is a "sodium void worth" where the atom density of sodium is modified everywhere in the model in a specified manner to emulate sodium voiding the specifics of which can be identified by inspecting the input file. It is important to note that the cross section evaluations are also switched when modeling this reactivity worth as done in this example. We also note that the RTFLUX and ATFLUX files are included in the "old" block which merely indicates that these files were generated before running VARI3D. Starting with the A.VARI input, the card #2 input is identical to the previous example and thus one should understand that this is the typical way of running A.VARI3D. The RTFLUX and ATFLUX files will automatically be inferred as the default ones where RTFLUX2, RTFLUX3 are recognized as the other version files.

The card #3 input on A.VARI specifies that this is a generalized perturbation theory problem and enables all of the group, space, balance edit breakdowns. The "2" at the end of the line specifies a specific treatment for the way the total and transport cross section are perturbed

$$\sigma'_{tg} = \sigma_{tg} + \delta\sigma_{tg} \quad (4.1)$$

$$\sigma'_{trg} = \sigma_{trg} + \delta\sigma_{tg} - \bar{\mu}\delta\sigma_{eg} \quad (4.2)$$

This is the default operation that is applied when the cross section is modified noting that a "1" would only perform equation 4.1 and a "3" would only perform equation 4.2. By far the most important part of the A.VARI input is the specification of multiple sensitivities. Taking the first input line as an example, it specifies a sensitivity named "VDu5" for the parameter "NAVD" seen in the A.PAR input with the model "U235" used to define the perturbation of the base and perturbed configurations of the "NAVD" parameter. The remaining values specify which edits to display. One can see the remaining lines are all identical except for the sensitivity name and the associated model. This is the typical way to invoke multiple sensitivities, and one should note that VARI3D will carry out a perturbed adjoint flux calculation when using generalized perturbation theory.

On the A.PAR input, besides the obvious specification of a generalized perturbation operation by the "11" input on the card #1, the input is straightforward, simply defining the type of edits to show and the usage of the "NAV" perturbation model. The "NAV" perturbation theory model is required to be the first A.MODL input in Figure 4.3 such that VARI3D carries out the perturbation first. In this input, one can clearly see that card #4 input is used to redirect compositions to regions, counter to the suggested input restriction that this not be done for sensitivity calculations. In this case it appears to work, but we suggest following the developer's guidelines of not using it.

After the DIF3D input is given, VARI3D will perform the stated perturbation theory problem. Each VARI3D block of data yields a separate restart-like input for VARI3D which is not checked until it is reached, so users should be careful of input mistakes. In the typical sensitivity sequence, one can see that the first block of VARI3D after the basic DIF3D input does not contain A.VARI input nor A.PAR. In fact it specifically is required that the A.PAR be "removed." This indicates to VARI3D that it should keep the existing parameter where duplicating the A.PAR input would cause an error.

```
BLOCK=OLD
DATASET=RTFLUX
DATASET=ATFLUX
DATASET=ISOTXS
BLOCK=VARI3D,3
UNFORM=A.VARI
01    ZPR6 ASSEMBLY 7 SENS COEF-CORE VOID-(Nu)-GR 01-33
02   9000000   000   000   001   001   000   001
03       001   001   001   001     0     2
04    VDu5  NAVD  U235    U235     1     0     1     1
04    VDu8  NAVD  U238    U238     1     0     1     1
04    VDpu8 NAVD  PU238  PU238    1     0     1     1
04    VDpu9 NAVD  PU239  PU239    1     0     1     1
04    VDpu0 NAVD  PU240  PU240    1     0     1     1
04    VDpu1 NAVD  PU241  PU241    1     0     1     1
04    VDpu2 NAVD  PU242  PU242    1     0     1     1
04    VDam1 NAVD  AM241  AM241    1     0     1     1
DATASET=A.PAR
01    NAVD     011   001   000   001   001
02         0     0NAV
DATASET=A.MODL
01    NAV   BASE       1
04    FI_VM FI    CENTR
04    FO_VM FO
...DIF3D input...
BLOCK=VARI3D,3
REMOVE=A.PAR
DATASET=A.MODL
01    U235  BASE       1
02    U-235I    11     0     0             1.01
02    U-235V    11     0     0             1.01
02    U-235O    11     0     0             1.01
02    U-235Z    11     0     0             1.01
02    U-235R    11     0     0             1.01
02    U-235B    11     0     0             1.01
02    U-235C    11     0     0             1.01
02    U-235D    11     0     0             1.01
02    U-235E    11     0     0             1.01
02    U-235F    11     0     0             1.01
BLOCK=VARI3D,3
REMOVE=A.PAR
DATASET=A.MODL
01    U238  BASE       1
02    U-238I    11     0     0             1.01
02    U-238V    11     0     0             1.01
02    U-238O    11     0     0             1.01
02    U-238Z    11     0     0             1.01
02    U-238R    11     0     0             1.01
02    U-238B    11     0     0             1.01
02    U-238C    11     0     0             1.01
02    U-238D    11     0     0             1.01
02    U-238E    11     0     0             1.01
02    U-238F    11     0     0             1.01
…
```

Figure 4.3. VARI3D Specific Input from Example Problem #4 Case #10

The new part of data that is required is another A.MODL input specifying how the sensitivity calculation is to be performed. In the first example, the model is named “U235” which matches the earlier specification of sensitivity in the A.VARI input. For this model, the list of isotopes to be impacted is specified on individual card #2. The “11” input on each card #2 indicates that

υ (neutrons emitted per fission) is to be modified while the 1.01 indicates a multiplier of 1.01 is to be applied to the existing value of υ. It is important to note that all of the isotopic changes specified on a model will be applied simultaneously and thus one can vary the factor to apply to each isotope for a given sensitivity. However, it is not clear why anyone would want to do that. The remaining VARI3D blocks are virtually identical to the one just describe noting that other isotopes are selected.

From this single example one should be able to understand how to construct input for other sensitivity problems. A considerable number of examples are provided. It is important to note that the sensitivity options in VARI3D only appear to be working with RZ geometry. The output returned from this specific benchmark is summarized in Figure 4.4. As can be seen, similar to the perturbation result in Figure 4.2, there is another "boxed" output which gives the total sensitivity value. In this case, the sensitivity of the sodium void worth in ZPR6-7 with respect to changes in υ in U235 is -0.0003467. It is important to note that at the bottom of the boxed section, the original reactivity worth of 0.004404 is given along with the absolute change in the parameter due to the modifications applied to all isotopes in all energy groups. This absolute term is not necessary meaningful in this case. The component breakdown of the sensitivity is also given in the boxed output which indicates the contribution to the total sensitivity by the direct term, the forward, and adjoint terms coming from the derivation. For the most part, only the total sensitivity and parameter value are relevant.

```
                    REACTN        REACTN        REACTN        REACTN
                      1             2             3             4
                     CAPT          FISS         NU-F S        OUT-SC     …
       GROUP
          1      -3.3771E-18   -4.4401E-18   1.1764E-06   -1.2214E-16   …
          2      -6.5850E-17   -7.8586E-17   1.1908E-05    3.8848E-18   …
          3      -3.7211E-16   -5.8129E-16   2.8073E-05    0.0000E+00   …
…
      SENS. BY GROUP TOTAL
       GROUP
          1       1.1764E-06
          2       1.1908E-05
          3       2.8073E-05
…
          * * * * * * * * * * * * * * * * * * * * * * * * * * * * * * *
          *                                                             *
          *  SENSITIVITY NAME                     =         VDu5       *
          *  SENSITIVITY NUMBER                   =              1     *
          *  VALUE (DELTA-PARAMETER/PARAMETER)    =  -3.46729725E-04   *
          *     NUMERATOR TERM                    =  -2.12492625E-05   *
          *     DENOMINATOR TERM                  =  -1.25056769E-04   *
          *     DELTA-FLUX TERM                   =   4.54605790E-04   *
          *     DELTA-ADJOINT TERM                =  -6.82456789E-04   *
          *     DELTA-K TERM                      =   2.74273050E-05   *
          *                                                             *
          *  PARAMETER NAME                       =         NAVD       *
          *  MODEL-CHANGE NAME                    =         U235       *
          *  DELTA-PARAMETER                      =  -1.52723160E-06   *
          *  VALUE OF BASE PARAMETER              =   4.40467455E-03   *
          *                                                             *
          * * * * * * * * * * * * * * * * * * * * * * * * * * * * * * *
```

Figure 4.4. VARI3D Example Output from Example Problem #4 Case #10

Also appearing in Figure 4.4 is the truncated sensitivity breakdown by group and the balance edit breakdown. The group wise breakdown is almost essential when performing uncertainty analysis and it is not clear why additional input is necessary to invoke it. One can also separate out the sensitivity contributions by region and area, but the tabulated data becomes quite vast and is not needed. The balance edit shown in Figure 4.4 shows the component-wise changes in the response parameter (i.e., the sodium void worth for this example) due to the model variation (i.e., cross sections changes) which is not really possible to obtain with the sensitivity functional. Close inspection shows it is just the reactivity worth balance edit divided by the total reactivity worth and multiplied by the total sensitivity value reported in the boxed section of Figure 4.4. We did not repeat this process in PERSENT as one can construct the same table given the perturbation balance table and any given value in the sensitivity output listing.

In summary, the preceding two example input and output descriptions should sufficiently describe the setup process for performing perturbation and sensitivity calculations using VARI3D. If a given compiled executable does not reproduce the reference output files provided with VARI3D within reason, one should be very cautious of using the VARI3D code noting that we have experienced problems with various compilers. We note that the set of verification problems does not cover all possible input options for VARI3D as many of those input options are rarely used. As a final note, DIF3D solves the inhomogeneous problems associated with the Lagrange multipliers using a fixed iteration scheme where convergence is not checked and it is thus up to the user to catch errors.

5 PERSENT INPUT AND OUTPUT

The main purpose of this document is to describe the PERSENT code, for which the input and output are discussed in this section. The detailed output and verification study is carried out in follow-on sections and thus we only consider the actual text based input and output generated by PERSENT. Unlike VARI3D, PERSENT was constructed to wrap around DIF3D rather than embed itself into the ARC system. In this sense, the DIF3D executable is treated as an external UNIX function that PERSENT can call via a standard Fortran system call. With this approach, we are free to define an input structure that is not restricted by the conventional ARC input process.

To begin, one should prepare the DIF3D input for the "base" or conventional steady state flux solution mode. The standard execution path for PERSENT is shown in Figure 5.1, and one can see it is rather linear noting that there are loops to account for multiple perturbation problems and sensitivity problems in the same input deck. The default input file PERSENT looks for is "persent.inp" but it can be overridden on the command line via: persent.x <input file>. As mentioned, PERSENT uses keyword input described in Tables 5.1 through 5.3. We can separate the PERSENT input into control input, perturbation theory input, and sensitivity input.

5.1 PERSENT Control Input

Some key subtleties in Figure 5.1 need to be addressed. First, PERSENT does not accept a file named ISOTXS as the standard cross section input as is the common approach for DIF3D and other ARC tools. The primary reason is that DIF3D itself requires ISOTXS for a given problem description and thus, in order for PERSENT to be able to execute DIF3D in the local directory, it must be able to define unique ISOTXS files. PERSENT thus overwrites the default ISOTXS file used in DIF3D which led to some rather interesting consequences for user ISOTXS files in the initial development phase. In general, one should never include a symbolic link (to non-executables) or an ISOTXS file in the PERSENT execution directory because PERSENT will delete any file named ISOTXS and potentially overwrite some of the other files the user might wish to actually keep. The default ISOTXS file PERSENT looks for is "user.ISOTXS", but this can overridden by the ISOTXS_INPUT variable as shown in Table 5.1. PERSENT will throw a fatal error if you attempt to use ISOTXS or ./ISOTXS as the file name. For cases where the root of the file system is to be utilized, one should enclose the entire file path with double quotes although this is not required. PERSENT also handles the special case when the ISOBCD input is included in the DIF3D input deck by moving the ISOTXS file after its creation by the null DIF3D run which can be found in Figure 5.1 (second step involving the dif3d_init.inp file).

Because of the computational expense of carrying out large energy group perturbation or sensitivity calculations, many users perform the DIF3D calculations external to PERSENT. Because this was expected, the entire PERSENT code was built to generate the necessary DIF3D input by setting the MAKE_INPUT_ONLY keyword input described in Table 5.1. It is important to note that PERSENT must have the forward and adjoint flux solutions in many of the sensitivity problems to be able to generate the input (i.e. fixed source for Γ) and thus two null runs of PERSENT might be necessary to generate all of the necessary input.

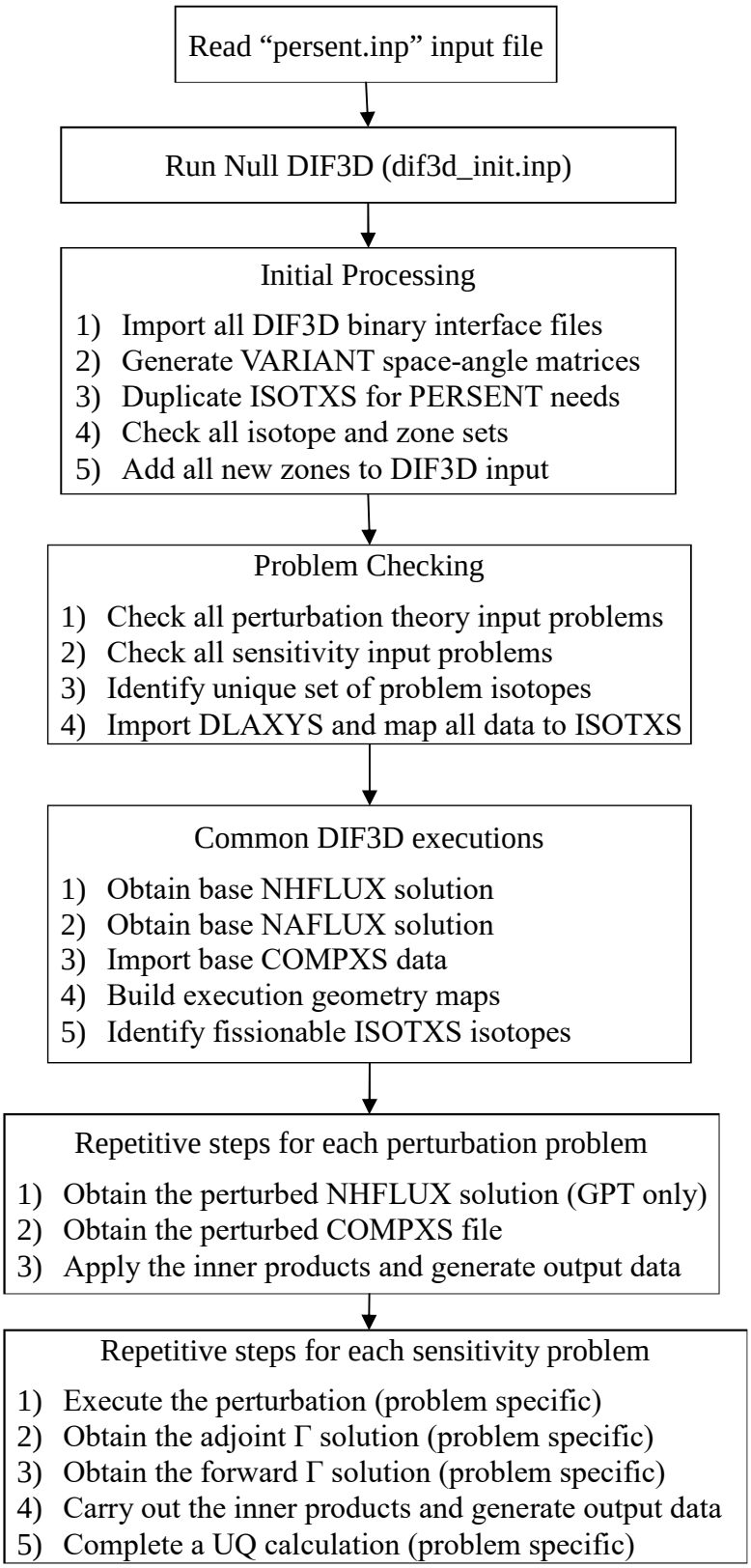

Figure 5.1. PERSENT Execution Path

Table 5.1. PERSENT Basic Control Input

Keyword	Description	Example Usage
FORCE_FULL_FLUX	Will adjust source and flux spatial approximation orders along with angular scattering order in the DIF3D input deck to ensure the flux vector is consistent	Force_full_flux yes Force_full_flux no
MAKE_INPUT_ONLY	Will skip all possible DIF3D flux solution calls so that only the exact DIF3D input needed for each call is generated.	Make_input_only yes Make_input_only no
ISOTXS_INPUT	Specifies the location/name of the ISOTXS file (Cannot be ./ISOTXS)	Isotxs_input ./user.ISOTXS Isotxs_input “/home/user/HFR/metal.33g.ISOTXS”
DLAYXS_INPUT	Specifies the location/name of the DLAYXS file	Dlayxs_input “/home/user/HFR/33g.DLAYXS”
DIF3D_INPUT	Specifies the location/name of the DIF3D base input deck	Dif3d_input ../dif3d.base.inp Dif3d_input “/home/user/HFR/hfr.inp”
DIF3D_EXECUTABLE	Specifies the location/name of the DIF3D executable	Dif3d_executible ./dif3d.x Dif3d_executible “/software/bin/dif3d.x”
FORWARD_FILE	Specifies the location of the base NHFLUX file containing the forward flux solution	Forward_file “/home/user/hfr.66133.NHFLUX” Forward_file “/scratch/hfr.66133.NHFLUX” Forward_file ./hfr.66133.NHFLUX
ADJOINT_FILE	Specifies the location of the base NAFLUX file containing the adjoint flux solution	Adjoint_file “/home/user/hfr.66133.NAFLUX” Adjoint_file “/scratch/hfr.66133.NAFLUX” Adjoint_file ./ hfr.66133.NAFLUX
ISOTOPE_LIST	Specifies a list of ISOTXS isotope names	Isotope_list all_fe FE56 FE57 FE58 Isotope_list all_u238 U238A U238B U238C
ZONE_LIST	Specifies a list of DIF3D A.NIP3 zone (composition) names	Zone_list core ICOREA ICOREB ICOREC ICORED Zone_list core IcoreA IcoreB IcoreC IcoreD
NEW_ZONE	Allows the inclusion of a new zone into the DIF3D input	New_zone blanket U238 0.02 U235 0.0001 New_zone blanket Na 0.03
SET_DELAY	Allows the mapping of ISOTXS isotopes to DLAYXS ones	Set_delay IU26A U238 Set_delay MU24A U235

Table 5.2. PERSENT Perturbation Inputs

Keyword	Description	Example
LAMBDA_BETA	Requests that Lambda and Beta be computed by PERSENT (requires DLAXYS file)	LAMBDA_BETA Yes LAMBDA_BETA No
ADJUST_XS	Specify a cross section perturbation reactivity worth	adjust_xs x1x2 generalized_pt all_u238 fission 1.0 -0.01 2 10 adjust_xs x1x2 generalized_pt all_u238 gamma 1.0 0.01 2 10
ADJUST_DENSITY	Specify a density perturbation reactivity worth	adjust_density UpNa generalized_pt CRHOLE 0.40
ADJUST_ZONE	Specify a zone perturbation reactivity worth	Adjust_zone C1C2 generalized_pt C1 C2 1.00
PROBLEM_EDITS	Specify the perturbation problem edits to display	Problem_edits UpNa print_by_mass print_balance Problem_edits lambda_beta print_by_isotope export_vtk
FORWARD_PERT_FILE	Location of the perturbed NHFLUX file	Forward_pert_file UpNa “/home/user/p.hfr.66133.NHFLUX”
ADJOINT_PERT_FILE	Location of the perturbed NAFLUX file	Adjoint_pert_file UpNa “/home/user/p.hfr.66133.NAFLUX”
COMMARA_INPUT	Specifies the location/name of the COMMARA formatted file	Commara_input bnl.1.apr.2011.commara
COMMARA_IGNORE-MISSINGDATA	Allows PERSENT to ignore co-variance data (yes is default)	Commara_ignoremissingdata no
COMMARA_ISOTOPE	Allows mapping of ISOTXS isotopes to co-variance isotope name ids	Commara_isotope FE56K Fe56 Commara_isotope NA23K Na Commara_isotope O16D O
COMMARA_REACTION	Allows mapping of PERSENT reaction names to co-variance reaction names	Commara_reaction n2n nxn

Table 5.3. PERSENT Sensitivity Inputs

Keyword	Description	Example
REACTION_RATE	Specify a reaction rate sensitivity (only valid for fixed source problems)	Reaction_rate FeSens all_fe everything core Reaction_rate NaSens all_Na gamma core
REACTION_RATIO	Specify a reaction rate ratio sensitivity	Reaction_ratio a29c28 a_p239 alpha core a_u238 gamma core
REACTION_WORTH	Specify a reactivity worth sensitivity	Reaction_worth SensUpNa UpNa
POWER_FRACTION	Specify a power fraction sensitivity	Power_fraction core MyListOfZones
SENSITIVITY_BETA	Request the β sensitivity	Sensitivity_beta sens_beta
SENSITIVITY_LAMBDA	Request the Λ_G sensitivity	Sensitivity_lambda sens_lambda
SENSITIVITY_KEFF	Request a $k_{effective}$ sensitivity	Senstivity_keff sens_basek
SELECT_ALPHA	Specify the alpha selection for sensitivity	Select_alpha sens_beta all_u238 everything Select_alpha FeSens all_Cl standardset Select_alpha FeSens all_Fe capture
SENSITIVITY_EDITS	Specify which edits are desired	Sensitivity_edits SensUpNa Print_perturbation
SENSITIVITY_DOUQ	Specify that the UQ computation is to be performed for the stated sensitivity	Sensitivity_douq beta_sens yes yes yes
GAMMA_FORWARD_FILE	Location of the Γ NHFLUX file	Gamma_forward_file SensUpNa ./hfr.inhomog.NHFLUX
GAMMA_ADJOINT_FILE	Location of the Γ NAFLUX file	Gamma_adjoint_file SensUpNa./hfr.inhomog.NAFLUX
LIMIT_OUTERS	Limits the number of outers between contamination removal	LIMIT_OUTERS 10
USE_SHIFT	Shift fission into scattering matrix	USE_SHIFT Yes
TREAT_UNIQUE	Generate individual sensitivity vectors for the isotopes listed on this line	TREAT_UNIQUE PU239A PU239B PU239D
USE_TOTALNU	Default is NO as sensitivities are to be produced in terms of prompt nu	USE_TOTALNU Yes
BILINEAR	Process the UQ with two different sensitivity vectors	BILINEAR coupledsens sens_beta sens_lambda

```
FORCE_FULL_FLUX  <yes/no>
MAKE_INPUT_ONLY  <no/yes>
ISOTXS_INPUT     <file_name>
DLAYXS_INPUT     <file_name>
DIF3D_INPUT      <file_name>
DIF3D_EXECUTABLE <file_name>
FORWARD_FILE     <file_name>
ADJOINT_FILE     <file_name>
ISOTOPE_LIST     <LIST_ISOTOPES> <ISOTXS isotope> <ISOTXS isotope> <ISOTXS isotope> <ISOTXS isotope> ...
ZONE_LIST        <LIST_ZONES>  <DIF3D zone> <DIF3D zone> <DIF3D zone> <DIF3D zone> ...
NEW_ZONE         <new DIF3D zone name> <ISOTXS isotope> <ISOTXS density> <ISOTXS isotope> <ISOTXS density> ...
SET_DELAY        <ISOTXS isotope> <DLAYXS isotope>
-----------------
LAMBDA_BETA      <no/yes>
ADJUST_XS         <problem_name> <METHOD> <LIST_ISOTOPES> <XS> <multiplicative factor> <add on factor> <start group> <end group>
ADJUST_DENSITY    <problem_name> <METHOD> <existing DIF3D zone> <density multiplicative factor>
ADJUST_ZONE       <problem_name> <METHOD> <existing DIF3D zone> <replacement zone> <density multiplicative factor>
PROBLEM_EDITS     <problem_name> <PRINT_BY_ISOTOPE> <PRINT_BY_MESH> <PRINT_BY_GROUP> <PRINT_BY_REGION> <PRINT_BY_AREA>
                                 <PRINT_BALANCE> <PRINT_BY_MASS> <PRINT_BY_UNIQUE> <PRINT_BY_FAMILY> <EXPORT_VTK> <file_name>
FORWARD_PERT_FILE <problem_name> <file_name>
ADJOINT_PERT_FILE <problem_name> <file_name>
-----------------
REACTION_RATE       <problem_name>  <LIST_ISOTOPES> <XS> <LIST_ZONES>
REACTION_RATIO      <problem_name>  <numer. LIST_ISOTOPES> <XS> <LIST_ZONES> <denom. LIST_ISOTOPES> <XS> <LIST_ZONES>
REACTION_WORTH      <problem_name>  <perturbation PROBLEM_NAME>
POWER_FRACTION      <problem_name>  <numerator LIST_ZONES>
SENSITIVITY_BETA    <problem_name>
SENSITIVITY_LAMBDA  <problem_name>
SENSITIVITY_KEFF    <problem_name>
SENSITIVITY_FILE    <problem_name> <file name>
BILINEAR            <problem_name>   <Sensitivity problem name 1> <Sensitivity problem name 2>
SELECT_ALPHA        <problem_name>  <LIST_ISOTOPES> <XS>
SENSITIVITY_EDITS   <problem_name>  <Print Perturbation?> <file_name>
SENSITIVITY_DOUQ    <problem_name>  <Print Reaction-wise table?> <Print Detailed Isotoped table?> <Print Isotope to Isotope Table?>
GAMMA_FORWARD_FILE  <problem_name>  <file_name>
GAMMA_ADJOINT_FILE  <problem_name>  <file_name>
LIMIT_OUTERS        <min iterations> <max iterations>
USE_SHIFT           <no/yes>
USE_TOTALNU         <no/yes>
TREAT_UNIQUE        <ISOTXS isotope> <ISOTXS isotope> ...  These isotopes will be uniquely treated in the sensitivity calculations
-----------------
COMMARA_INPUT     <file_name>
COMMARA_IGNOREMISSINGDATA <no/yes>
COMMARA_ISOTOPE   <ISOTXS isotope> <COMMARA isotope>
COMMARA_REACTION  <PERSENT reaction> <COMMARA reaction>
-----------------
<METHOD> = <FIRST_ORDER_PT> <GENERALIZED_PT> <NS_FIRST_ORDER>
<XS> = <TOTAL> <NU> <NUFISSION> <CHI> <CHI_NORM> <FISSION> <CAPTURE> <GAMMA> <ALPHA> <PROTON> <TRITIUM> <DEUTERIUM>
       <SCATTER> <ELASTIC> <INELASTIC> <N2N> <P1SCATTER> <P1ELASTIC> <P1INELASTIC> <P1N2N> <STANDARDSET> <EVERYTHING>
```

Figure 5.2. PERSENT Quick Guide Input Commands

Depending upon the way PERSENT is executed, it will generate the files shown in Table 5.4. In a non-null PERSENT run, file names with the generic dif3d_problem name are created according to the order in which they are executed. Take note that all NHFLUX and NAFLUX files from any specific execution are stored by the problem name. Most users do not run in this mode when DIF3D takes considerable time to run, but routinely provide NHFLUX and NAFLUX files externally via the input.

Table 5.4. Example PERSENT Input and Output Files

MAKE_INPUT_ONLY=NO	MAKE_INPUT_ONLY=YES
ISOTXS.unmodified	ISOTXS.unmodified
dif3d_init.inp	dif3d_init.inp
dif3d_init.out	dif3d_init.out
dif3d_adjoint.inp	BaseAdjoint.inp
dif3d_adjoint.out	BaseForward.inp
dif3d_forward.inp	BaseForwardorAdjoint.GEODST
dif3d_forward.out	BaseForwardorAdjoint.ISOTXS
P_dif3d_problem0001.inp	BaseForwardorAdjoint.LABELS
P_dif3d_problem0001.out	BaseForwardorAdjoint.NDXSRF
P_dif3d_problem0002.inp	BaseForwardorAdjoint.ZNATDN
P_dif3d_problem0002.out	base.NHFLUX
S_dif3d_problem0002_A.inp	base.NAFLUX
S_dif3d_problem0002_A.out	P_PT_DOPPLER____01.inp
S_dif3d_problem0002.inp	P_PT_DOPPLER____01.GEODST
S_dif3d_problem0002.out	P_PT_DOPPLER____01.ISOTXS
S_dif3d_problem0003.AdjointGamma.inp	P_PT_DOPPLER____01.LABELS
S_dif3d_problem0003.AdjointGamma.out	P_PT_DOPPLER____01.NDXSRF
	P_PT_DOPPLER____01.ZNATDN
	S_PT_DOPPLER____01.inp
	S_PT_DOPPLER____01_A.inp
	S_PT_DOPPLER____01.GEODST
	S_PT_DOPPLER____01.ISOTXS
	S_PT_DOPPLER____01.LABELS
	S_PT_DOPPLER____01.NDXSRF
	S_PT_DOPPLER____01.ZNATDN
	S_PT_DOPPLER____01.NHFLUX
	S_PT_DOPPLER____01.NAFLUX
	S_PT_DOPPLER____01_AdjointGamma.inp
	S_PT_DOPPLER____01_Adjoint.VARSRC

As seen in Table 5.4, a null PERSENT run generates files including either the perturbation or sensitivity problem name (PT_DOPPER in this case) to make identification straightforward. Note that in this situation, the binary interface files are also generated which can lead to multiple copies of files that are identical. The descriptions and purposes of each of these files can be found in the DIF3D manual [1]. It is important to note that for sensitivity problems the VARSRC files are used to define inhomogeneous fixed source problems, which subsequently

requires the use of the inhomogeneous solver discussed later in this section. Note that PERSENT creates output files for each input file when MAKE_INPUT_ONLY option is enabled, which can be ignored. Also note that each input file will have to be modified to change the number of outer iterations to a more realistic value in order to run DIF3D. As a final note, the forward and adjoint binary files are identical for the base case and thus only a single copy is provided.

The main goal of running the DIF3D calculations is to generate the NHFLUX and NAFLUX files needed by PERSENT for computing the perturbations or sensitivities. From Tables 5.1 through 5.3, one can identify the keyword inputs required to externally include these files as: FORWARD_FILE, ADJOINT_FILE, FORWARD_PERT_FILE, ADJOINT_PERT_FILE, GAMMA_FORWARD_FILE, and GAMMA_ADJOINT_FILE. The first two cases are used to include the forward and adjoint flux files for the base DIF3D geometry. The next two cases (*_pert_file) are specific inputs for each perturbation problem depending upon what is needed and thus include an additional specification for the associated perturbation theory problem name. The final inputs (gamma_*_file) are used for the sensitivity cases and thus specify the flux solutions for the inhomogeneous Lagrange multipliers.

The remaining control inputs are primarily found in Table 5.1 and consist of: force_full_flux, dlayxs_input, dif3d_input, and dif3d_executable. The last three allow the user to select alternative locations for the DLAYXS file (default is ./DLAYXS), the DIF3D input deck (default is ./dif3d.inp), and the DIF3D executable (./dif3d.x). The most difficult control input to explain and understand is the force_full_flux input. This input is an artifact of the historical usage of the DIF3D code and is by default turned on. In the conventional VARIANT methodology, the flux within each node can be expanded into a high order set of spherical harmonics such as P_7. If a P_3 scattering kernel is used, the conventional DIF3D-VARIANT code obviously only needs a P_3 flux expansion to apply to the scattering kernel and thus only builds P_3 sized matrices and vectors for the final iterative system. In this situation, the resulting NHFLUX file does not contain sufficient information to apply the P_7 operator (it only has the P_3 moments) thus resulting in a residual amount of error in the perturbation or sensitivity calculations. Consequently, it is strongly suggested that this flag always be turned on, as it will force DIF3D-VARIANT to produce a NHFLUX file with the full P_7 expansion. Note that this does result in more computational expense, but should yield the most accurate result possible. Also note that PERSENT does not allow the NHFLUX file provided to be of higher order than the operator, but it does allow a lower order NHFLUX file to be used such that one can assess the importance of the truncation.

In order to use the perturbation or sensitivity inputs, we will routinely need to group isotopes or compositions together and thus the ISOTOPE_LIST and ZONE_LIST were included. The “isotope_list” input can be found in Figure 5.1, and its purpose is to conglomerate the treatment of different isotopes as one although with the updated sensitivity input, it is not really needed for anything other than cross section perturbations. In many fast reactor problems, it is not uncommon to evaluate isotope wise cross section data at different regions of the domain when using a coarse energy group structure (say 33 groups). This typically leads to multiple definitions of each isotope in the problem (or ISOTXS file) which should all change in the same manner. To manage this, the perturbation and sensitivity codes were set up to manipulate an isotope set rather an individual isotope as discussed in Section 3. The “zone_list” input has a

similar purpose except it is typically used to define specific areas (such as that needed for power fraction) which are required for some sensitivity calculations.

5.2 PERSENT Perturbation Input

The primary usage of PERSENT today is on perturbation problems used to calculate point kinetics parameters. The most common of these is the Λ and β operations which are engaged by including the keyword input "lambda_beta yes" as shown in Table 5.2 and Figure 5.1. Because both of these constants only require the forward and adjoint fluxes, they are handled simultaneously rather than independently. This is consistent with the fact that the routines which generate Λ and β are not appropriate for use within the sensitivity calculations discussed later. The act of requesting Λ and β tells PERSENT to look for the DLAYXS file in the path specified by the associated input.

One issue to deal with is that the mapping between ISOTXS and DLAYXS isotopes is not entirely clear. Noting that ISOTXS allows users to assign an alias to each isotope (u238a, u238b, u238c, etc.) stored in HISONM on ISOTXS, the assumption by VARI3D and PERSENT is that the original "ENDF" isotope name is stored in the isotope-wise HABSID location on ISOTXS. The DLAYXS file is typically stored using the HABSID name noting that the mapping is thus obvious by comparison of HABSID on the ISOTXS and DLAYXS. This is the assumed approach, however, PERSENT also checks the HISONM against the HABSID name assuming that some users might create cross section data by hand. If fissionable isotopes are not mapped successfully, PERSENT will issue a warning of the form:

```
[PERSENT]...Warning::: Fissionable ISOTXS isotope PU239H   is not mapped to any DLAYXS data
[PERSENT]...Warning::: Fissionable ISOTXS isotope U238H    is not mapped to any DLAYXS data
```

Clearly this will be a serious problem in this example as these isotopes should have delay neutron data present. To fix these issues, one must use the SET_DELAY option which will assign a given ISOTXS HISONM to a given DLAYXS HABSID as directed by the user. For the above warnings, one might utilize the input

```
SET_DELAY U238H  U-2387
SET_DELAY PU239H PU2397
```

The remaining perturbation problem inputs are: Adjust_XS, Adjust_Density, and Adjust_Zone. Starting with Adjust_XS, from Figure 5.2, one can see that the user needs to assign a problem name followed by the METHOD, the options for which are specified at the bottom of Figure 5.2. The suggested usage is GENERALIZED_PT although the FIRST_ORDER_PT option now provides the desired quantity as discussed in Section 3. The remaining inputs for Adjust_XS are the specification of an isotope list, the cross section to manipulate, and how it is to be manipulated. As an example, one can specify the input:

```
ADJUST_XS u238gamma GENERALIZED_PT all_u238 gamma 1.01 0.0 3 3
```

In this case, the user named the perturbation u238gamma, selected all U238 in the domain (assumed what was in the isotope list), selected the group 3 gamma cross section and modified

it by multiplying by 1.01 and adding 0.0. To impose multiple changes to a given perturbation, one only needs to include multiple lines with the same perturbation problem name such as:

```
ADJUST_XS u238gamfis GENERALIZED_PT all_u238 gamma   1.01 0.0 1 1
ADJUST_XS u238gamfis GENERALIZED_PT all_u238 gamma   1.03 0.0 2 2
ADJUST_XS u238gamfis GENERALIZED_PT all_u238 gamma   1.05 0.0 3 3
ADJUST_XS u238gamfis GENERALIZED_PT all_u238 fission 0.99 0.0 1 1
```

Note that the given perturbation problem must be of the same type and that TOTAL, NUFISSION, CHI, POWER, STANDARDSET, and EVERYTHING are not valid selections for the XS modification.

The input for the Adjust_Density perturbation problem is very simple and only done to avoid introducing a new composition (zone) into the DIF3D problem. A simple example using multiple lines in a single perturbation can be written as

```
ADJUST_Density coredensity GENERALIZED_PT icore 1.10
ADJUST_Density coredensity GENERALIZED_PT mcore 0.93
ADJUST_Density coredensity GENERALIZED_PT ocore 1.04
```

As can be seen, the treatment is similar to ADJUST_XS except for the reduced content of information.

The ADJUST_ZONE input is by far the most used perturbation option of the three. Its purpose is to replace zones in the problem to simulate partial material density changes (such as sodium) or changes in temperature or control rods. Much like the preceding two inputs, we can write a simple example as

```
ADJUST_ZONE doppler GENERALIZED_PT icore icoreT
ADJUST_ZONE doppler GENERALIZED_PT mcore mcoreT  1.01
ADJUST_ZONE doppler GENERALIZED_PT ocore ocoreT
```

It is important to note that this input not only replaces the zone, but also adjusts the density and thus can duplicate the ADJUST_DENSITY perturbation option. In most cases, users only replace zones rather than adjust the density.

All of the perturbation problems will be thoroughly checked to ensure the proposed change is possible and not recursive. As an example, one cannot change composition C1 to composition C2 and have another line in the same problem that then changes composition C2 to composition C3. More importantly, part of the DIF3D structure allows a given composition to be dependent upon other compositions. This setup is described as zones (compositions) composed of subzones (materials or other compositions). As an example, an assembly homogenized composition can be composed of fuel, structure, and coolant. The fuel, structure, and coolant can be defined as subzones of the assembly zone. The PERSENT perturbation inputs will allow you to select either a zone or subzone in the problem for the modification, noting that if the same subzone (say structure) is used in multiple zones, all such zones will be modified by the perturbation input. There are thus four possible results and PERSENT will inform the user as to which option is being used for each input line for a given perturbation problem:

```
[PERSENT]...Replacing zone     IC21D    with copy of zone     IC21DM
[PERSENT]...Replacing zone     IC21E    with copy of subzone  IC21EM
[PERSENT]...Replacing subzone  IC21F    with copy of zone     IC21FM
[PERSENT]...Replacing subzone  IC21G    with copy of subzone  IC21GM
```

Note that replacement of a subzone can impact multiple zones and that one can specify the promotion (duplication) of a subzone as a zone.

5.3 PERSENT Problem Edits Input

The last part of the perturbation input is likely the most important: PROBLEM_EDITS. Figure 5.1 shows the full listing of options which can be summarized as: isotope, mesh, group, region, area, balance, mass, unique, family, export_vtk, file_name. Table 5.4 indicates which output options are supported by which perturbation problems.

Table 5.5. Supported Problem Edits for Perturbation Problems

Input Option	Λ	β	XS	Density	Zone
PRINT_BY_ISOTOPE		X			
PRINT_BY_MESH	X	X	X	X	X
PRINT_BY_GROUP	X	X	X	X	X
PRINT_BY_REGION	X	X	X	X	X
PRINT_BY_AREA	X	X	X	X	X
PRINT_BALANCE	X	X	X	X	X
PRINT_BY_MASS					X
PRINT_BY_UNIQUE		X			
PRINT_BY_FAMILY		X			
file_name	X	X	X	X	X
EXPORT_VTK	X	X	X	X	X

As seen in Table 5.4, all of the perturbation problems support the export of the result to an external file (file_name) rather than the standard output (screen). All of them also support the exporting of data to a VTK file [25] which can be used to view the geometry and distribution of the perturbation using a tool like VISIT [26]. In the case of β, only the total value (i.e. sum over all families) is exported for visualization. Note that if EXPORT_VTK is enabled, the problem name will be used in the outputted VTK file such as: “LAMBDA.vtk”.

Of the remaining edits, PRINT_BY_MESH and PRINT_BY_GROUP are the easiest to understand. They will generate massive tables of data associated with the mesh and energy breakdown of a given perturbation. PRINT_BY_REGION will generate output of the form:

```
[PERSENT]...|Region| Numerator  | Numerator /
[PERSENT]...|      |            | Sum[Denominator] |
[PERSENT]...|ROD1  | -1.266E+20|        -2.851E-02|
[PERSENT]...|CORE1 |  0.000E+00|         0.000E+00|
[PERSENT]...|ROD2  | -3.065E+20|        -6.901E-02|
[PERSENT]...|ROD3  | -3.065E+20|        -6.901E-02|
[PERSENT]...|CORE2 |  0.000E+00|         0.000E+00|
[PERSENT]...|ROD4  | -1.312E+20|        -2.954E-02|
[PERSENT]...|ROD5  | -1.312E+20|        -2.954E-02|
[PERSENT]...|BLAN  |  0.000E+00|         0.000E+00|
[PERSENT]...|REFL  |  0.000E+00|         0.000E+00|
```

The CORE1 and CORE2 regions are DIF3D regions as defined by geometry input in the DIF3D input file. By adding the PRINT_BALANCE option, this table of data will be modified to include:

```
[PERSENT]...|Region| Numerator  | Numerator /      = Leakage  +  Capture  …
[PERSENT]...|      |            | Sum[Denominator] |          |           …
[PERSENT]...|ROD1  | -1.266E+20|        -2.851E-02| 4.367E-05|-2.598E-02 …
[PERSENT]...|CORE1 |  0.000E+00|         0.000E+00| 0.000E+00| 0.000E+00 …
[PERSENT]...|ROD2  | -3.065E+20|        -6.901E-02| 5.035E-04|-6.395E-02
[PERSENT]...|ROD3  | -3.065E+20|        -6.901E-02| 5.035E-04|-6.395E-02
[PERSENT]...|CORE2 |  0.000E+00|         0.000E+00| 0.000E+00| 0.000E+00
[PERSENT]...|ROD4  | -1.312E+20|        -2.954E-02| 3.562E-03|-3.044E-02
[PERSENT]...|ROD5  | -1.312E+20|        -2.954E-02| 3.562E-03|-3.044E-02
[PERSENT]...|BLAN  |  0.000E+00|         0.000E+00| 0.000E+00| 0.000E+00
[PERSENT]...|REFL  |  0.000E+00|         0.000E+00| 0.000E+00| 0.000E+00
```

where the remaining column wise output is

```
+ Fission  + Out Scatter - In Scatter - Production  ||   n,2n   |
|          |             |            |             ||          |
| 0.000E+00|   -1.700E-02|  -1.444E-02|    0.000E+00|| 0.000E+00|
| 0.000E+00|    0.000E+00|   0.000E+00|    0.000E+00|| 0.000E+00|
| 0.000E+00|   -4.367E-02|  -3.811E-02|    0.000E+00|| 0.000E+00|
| 0.000E+00|   -4.367E-02|  -3.811E-02|    0.000E+00|| 0.000E+00|
| 0.000E+00|    0.000E+00|   0.000E+00|    0.000E+00|| 0.000E+00|
| 0.000E+00|   -2.089E-02|  -1.823E-02|    0.000E+00|| 0.000E+00|
| 0.000E+00|   -2.089E-02|  -1.823E-02|    0.000E+00|| 0.000E+00|
| 0.000E+00|    0.000E+00|   0.000E+00|    0.000E+00|| 0.000E+00|
| 0.000E+00|    0.000E+00|   0.000E+00|    0.000E+00|| 0.000E+00|
```

From these two segments of output, the total value is taken to be Numerator/Sum [Denominator]. In the balance edit this is equal to the sum of leakage, capture, fission, out scatter, in scatter and production. These are not the absolute values, but merely the change in the quantities for the perturbation being studied. One can see there is no change in the fission cross section for this problem. It is also important to note that we provide the N2N as an auxiliary output with the balance edits. All of these terms are easy to understand and are implemented using classic diffusion theory. This means that any error resulting from using a transport versus diffusion representation is dumped into the “leakage” term. As a consequence, the balance numbers can only be considered estimates unless DIF3D-VARIANT is being used on a diffusion calculation.

The PRINT_BY_AREA option is virtually identical to the PRINT_BY_REGION option except it reports the breakdown for the user defined “areas” provided in the base DIF3D

deck. If no areas are defined, no data will be printed. It is important to note that great care was taken to ensure that duplicate regions included in a given area do not produce an invalid result for those areas.

From Table 5.5, the PRINT_BY_MASS option is only available for the zone perturbation option. This option generates the change in unique isotopic mass resulting from the perturbation, for example:

```
[PERSENT]...This perturbation has total core changes in mass of
[PERSENT]...NA23 5             0.8212 kg
[PERSENT]...FE   5             6.4376 kg
[PERSENT]...O-16 5            -3.3761 kg
[PERSENT]...U-238S           -25.1226 kg
```

As shown in Figure 5.1, a unique set of isotopes is constructed by looking at the isotope masses included in ISOTXS and mapping to a given HABSID name of each unique isotope. In this particular case, the perturbation involves a considerable change in the U238 mass along with changes in oxygen, iron, and sodium. The mass breakdown is also printed with respect to region, area, and mesh depending upon the selections chosen, but note that balance and group edits do not make sense and are not printed. Note that the mass edit can also be exported to a VTK file to verify the intended zone perturbation was applied as expected. Two additional VTK files are generated with tailing names “per_mass_kg” referring to the reactivity worth per unit mass and “just_mass_kg” referring to the net mass change. Because the absolute reactivity worth change can vary by mesh size, the reactivity worth divided by the total mass change in the mesh (region or area) is also printed out such that the visualization of the reactivity worth is more meaningful (“per_mass_kg”).

The remaining options PRINT_BY_ISOTOPE, PRINT_BY_UNIQUE, and PRINT_BY_FAMILY are only relevant to the delayed neutron fraction. If the print_by_isotope option is triggered, the total delay neutron fraction will be broken into contributions by each isotope in the ISOTXS file. The print_by_family option is only a modifier on the print_by_isotope option which invokes a print out of the detailed family breakdown by each ISOTXS isotope. The print_by_isotope option will also cause the coalesced beta parameters to be generated by ISOTXS isotope. The print_by_unique option only applies to the coalesced beta parameters such that data for unique isotopes is displayed.

Unlike VARI3D, the total value for any perturbation is printed on a single line. The adjust_zone, adjust_xs, and adjust_density perturbations will all yield virtually identical output lines. The Λ and β cases have considerably different output files where we summarize all of them as:

```
=PERSENT...Parameter General PT of TEST1    is -5.00000E-01 k-eff A  8.2219642E-01 F  5.8266324E-01
=PERSENT...Parameter First O PT of FO_TEST1 is -5.00000E-01 k-eff A  8.2219642E-01 F  8.2219642E-01
=PERSENT...Parameter General PT of TEST7    is -7.52291E-01 k-eff A  8.2219642E-01 F  5.0798881E-01
=PERSENT...Parameter LAMBDA Gen time  3.54011E-07 Prompt Lifetime  4.38089E-07 k-eff  1.2375001E+00
=PERSENT...Parameter BETA is         1.89813E-03 denominator  1.11773E+21 k-eff  1.2375001E+00
=PERSENT...Domain coalesced kinetics parameters for unique isotope PU239S
=PERSENT...Family     beta(i)    lambda(i)
=PERSENT...   1   9.83991E-04  3.00000E-02
=PERSENT...   2   9.14141E-04  1.00000E+00
=PERSENT...Domain coalesced effective point kinetics parameters
=PERSENT...Family     beta(i)    lambda(i)
=PERSENT...   1   9.83991E-04  3.00000E-02
=PERSENT...   2   9.14141E-04  1.00000E+00
```

(Note that we have stripped off the "denominator" part of each line from all but the beta output in order to display the above output.) From this example output, one should note the adjoint eigenvalue of the perturbed configuration and forward eigenvalue of the base case are provided, which should yield an identical reactivity worth to that given on each line (assuming Generalized PT or General PT above). Any errors observed in between the reported value and the one obtained with the two eigenvalues has typically been found to be a result of an insufficient spatial approximation or failure to use the force_full_flux option. Note that for Λ, PERSENT gives the generation time Λ_G in addition to the targeted prompt neutron lifetime. For β, it is common to get the total delayed neutron fraction as done in the example, but it is also common to produce a set of core coalesced parameters which appear after the total β value is given. These are the values that typically will be used in a point kinetics code and we note that they are broken down by unique isotope as indicated in the example. In this case, the λ_i values correspond to the delay constants for each family.

5.4 PERSENT Sensitivity Input

The sensitivity problem inputs for PERSENT are not much different from the perturbation problem inputs. From Figure 5.1 one can see that the sensitivity problems are done sequentially with respect to the perturbation problems but that each sensitivity problem can invoke a perturbation problem. In PERSENT, any perturbation problem that is identified as a sensitivity case is eliminated from the list of perturbation problems and thus a subsidiary of the sensitivity problems. It should be obvious that the UQ calculation of a specified sensitivity calculation must follow the sensitivity calculation and in general the output will appear immediately after the sensitivity output. With regard to combining sensitivities in a UQ calculation, these are treated identically to sensitivity problems with steps 1 through 4 in Figure 5.1, skipped given they were already completed for the needed sensitivities. The combined sensitivity problems will always be completed after all regular sensitivity calculations are completed.

Much like the PROBLEM_EDITS input for perturbation problems, the SENSITIVITY_EDITS input is used to define additional edits for a sensitivity problem. Given a valid sensitivity problem name, there are only two other valid inputs: file_name and print_perturbation. The file_name specifies the file to which the sensitivity data is to be written instead of writing to the screen. The print_perturbation input is optional noting that the problem edits specified for any perturbation problem that is subsidiary to a given sensitivity problem are disabled by default.

Starting with the Λ and β calculations, the sensitivity operation on either Λ or β is independent of the other and thus we have two separate sensitivity inputs: SENSITIVITY_LAMBDA and SENSITIVITY_BETA. The input for these two is very simple and only requires a problem name as shown in Figure 5.2. One can invoke multiple sensitivities of each parameter using different problem names as desired. The LAMBDA_BETA input option does not have to be used to invoke either sensitivity. The SENSITIVITY_BETA option was updated to produce a breakdown of the sensitivity by family as discussed in Section 3 noting that it is nothing more than a scaling of the total result.

The sensitivity input option SENSITIVITY_KEFF is very similar to Λ and β in that it only requires a problem name. The REACTION_WORTH input is a bit more difficult to understand but it merely requires a problem name followed by the associated perturbation problem name. In this latter case, we refer to the problem name assigned on an adjust_xs, adjust_density, or adjust_zone input card. As mentioned, this will cause all parts of the perturbation problem to be done as a subsidiary part of the sensitivity problem where all input options on the problem_edits are propagated through. We note that print_perturbation must be assigned to the given sensitivity problem. *For reaction worth sensitivities, first order perturbations are not supported, and thus all first order perturbation theory methodologies will be automatically promoted to generalized perturbation ones*.

The remaining sensitivity options are more complex: REACTION_RATE, REACTION_RATIO, and POWER_FRACTION. The power_fraction only requires a zone list beyond the normal problem name definition. In this case, the zones that are to appear in the numerator of the power fraction are provided via a ZONE_LIST input. The reaction_rate input is similar to the power_fraction, however, the key difference is that by using separate reaction_rate lines, one can isolate the contributions from similar isotopes in different zones to the reaction rate of interest. From Figure 5.2, one can define input of the form

```
REACTION_RATE  CAPTURE_C1_C2  ALL_NA CAPTURE C1_REGIONS
REACTION_RATE  CAPTURE_C1_C2  ALL_FE CAPTURE C2_REGIONS
```

In this case, the capture from any Na isotopes appearing in the C2 regions will not be included in the reaction rate. Note that use of the reaction rate sensitivity is only valid for a homogeneous or inhomogeneous fixed source problem.

The REACTION_RATIO sensitivity is very similar to the reaction_rate input but has double the input because it contains the ratio of two reaction rates. From Figure 5.2, the numerator selection of isotopes comes before the denominator set such that an example input would have the form:

```
REACTION_RATIO Alpha_U28c ALL_ISO  ALPHA C1_ZONES  ALL_U238 CAPTURE ENTIRE_CORE
REACTION_RATIO Alpha_U28c ALL_U238 ALPHA C2_ZONES  ALL_U238 CAPTURE ENTIRE_CORE
```

In this example, we select the alpha production from all isotopes in the C1 zones and the alpha production from just U-238 isotopes in the C2 zones as the numerator. In the denominator, we include the capture rate of all U-238 in the core. Similar to the reaction_rate input, the isotopes and regions of both the numerator and denominator reaction rate are not assumed to overlap. In all cases, the reaction rate used in either the numerator or denominator must be constant. Note that power_fraction is therefore a special case of the reaction_ratio input. As a final note, NU, CHI, P1SCATTER, P1ELASTIC, P1INELASTIC, P1N2N, STANDARDSET, and EVERYTHING are invalid as reaction rate selections for the reaction_rate and reaction_ratio sensitivities.

The only remaining sensitivity-related input is the selection of alpha (i.e., the type of cross section to change and the magnitude of variation in the finite difference approximation of the derivative) controlled by SELECT_ALPHA. *In the updated version of PERSENT, all sensitivities for all unique isotopes are computed automatically. Thus the SELECT_ALPHA*

input has its meaning switched from the targeted set of work to complete to the targeted set of data to print. The default selection is to print all isotope data for STANDARDSET which will be invoked if no SELECT_ALPHA line is given for a sensitivity problem. The STANDARDSET option will automatically invoke NU, FISSION, CAPTURE, ELASTIC, INELASTIC, N2N, and P1SCATTER, P1INELASTIC, CHI print outs. The user can neglect providing an isotope set by including a name that does not correspond to an existing isotope set and PERSENT will interpret this as the desire to print all isotope sensitivities for the stated reaction. The user can also neglect providing a reaction type for a given isotope list and PERSENT will assume the user wants the STANDARDSET.

It is important to note in the updated version of PERSENT the υ (NU) sensitivity can be done with respect to the prompt υ or the total υ. In the previous version only the total υ value was allowed which was an oversight compared with conventional sensitivity codes. In this regard, to use the prompt υ, the user must provide a DLAYXS file. If no DLAYXS file is provided and the USE_TOTALNU is not set to YES (default is NO), PERSENT will issue a fatal error and quit. This check acts as a safety valve to ensure users understand what they are using for their sensitivity and uncertainty calculations when selecting a total υ.

An example usage of alpha for a sensitivity problem can be written as

```
SELECT_ALPHA Alpha_U28c ALL_U238 GAMMA
SELECT_ALPHA Alpha_U28c ALL_U238 PROTON
SELECT ALPHA Alpha U28c ALL P239 STANDARDSET
```

In this example, we have three separate inputs specifying different combinations of isotopes and reactions. For the first line, we select all U-238 in the domain and compute the sensitivity with respect to changes in the gamma cross section. The second line specifies the proton cross section of all U-238. The last line is the typical user input which will invoke the print out of the standard sensitivities to all cross sections of all Pu-239 isotopes in the domain. In this context the alpha selection print out will have GAMMA, PROTON, NU, FISSION, CAPTURE, ELASTIC, INELASTIC, N2N, P1SCATTER, P1INELASTIC, and CHI for all of the selected isotopes in the stated isotope sets. The CAPTURE selection merges the contributions from GAMMA, ALPHA, PROTON, DEUTERON, and TRITIUM. Similarly, the SCATTER will merge the contributions from ELASTIC, INELASTIC, and N2N while P1SCATTER will merge the P1ELASTIC, P1INELASTIC, and P1N2N options.

With regard to the isotopes chosen, there is no need to select all O-16 isotope evaluations in the isotope set as they are categorized by ENDF or MC2 assigned named. The following example shows the new output section produced by PERSENT when any sensitivity input is given. In this example, one can see that numerous user element isotopes are identified as FE__SV which is the old MC^2-2 name assigned to the ENDF/B-V element iron data. The other isotopes are similarly mapped according to name. If there is an error in this list, the user must correct their ISOTXS file as it fundamentally either contains an incorrect isotope name or isotope data. If the user provides unique isotope names for every isotope with no commonality, then PERSENT will compute individual sensitivities for every isotope in ISOTXS even if they do not appear in the input geometry. The sensitivity SELECT_ALPHA isotope list can either select a reference isotope name (i.e. MC2 name) or their region assigned name. The isotope list

can contain all isotopes of data that are interested where the output data order will identically match the unique id ordering shown in the above example.

```
Index Unique  ISOTXS ->
    1 FE  SV  FEX      FEI      FEY      FEM      FEZ      FEO      FEB
    2 NP237V  N237X    N237I    N237Y    N237M    N237Z    N237O    N237B
    3 AM243V  A243X    A243I    A243Y    A243M    A243Z    A243O    A243B
    4 ZR  SV  ZIRCX    ZIRCI    ZIRCY    ZIRCM    ZIRCZ    ZIRCO    ZIRCB
    5 AM242M  A24MX    A24MI    A24MY    A24MM    A24MZ    A24MO    A24MB
    6 PU239V  P239X    P239I    P239Y    P239M    P239Z    P239O    P239B
    7 LFPMO2  LFPPX    LFPPI    LFPPY    LFPPM    LFPPZ    LFPPO    LFPPB
    8 CM2415  C241X    C241I    C241Y    C241M    C241Z    C241O    C241B
    9 CM2425  C242X    C242I    C242Y    C242M    C242Z    C242O    C242B
   10 NA23 S  NA23X    NA23I    NA23Y    NA23M    NA23Z    NA23O    NA23B
   11 AL27 5  AL27     AL27V    AL27T    AL27W
   12 XE1355  X135     X135V    X135T    X135W
   13 K    5  K        KV       KT       KW
   14 MO   S  MOX      MOI      MOY      MOM      MOZ      MOO      MOB
   15 CR   S  CRX      CRI      CRY      CRM      CRZ      CRO      CRB
   17 N-14 5  N-14I    N-14M    N-14O    N-14B    N-14IV   N-14MV   N-14OV
   18 O-16 5  O-16X    O-16I    O-16Y    O-16M    O-16Z    O-16O    O-16B
   19 PU2405  P240X    P240I    P240Y    P240M    P240Z    P240O    P240B
   20 PU2415  P241X    P241I    P241Y    P241M    P241Z    P241O    P241B
   25 HE4  5  HE-4     HE-4V    HE-4T    HE-4W
```

5.5 Co-variance and Uncertainty Input Specification

As discussed earlier, an uncertainty quantification (UQ) computation capability was added to PERSENT. The initial version included an explicit connection to the COMMARA data set. In the updated version, the input structure was generalized although the basic file format of COMMARA was still assumed as were the input names. Four additional PERSENT input options were added to main PERSENT input as shown in Figure 5.2. The following example shows how to use them

```
COMMARA_INPUT   bnl.1.apr.2011.commara.with.chi.mubar.matrix
COMMARA_IGNOREMISSINGDATA yes
COMMARA_ISOTOPE FE56K   Fe56
COMMARA_ISOTOPE NA23K   Na
COMMARA_ISOTOPE O16D    O
COMMARA_ISOTOPE U235D   U235
COMMARA_ISOTOPE U238D   U238
COMMARA_ISOTOPE P239D   Pu239
COMMARA_ISOTOPE P240D   Pu240
COMMARA_ISOTOPE P241D   Pu241
COMMARA_REACTION n2n    nxn
```

The COMMARA_INPUT simply allows the user to target a generic file for use as the co-variance matrix. The COMMARA file format can be found in the literature and is not included in this manual. The COMMARA_IGNOREMISSINGDATA is set to YES in the example which is done to avoid a fatal error when data is missing. As an example, if the Fe56 sensitivity data was calculated by PERSENT but is missing in the co-variance matrix PERSENT will die with a fatal error. Conversely, if the Fe56 co-variance data is present but no Fe56 sensitivity data is provided by PERSENT, PERSENT will give a warning. PERSENT will issue warnings if reactions are not present and will exit with a fatal error if no mappings exist between the co-variance data and ISOTXS. In that regard, setting COMMARA_IGNOREMISSINGDATA to YES will always execute if at least one isotope and reaction are mapped properly to the ISOTXS

data set *and omit* the stated warnings and error messages as it assumes the user already has accepted these issues as correct. In that regard, the user should always execute the software with it set to NO initially followed by YES after reviewing the mapping issues. In the example provided, one can clearly see that several co-variance isotopes are mapped to ISOTXS isotopes and only a single reaction is mapped to a PERSENT recognized reaction. By rule, PERSENT is setup to recognize its own names and the COMMARA standard reaction listing and thus a set of COMMARA_REACTION input lines are unnecessary.

To perform an uncertainty calculation, one must use either the SENSITIVITY_DOUQ or BILINEAR input for PERSENT from Figure 5.2. The following example shows how to use sensitivity vectors computed in the PERSENT input and those obtained from files in uncertainty calculations.

```
SENSITIVITY_KEFF  ReferenceCore
SELECT_ALPHA      ReferenceCore  ALL_ISO standardset
SENSITIVITY_EDITS ReferenceCore  PRINT_PERTURBATION ReferenceCore.sens
SENSITIVITY_DOUQ  ReferenceCore  YES YES YES

REACTION_WORTH    S_Change_OFUEL  Change_OFUEL
SELECT_ALPHA      S_Change_OFUEL  ALL_ISO STANDARDSET
SENSITIVITY_EDITS S_Change_OFUEL  PRINT_PERTURBATION
SENSITIVITY_DOUQ  S_Change_OFUEL  NO NO NO

Bilinear CheckLogic ReferenceCore S_Change_OFUEL
SENSITIVITY_DOUQ  CheckLogic  YES YES YES

SENSITIVITY_FILE  LoadFile ReferenceCore.sens

Bilinear CheckFile LoadFile S_Change_OFUEL
SENSITIVITY_DOUQ  CheckFile  YES YES YES
```

As can be seen, we define an eigenvalue (ReferenceCore) and reactivity worth (S_Change_OFUEL) sensitivity operations. In each case, we perform the uncertainty calculation using the calculated sensitivity vector to collapse the co-variance matrix as defined in equation 3.80 where $s_1 = s_2$. In the eigenvalue sensitivity, we export the sensitivity vector to the file "ReferenceCore.sens" which is later loaded using the SENSITIVITY_FILE input as problem LoadFile. With two different sensitivity vectors, the user can use the BILINEAR co-variance matrix operation where the first problem specifies s_1 and the second one defines s_2 in equation 3.80. The file format of the sensitivity file is discussed later in Section 5.8.

Internal to PERSENT, all standard sensitivity calculations are executed followed immediately by their uncertainty calculations. The sensitivity file load operations are treated as sensitivity operations and thus the above input only works because the ReferenceCore input occurs before the LoadFile sensitivity input specification. Only after all sensitivity calculations are complete will PERSENT attempt to apply any BILINEAR operations. As is the case with all other inputs, PERSENT will check the logic of the user inputs before executing any flux or sensitivity calculations excluding the physical import of file based data.

One key feature not described in the previous example is how PERSENT maps the isotopes from one sensitivity file to that of the present one. In ISOTXS, the reference library isotope name is preserved such that PERSENT automatically knows the isotope mapping

between any sensitivity files so long as the reference library was the same. In this regard, assuming the user provided isotope mapping from ISOTXS, see example at the end of Section 5.4, is correct for the sensitivity file, no additional mapping is required by PERSENT. If the mapping is not appropriate, the user must ***manually*** modify the sensitivity file to ensure that the base library isotope mapping between the two sensitivity vectors is consistent. In this regard, if two ISOTXS files with different base libraries (say JENDL and ENDF are used), the user must manually remap the isotopes from one data set to another by modifying the sensitivity file to agree with the user provided ISOTXS. See section 5.8 to understand how to setup the isotope reference names in the sensitivity file. PERSENT will produce warnings for all isotope sensitivities that are not usable due to missing mapping information.

To understand how the representativity calculation process works, we will assume the three reactor problems in Table 5.6. As can be seen, the primary difference between the three problems are reactor size and isotope content. The volume of the reactor has no bearing on the representativity calculation in PERSENT. It is only included in the table to indicates that it is a factor to consider with regard to how the sensitivities of the two systems can be related and just to give the impression that these reactors are physically different. In this example, we thus assume that the user has already decided that these three problems are reasonable to compare. We also note that Table 5.6 does not list any details of the ENDF evaluation of the isotopes and thus assume the isotope mapping to COMMARA data is consistent on the isotopic/elemental basis as appropriate. In this regard, the only factor of interest in Table 5.6 is the fact that isotope data is not consistent between the three reactor problems and thus the user wants to understand how to properly use PERSENT to compute the representativity.

Table 5.6. Hypothetical Representativity Cases

	Reactor Problem 1	Reactor Problem 2	Reactor Problem 3
Volume m^3	2.0	3.0	2.5
U-235	Y	Y	Y
U-238	Y	Y	Y
Pu-239	Y	N	N
Na	Y	Y	Y
Fe	Y	Y	Y
Ni	Y	N	Y
Pu-240	Y	Y	N
File Name	RP1.sens	RP2.sens	RP3.sens

If we want to compute the representativity from reactor 1 to reactor 2, we first take note that reactor problem 1 contains all of the isotopes of interest in reactor problem 2 while reactor problem 2 does not contain all of those in reactor problem 1. In this regard, we know that the bilinear operation defined earlier in equation 3.80 will have zero representativity components coming from reactor problem 2 into reactor problem 1. The best PERSENT input should take the reactor problem 1 as its “base” state and have the input of:

```
!Appropriate Input Example Reactor 1 to Reactor 2
DIF3D_INPUT        reactor1.inp
ISOTXS_INPUT       reactor1.ISOTXS

SENSITIVITY_FILE Reactor1 RP1.sens
SENSITIVITY_DOUQ Reactor1

SENSITIVITY_FILE Reactor2 RP2.sens
SENSITIVITY_DOUQ Reactor2

BILINEAR Numer Reactor1 Reactor2
SENSITIVITY_DOUQ Numer
```

From this example input, one can see that the DIF3D and ISOTXS input refer to the reactor 1 related data. This is very important as the COMMARA mapping will be bound by the set of isotopes found in the reactor1.ISOTXS file and thus reactor problem 1. To get all of the output in the same file, we can have PERSENT perform the UQ calculations for each reactor problem (1 & 2) upon loading the sensitivity files and then the bilinear operation at the end. The results of these UQ calculations can be combined to give the representativity using the standard technique

$$R = \frac{s_1^T \cdot D \cdot s_2}{\sqrt{s_1^T \cdot D \cdot s_1} \cdot \sqrt{s_2^T \cdot D \cdot s_2}}. \tag{5.1}$$

In the output, PERSENT will issue the following warnings associated with loading the RP2.sens file:

```
[PERSENT]...No sensitivity data was provided for unique isotope PU239
[PERSENT]...No sensitivity data was provided for unique isotope NI
```

These warnings just indicate that PERSENT is going to assume zero sensitivities for reactor problem 2 with respect to the Pu239 and Ni isotopes which is the only thing it can do.

An alternative input setup with respect to reactor problem 2 can be written as:

```
! Inappropriate setup example Reactor 1 to Reactor 2
DIF3D_INPUT        reactor2.inp
ISOTXS_INPUT       reactor2.ISOTXS

SENSITIVITY_FILE Reactor1 RP1.sens
SENSITIVITY_DOUQ Reactor1             ! This will yield an invalid UQ result

SENSITIVITY_FILE Reactor2 RP2.sens
SENSITIVITY_DOUQ Reactor2

BILINEAR Numer Reactor1 Reactor2
SENSITIVITY_DOUQ Numer
```

With respect to the UQ calculation, the “Numer” and “Reactor2” calculations will yield identical results to that of the first example above. However, the “Reactor1” calculation will not produce the same UQ result as the previous one as PERSENT will artificially zero out the sensitivity data from Pu239 and Ni as indicated by the warning messages:

```
[PERSENT]...The sensitivity data from file isotope PU239 has no storage destination
[PERSENT]...The sensitivity data from file isotope NI    has no storage destination
```

It is important to note the difference in meaning between these warnings from PERSENT and the earlier ones such that the latter set should always be checked for acceptability. In this case it is an indication to the user they are going to get an incorrect UQ assessment.

In the next example, we consider the representativity of mapping reactor problem 2 to reactor 3 in Table 5.6. In this case, the set of isotopes in either model is missing a key isotope from the other model. Because these isotopes are likely to be important for the sensitivity calculation it is strongly advised not to have PERSENT perform the UQ calculation for one of the two file load operations, but instead to have it generate that result when creating the sensitivity vector file or in a separate PERSENT calculation (not shown). The best input for the bilinear operation in this case is:

```
!Appropriate Input Example Reactor 2 to Reactor 3
DIF3D_INPUT        reactor2.inp
ISOTXS_INPUT       reactor2.ISOTXS

SENSITIVITY_FILE Reactor2 RP2.sens
SENSITIVITY_DOUQ Reactor2

SENSITIVITY_FILE Reactor3 RP3.sens
!SENSITIVITY_DOUQ Reactor3  This would produce an invalid UQ result

BILINEAR Numer Reactor2 Reactor3
SENSITIVITY_DOUQ Numer
```

The output warnings from PERSENT when loading RP3.sens in this case will be:

```
[PERSENT]...No sensitivity data was provided for unique isotope PU240
[PERSENT]...The sensitivity data from file isotope NI    has no storage destination
```

Note that there is a warning about both missing data on the file and data that cannot be used. These are acceptable as PERSENT will discard the unusable data and set the missing data to zero as is appropriate.

The primary motivation behind the preceding setup of PERSENT is to allow the user to perform the necessary UQ and representativity calculations without having to modify their existing reactor models. While users should be very careful to understand and check any mapping issues reported by the COMMARA mapping or the PERSENT mapping for their isotopic data, the preceding setup is the most logical approach to handling the issue of different isotopic vectors for different reactors which is a standard problem when comparing operational reactors against experimental mockups.

5.6 Example PERSENT Output

From the preceding discussion, it should not be necessary to completely display a PERSENT perturbation or sensitivity input deck. Consequently, we assume the reader can review the DIF3D and PERSENT example inputs when discussing the output of PERSENT in this section. The first problem to study is example problem #5. It is a two-dimensional hexagonal geometry and has a series of perturbation problems. An excerpt of the output from the RC_TO_RD perturbation from example #5 is given in Figure 5.3.

As can be seen in Figure 5.3, each PERSENT perturbation problem is signaled with stating the problem name (RC_TO_RD), its type (zone perturbation), and the methodology (generalized perturbation theory). It also indicates which DIF3D output file is associated with the perturbation (P_dif3d_problem0001.out). Given that this is a zone perturbation (ADJUST_ZONE) the input immediately appearing after the header is the list of which zones modified in order to impose the perturbation (zone RC is replaced with zone RD). After this is

complete, the input is fully prepared and, given that this is a generalized perturbation theory problem, DIF3D is invoked to obtain the perturbed NHFLUX file. In a first order perturbation theory problem, DIF3D will be invoked to obtain the homogenized cross section data.

After the DIF3D code returns the solution of the perturbed problem, PERSENT issues a single line of output to indicate that it is performing the numerator and denominator inner products which it subsequently displays according to the selected problem_edits. In this case, the selection clearly chose PRINT_BY_MESH, PRINT_BY_REGION, and PRINT_BALANCE. The total reactivity worth was computed to be -0.2256. One can easily use the unix "grep" function to extract the perturbation output out of a complicated output file due to the leading "=PERSENT" printing on the relevant output lines.

The next section of output is taken from the same example problem but for the FO_RC_TO_RD perturbation. In this case, we have truncated the output in Figure 5.4. Note that the PRINT_BY_MASS option was clearly invoked in this case along with the options used for RC_TO_RD. The inclusion of print_by_mass nearly triples the output where the first section of output is just the total mass change (mostly a change in iron). Focusing only on the total values, one finds a 3.67 kg change in mass resulted from this perturbation yielding a total change in reactivity of -0.331 and -0.0902 change in reactivity per unit change in mass. The region edits provide the total mass change by region, the reactivity worth breakdown by region and balance edit, along with the reactivity worth per unit mass change in *each region* also broken down into the balance edits. It is important to note that the worth/mass edit cannot be directly summed to give the total worth/mass result!

The Λ and β output from example problem #5 is displayed in Figure 5.5. In this case the user cannot assign the problem name (LAMBDA_BETA) nor the methodology, but the same type of header is included at the beginning of the perturbation problem. Noting that the input only specifies PRINT_BALANCE and PRINT_BY_UNIQUE, one can see the former clearly forces the region wise edits to be engaged. The total values of Λ and β are again included on lines starting with "=PERSENT" and found to be $4.4 \cdot 10^{-7}$ for Λ_G, and $5.0 \cdot 10^{-7}$ for Λ, and 0.00318 for β. Much like the other reactivity worths, the two components are broken down by region where the sum of regions for lambda yields Λ_G. Because the user selected PRINT_BY_UNIQUE, the coalesced kinetics parameters are exported for the unique isotopes. By default, PERSENT will always generate the coalesced kinetics parameters for the whole domain when the LAMBDA_BETA option is invoked.

```
[PERSENT]....................................................................
[PERSENT]...Problem RC_TO_RD         is a zone perturbation using GENERALIZED_PT
[PERSENT]...Associated DIF3D output is P_dif3d_problem0001.out
[PERSENT]....................................................................
[PERSENT]...Replacing zone     RC       with copy of zone     RD
[PERSENT]...Running DIF3D to get the perturbed forward solution
[PERSENT]...Performing the DIF3D-VARIANT numerator/denominator operations
[PERSENT]...Start of numerator/sum(denominator) table for General PT of RC_TO_RD
               1          2          3          4          5          6          7          8          9         10         11
    11  0.000E+00  0.000E+00  0.000E+00  0.000E+00  0.000E+00  0.000E+00  0.000E+00  0.000E+00  0.000E+00  0.000E+00  0.000E+00
    10  0.000E+00  0.000E+00  0.000E+00  0.000E+00  0.000E+00  0.000E+00  0.000E+00  0.000E+00  0.000E+00  0.000E+00  0.000E+00
     9  0.000E+00  0.000E+00  0.000E+00  0.000E+00  0.000E+00  0.000E+00  0.000E+00  0.000E+00  0.000E+00  0.000E+00  0.000E+00
     8  0.000E+00  0.000E+00  0.000E+00  0.000E+00  0.000E+00  0.000E+00  0.000E+00  0.000E+00  0.000E+00  0.000E+00  0.000E+00
     7  0.000E+00  0.000E+00  0.000E+00  0.000E+00  0.000E+00  0.000E+00  0.000E+00  0.000E+00  0.000E+00  0.000E+00  0.000E+00
     6 -9.847E-03  0.000E+00  0.000E+00  0.000E+00  0.000E+00 -9.847E-03  0.000E+00  0.000E+00  0.000E+00  0.000E+00  0.000E+00
     5  0.000E+00  0.000E+00  0.000E+00  0.000E+00  0.000E+00  0.000E+00  0.000E+00  0.000E+00  0.000E+00  0.000E+00  0.000E+00
     4 -2.300E-02  0.000E+00  0.000E+00 -2.300E-02  0.000E+00  0.000E+00  0.000E+00  0.000E+00  0.000E+00  0.000E+00  0.000E+00
     3  0.000E+00  0.000E+00  0.000E+00  0.000E+00  0.000E+00  0.000E+00  0.000E+00  0.000E+00  0.000E+00  0.000E+00  0.000E+00
     2  0.000E+00  0.000E+00  0.000E+00  0.000E+00  0.000E+00  0.000E+00  0.000E+00  0.000E+00  0.000E+00  0.000E+00  0.000E+00
     1 -2.851E-02  0.000E+00  0.000E+00 -2.300E-02  0.000E+00 -9.847E-03  0.000E+00  0.000E+00  0.000E+00  0.000E+00  0.000E+00
[PERSENT]...Region edits for General PT of RC_TO_RD
[PERSENT]...|Region| Numerator | Numerator /      = Leakage  +  Capture + Fission  + Out Scatter - In Scatter - Production  ||   n,2n    |
[PERSENT]...|      |           | Sum[Denominator] |          |          |           |              |              |              ||           |
[PERSENT]...|ROD1  | -1.266E+20|        -2.851E-02| 4.367E-05|-2.598E-02| 0.000E+00|   -1.700E-02|  -1.444E-02|    0.000E+00|| 0.000E+00|
[PERSENT]...|CORE1 |  0.000E+00|         0.000E+00| 0.000E+00| 0.000E+00| 0.000E+00|    0.000E+00|   0.000E+00|    0.000E+00|| 0.000E+00|
[PERSENT]...|ROD2  | -3.065E+20|        -6.901E-02| 5.035E-04|-6.395E-02| 0.000E+00|   -4.367E-02|  -3.811E-02|    0.000E+00|| 0.000E+00|
[PERSENT]...|ROD3  | -3.065E+20|        -6.901E-02| 5.035E-04|-6.395E-02| 0.000E+00|   -4.367E-02|  -3.811E-02|    0.000E+00|| 0.000E+00|
[PERSENT]...|CORE2 |  0.000E+00|         0.000E+00| 0.000E+00| 0.000E+00| 0.000E+00|    0.000E+00|   0.000E+00|    0.000E+00|| 0.000E+00|
[PERSENT]...|ROD4  | -1.312E+20|        -2.954E-02| 3.562E-03|-3.044E-02| 0.000E+00|   -2.089E-02|  -1.823E-02|    0.000E+00|| 0.000E+00|
[PERSENT]...|ROD5  | -1.312E+20|        -2.954E-02| 3.562E-03|-3.044E-02| 0.000E+00|   -2.089E-02|  -1.823E-02|    0.000E+00|| 0.000E+00|
[PERSENT]...|BLAN  |  0.000E+00|         0.000E+00| 0.000E+00| 0.000E+00| 0.000E+00|    0.000E+00|   0.000E+00|    0.000E+00|| 0.000E+00|
[PERSENT]...|REFL  |  0.000E+00|         0.000E+00| 0.000E+00| 0.000E+00| 0.000E+00|    0.000E+00|   0.000E+00|    0.000E+00|| 0.000E+00|
=PERSENT...Parameter General PT of RC_TO_RD          is -2.25609E-01 denominator  4.44105E+21 k-eff A  1.1444027E+00 F  9.0956324E-01
```

Figure 5.3. PERSENT Output for RC_TO_RD Perturbation from Example Problem #5.

```
[PERSENT]...Problem FO_RC_TO_RD      is a zone perturbation using FIRST_ORDER_PT
…
[PERSENT]...This perturbation has total core changes in mass of
[PERSENT]...NA23 5            -0.6254 kg
[PERSENT]...FE   5             2.3705 kg
[PERSENT]...O-16 5             0.5589 kg
[PERSENT]...B-10 5             0.2113 kg
[PERSENT]...C    5             1.1595 kg
[PERSENT]...Region edits for mass(kg) change for FO_RC_TO_RD
[PERSENT]...|Region| Numerator | Numerator /      |
[PERSENT]...|      |           | Sum[Denominator] |
[PERSENT]...|ROD1  |  0.000E+00|         2.827E-01|
[PERSENT]...|CORE1 |  0.000E+00|         0.000E+00|
[PERSENT]...|ROD2  |  0.000E+00|         8.480E-01|
[PERSENT]...|ROD3  |  0.000E+00|         8.480E-01|
[PERSENT]...|CORE2 |  0.000E+00|         0.000E+00|
[PERSENT]...|ROD4  |  0.000E+00|         8.480E-01|
[PERSENT]...|ROD5  |  0.000E+00|         8.480E-01|
[PERSENT]...|BLAN  |  0.000E+00|         0.000E+00|
[PERSENT]...|REFL  |  0.000E+00|         0.000E+00|
=PERSENT...Parameter mass(kg) change for FO_RC_TO_RD  is  3.67485E+00 denominator  0.00000E+00 k-eff A  0.0000000E+00 F  0.0000000E+00
[PERSENT]...Region edits for First O PT of FO_RC_TO_RD
[PERSENT]...|Region| Numerator | Numerator /      = Leakage  +  Capture + Fission  + Out Scatter - In Scatter - Production  ||   n,2n    |
[PERSENT]...|      |           | Sum[Denominator] |          |          |          |              |              |             ||           |
[PERSENT]...|ROD1  | -2.027E+20|        -4.497E-02| 6.657E-06|-4.192E-02| 0.000E+00|   -2.014E-02|  -1.709E-02|    0.000E+00|| 0.000E+00|
[PERSENT]...|CORE1 |  0.000E+00|         0.000E+00| 0.000E+00| 0.000E+00| 0.000E+00|    0.000E+00|   0.000E+00|    0.000E+00|| 0.000E+00|
[PERSENT]...|ROD2  | -4.594E+20|        -1.019E-01| 1.074E-03|-9.672E-02| 0.000E+00|   -4.898E-02|  -4.273E-02|    0.000E+00|| 0.000E+00|
[PERSENT]...|ROD3  | -4.594E+20|        -1.019E-01| 1.074E-03|-9.671E-02| 0.000E+00|   -4.898E-02|  -4.273E-02|    0.000E+00|| 0.000E+00|
[PERSENT]...|CORE2 |  0.000E+00|         0.000E+00| 0.000E+00| 0.000E+00| 0.000E+00|    0.000E+00|   0.000E+00|    0.000E+00|| 0.000E+00|
[PERSENT]...|ROD4  | -1.863E+20|        -4.132E-02| 7.410E-03|-4.575E-02| 0.000E+00|   -2.333E-02|  -2.035E-02|    0.000E+00|| 0.000E+00|
[PERSENT]...|ROD5  | -1.863E+20|        -4.131E-02| 7.410E-03|-4.575E-02| 0.000E+00|   -2.333E-02|  -2.035E-02|    0.000E+00|| 0.000E+00|
[PERSENT]...|BLAN  |  0.000E+00|         0.000E+00| 0.000E+00| 0.000E+00| 0.000E+00|    0.000E+00|   0.000E+00|    0.000E+00|| 0.000E+00|
[PERSENT]...|REFL  |  0.000E+00|         0.000E+00| 0.000E+00| 0.000E+00| 0.000E+00|    0.000E+00|   0.000E+00|    0.000E+00|| 0.000E+00|
=PERSENT...Parameter First O PT of FO_RC_TO_RD        is -3.31367E-01 denominator  4.50882E+21 k-eff A  1.1444033E+00 F  1.1444027E+00
[PERSENT]...Region edits/mass(kg) for First O PT of FO_RC_TO_RD
[PERSENT]...|Region| Numerator | Numerator /      = Leakage  +  Capture + Fission  + Out Scatter - In Scatter - Production  ||   n,2n    |
[PERSENT]...|      |           | Sum[Denominator] |          |          |          |              |              |             ||           |
[PERSENT]...|ROD1  | -7.172E+20|        -1.591E-01| 2.355E-05|-1.483E-01| 0.000E+00|   -7.124E-02|  -6.045E-02|    0.000E+00|| 0.000E+00|
[PERSENT]...|CORE1 |  0.000E+00|         0.000E+00| 0.000E+00| 0.000E+00| 0.000E+00|    0.000E+00|   0.000E+00|    0.000E+00|| 0.000E+00|
[PERSENT]...|ROD2  | -5.417E+20|        -1.201E-01| 1.267E-03|-1.140E-01| 0.000E+00|   -5.775E-02|  -5.039E-02|    0.000E+00|| 0.000E+00|
[PERSENT]...|ROD3  | -5.417E+20|        -1.201E-01| 1.267E-03|-1.140E-01| 0.000E+00|   -5.775E-02|  -5.039E-02|    0.000E+00|| 0.000E+00|
[PERSENT]...|CORE2 |  0.000E+00|         0.000E+00| 0.000E+00| 0.000E+00| 0.000E+00|    0.000E+00|   0.000E+00|    0.000E+00|| 0.000E+00|
[PERSENT]...|ROD4  | -2.197E+20|        -4.872E-02| 8.738E-03|-5.395E-02| 0.000E+00|   -2.751E-02|  -2.400E-02|    0.000E+00|| 0.000E+00|
[PERSENT]...|ROD5  | -2.197E+20|        -4.872E-02| 8.738E-03|-5.395E-02| 0.000E+00|   -2.751E-02|  -2.400E-02|    0.000E+00|| 0.000E+00|
[PERSENT]...|BLAN  |  0.000E+00|         0.000E+00| 0.000E+00| 0.000E+00| 0.000E+00|    0.000E+00|   0.000E+00|    0.000E+00|| 0.000E+00|
[PERSENT]...|REFL  |  0.000E+00|         0.000E+00| 0.000E+00| 0.000E+00| 0.000E+00|    0.000E+00|   0.000E+00|    0.000E+00|| 0.000E+00|
=PERSENT...Parameter First O PT of FO_RC_TO_RD        is -9.01715E-02 denominator  4.50882E+21 k-eff A  1.1444033E+00 F  1.1444027E+00
```

Figure 5.4. PERSENT Output for FO_RC_TO_RD Perturbation from Example Problem #5.

```
[PERSENT]....................................................................
[PERSENT]...Problem LAMBDA_BETA      is infamous
[PERSENT]....................................................................
[PERSENT]...Region edits for LAMBDA
[PERSENT]...|Region| Numerator | Numerator /      |
[PERSENT]...|      |           | Sum[Denominator] |
[PERSENT]...|ROD1  |  2.640E+13|         5.854E-09|
[PERSENT]...|CORE1 |  6.922E+14|         1.535E-07|
[PERSENT]...|ROD2  |  6.095E+13|         1.352E-08|
[PERSENT]...|ROD3  |  6.095E+13|         1.352E-08|
[PERSENT]...|CORE2 |  9.658E+14|         2.142E-07|
[PERSENT]...|ROD4  |  2.884E+13|         6.397E-09|
[PERSENT]...|ROD5  |  2.884E+13|         6.396E-09|
[PERSENT]...|BLAN  |  1.168E+14|         2.589E-08|
[PERSENT]...|REFL  |  6.088E+12|         1.350E-09|
=PERSENT...Parameter LAMBDA Generation time  4.40659E-07 Prompt Lifetime  5.04291E-07 denominator  4.50882E+21 k-eff  1.1444027E+00
[PERSENT]...Region edits for Parameter BETA is
[PERSENT]...|Region| Numerator | Numerator /      |
[PERSENT]...|      |           | Sum[Denominator] |
[PERSENT]...|ROD1  |  0.000E+00|         0.000E+00|
[PERSENT]...|CORE1 |  5.210E+18|         1.156E-03|
[PERSENT]...|ROD2  |  0.000E+00|         0.000E+00|
[PERSENT]...|ROD3  |  0.000E+00|         0.000E+00|
[PERSENT]...|CORE2 |  8.509E+18|         1.887E-03|
[PERSENT]...|ROD4  |  0.000E+00|         0.000E+00|
[PERSENT]...|ROD5  |  0.000E+00|         0.000E+00|
[PERSENT]...|BLAN  |  6.073E+17|         1.347E-04|
[PERSENT]...|REFL  |  0.000E+00|         0.000E+00|
=PERSENT...Parameter BETA is         3.17745E-03 denominator  4.50882E+21 k-eff  1.1444027E+00
=PERSENT...Domain coalesced kinetics parameters for unique isotope PU239S
=PERSENT...Family     beta(i)    lambda(i)
=PERSENT...   1   9.65630E-04  3.00000E-02
=PERSENT...   2   8.69196E-04  1.00000E+00
=PERSENT...Domain coalesced kinetics parameters for unique isotope U-238S
=PERSENT...Family     beta(i)    lambda(i)
=PERSENT...   1   4.26895E-04  3.00000E-02
=PERSENT...   2   9.15729E-04  1.00000E+00
=PERSENT...Domain coalesced effective point kinetics parameters
=PERSENT...Family     beta(i)    lambda(i)
=PERSENT...   1   1.39252E-03  3.00000E-02
=PERSENT...   2   1.78492E-03  1.00000E+00
```

Figure 5.5. PERSENT Output for Lambda and Beta from Example Problem #5.

The next input of interest is a sensitivity problem for which we choose example problem #14. This problem is identical to example problem #5 except for the perturbations chosen for study in PERSENT. In example #14, a cross section perturbation and zone density perturbation are studied using the sensitivity option. In addition to these reactivity worth sensitivities, an eigenvalue and power fraction sensitivity are provided. Figure 5.6 gives the sensitivity output for the eigenvalue sensitivity and two reactivity worths while Figure 5.7 gives the sensitivity output for the power fraction and reaction rate ratio problems. Note that the accuracy of the sensitivity calculations is assessed in Section 7 of this report.

As seen in Figure 5.6, each sensitivity problem is reported with a header giving the problem name, the type of sensitivity, and the associated DIF3D output file. For the eigenvalue sensitivity, the input provided to PERSENT consists of:

```
SENSITIVITY_KEFF  ReferenceCore
SELECT_ALPHA      ReferenceCore  JUST_U238 everything
SENSITIVITY_EDITS ReferenceCore  PRINT_PERTURBATION
```

Looking at the output for the eigenvalue sensitivity in Figure 5.6, one can identify the table of sensitivities which is preceded by a single line of output specifying an eigenvalue and the current isotope set that yields the table of sensitivity data. From the table of data, one can see that there are no sensitivities to the P_1 scattering data which is due to the fact that there are no anisotropic scattering cross sections in this problem. The remaining sensitivities vary considerably in terms of their magnitude, and one would have to do a detailed comparison with the cross section data to make sense of the results. Take note that a TOTAL cross section sensitivity result is printed which is the sensitivity computed if all principle and scattering cross sections are computed except for υ, and the anisotropic P_N scattering are perturbed and should be the logical sum of all of the other components. A NUFISSION sensitivity is also computed but it is always identical to the FISSION cross section sensitivity. Finally, the POWER sensitivity is also printed but since it is not a physical cross section, it will always be zero for all sensitivities of all isotopes.

The output in Figure 5.6 continues with the cross section reactivity worth sensitivity which has similar output structure to the preceding eigenvalue sensitivity. In both cases, the total reactivity worth of the perturbation is generated with the familiar “=PERSENT” line. In the first case, the adjust_xs related worth is reported to be -7.5E-5 while the adjust_density related worth is 8.0E-5 (see the actual physical output). In both cases the same isotope set is chosen for the sensitivity. Given the relative magnitude of the perturbation, one can compare the two results against each other and find that the sensitivities depend upon the actual reaction rates impact upon the given reactivity worth.

Moving on to Figure 5.7, one again sees the same type of output observed in Figure 5.6 except we now have inhomogeneous solver output which we have truncated. We have also truncated the sensitivity data to remove zeros. As can be seen, the inhomogeneous solver repeatedly calls DIF3D, requiring 36 iterations for the power fraction problem and 30 for the reaction rate ratio problem to achieve the desired convergence. The “Outers” column indicates the number of outer iterations used in each DIF3D call while the “Total” column tracks the total number used.

```
[PERSENT]..................................................
[PERSENT]...Problem REFERENCECORE    is a eigenvalue sensitivity
[PERSENT]...Associated DIF3D output is S_dif3d_problem0001.out
[PERSENT]..................................................
[PERSENT]...Sensitivity of the eigenvalue      1.173141 to isotope:         U-238S
[PERSENT]...GROUP   ALPHA->    TOTAL         NU            NUFISSION     FISSION       CAPTURE       GAMMA         ALPHA
[PERSENT]...    1             2.880769E-02  9.802353E-02  5.533640E-02  5.533640E-02 -9.736371E-03 -9.736371E-03  0.000000E+00
[PERSENT]...    2            -4.678183E-02  3.176629E-04  1.857303E-04  1.857303E-04 -5.414296E-02 -5.414296E-02  0.000000E+00
[PERSENT]...    3            -1.579440E-01  9.118740E-05  5.939785E-05  5.939785E-05 -1.668846E-01 -1.668846E-01  0.000000E+00
[PERSENT]...COLUMN SUM       -1.759182E-01  9.843238E-02  5.558153E-02  5.558153E-02 -2.307639E-01 -2.307639E-01  0.000000E+00
  PROTON        TRITIUM       DEUTERIUM     SCATTER       ELASTIC       INELASTIC     N2N           P1SCATTER     P1ELASTIC
 0.000000E+00  0.000000E+00  0.000000E+00 -1.801875E-02  5.394987E-03 -2.316254E-02 -2.511912E-04  0.000000E+00  0.000000E+00
 0.000000E+00  0.000000E+00  0.000000E+00  7.170177E-03  1.348093E-02 -6.310751E-03  0.000000E+00  0.000000E+00  0.000000E+00
 0.000000E+00  0.000000E+00  0.000000E+00  8.976344E-03  8.953683E-03  2.266144E-05  0.000000E+00  0.000000E+00  0.000000E+00
 0.000000E+00  0.000000E+00  0.000000E+00 -1.872226E-03  2.782960E-02 -2.945063E-02 -2.511912E-04  0.000000E+00  0.000000E+00
  P1INELASTIC   P1N2N         POWER         CHI           CHI_FD             ROW SUM
 0.000000E+00  0.000000E+00  0.000000E+00  7.891214E-02  1.443508E-01  4.052567E-01
 0.000000E+00  0.000000E+00  0.000000E+00  1.876346E-02  3.440329E-02 -8.687153E-02
 0.000000E+00  0.000000E+00  0.000000E+00  6.716501E-04  1.237495E-03 -4.716414E-01
 0.000000E+00  0.000000E+00  0.000000E+00  9.834725E-02  1.799915E-01 -1.532563E-01
[PERSENT]..................................................................................................
[PERSENT]...Problem S_MODIFY_GAMMA   is a reactivity worth sensitivity
[PERSENT]...Associated DIF3D output is S_dif3d_problem0002.out
[PERSENT]..................................................................................................
[PERSENT]...Sensitivity of a cross section perturbation reactivity worth -7.536463E-05 to isotope:         U-238S
[PERSENT]...GROUP   ALPHA->    TOTAL         NU            NUFISSION     FISSION       CAPTURE       GAMMA         ALPHA
[PERSENT]...    1            -5.980063E-02 -1.939188E-01 -1.489109E-01 -1.489109E-01  1.026571E-02  1.026571E-02  0.000000E+00
[PERSENT]...    2             9.420552E-02 -6.213701E-04 -5.347875E-04 -5.347875E-04  3.553211E-02  3.553211E-02  0.000000E+00
[PERSENT]...    3            -4.435073E-01  3.796585E-05 -5.200737E-05 -5.200737E-05 -4.723296E-01 -4.723296E-01  0.000000E+00
[PERSENT]...COLUMN SUM       -4.091024E-01 -1.945022E-01 -1.494977E-01 -1.494977E-01 -4.265317E-01 -4.265317E-01  0.000000E+00
   PROTON        TRITIUM       DEUTERIUM     SCATTER       ELASTIC       INELASTIC     N2N           P1SCATTER     P1ELASTIC
  0.000000E+00  0.000000E+00  0.000000E+00  8.013762E-02 -6.048697E-03  8.527929E-02  9.070254E-04  0.000000E+00  0.000000E+00
  0.000000E+00  0.000000E+00  0.000000E+00  5.921162E-02  8.015875E-03  5.119574E-02  0.000000E+00  0.000000E+00  0.000000E+00
  0.000000E+00  0.000000E+00  0.000000E+00  2.914374E-02  2.907016E-02  7.357551E-05  0.000000E+00  0.000000E+00  0.000000E+00
  0.000000E+00  0.000000E+00  0.000000E+00  1.684930E-01  3.103734E-02  1.365486E-01  9.070254E-04  0.000000E+00  0.000000E+00
   P1INELASTIC   P1N2N         POWER         CHI           CHI_FD             ROW SUM
  0.000000E+00  0.000000E+00  0.000000E+00 -1.621719E-01 -1.567466E-01 -6.896530E-01
  0.000000E+00  0.000000E+00  0.000000E+00 -3.155740E-02 -2.443443E-02  2.260102E-01
  0.000000E+00  0.000000E+00  0.000000E+00 -4.013025E-04  4.788948E-04 -1.329867E+00
  0.000000E+00  0.000000E+00  0.000000E+00 -1.941306E-01 -1.807021E-01 -1.793510E+00
```

Figure 5.6. PERSENT Sensitivity Output for the Eigenvalue and Cross Section Perturbations from Example Problem #14.

```
[PERSENT]....................................................................
[PERSENT]...Problem S_POWER_FRACTION is a power fraction sensitivity
[PERSENT]...Associated DIF3D output is S_dif3d_problem0004.out
[PERSENT]....................................................................
[PERSENT]...Calling the inhomogeneous fixed source driver for the adjoint Gamma
[PERSENT]...|Iter|Outers|Total |pM| Full Error | Target |Flat P0 Err |   Target   | FM removal  initial |
%PERSENT]...|   1|     5|     5|Y | 1.5969E+00 > 1.0E-3 | 1.7321E+00 >  1.0000E-05| 2  1.0E-15  7.3E-01 |
…
%PERSENT]...|   6|     5|    30|Y | 7.0103E-03 > 1.0E-3 | 1.3762E-05 >  1.0000E-05| 2  1.8E-17  6.4E-01 |
%PERSENT]...|   7|     2|    32|N | 1.6223E+01 > 1.0E-3 | 1.4602E+01 >  1.0000E-05| 2  6.7E-17  1.6E-02 |
…
%PERSENT]...|  36|     1|    66|N | 3.8714E-06 < 1.0E-3 | 2.6136E-06 <  1.0000E-05| 2  3.9E-18  1.8E-01 |
 [PERSENT]...Sensitivity of the power fraction      0.692956 to isotope:         U-238S
[PERSENT]...GROUP   ALPHA->    TOTAL         NU            NUFISSION     FISSION       CAPTURE       GAMMA         SCATTER
[PERSENT]...    1            -3.013735E-03 -4.918478E-03 -2.706025E-02 -2.706025E-02  5.635472E-04  5.635472E-04  2.357533E-02
[PERSENT]...    2             2.114555E-04 -2.059690E-05 -1.901696E-04 -1.901696E-04 -3.367451E-03 -3.367451E-03  3.768945E-03
[PERSENT]...    3            -1.172589E-02 -6.199194E-06 -7.752252E-05 -7.752252E-05 -1.258008E-02 -1.258008E-02  9.326474E-04
[PERSENT]...COLUMN SUM       -1.452817E-02 -4.945274E-03 -2.732794E-02 -2.732794E-02 -1.538398E-02 -1.538398E-02  2.827692E-02
   ELASTIC       INELASTIC     N2N            CHI_FD            ROW SUM
  5.346632E-03  1.806190E-02  1.667981E-04  -1.537128E-02 -2.914623E-02
  4.437706E-03 -6.687613E-04  0.000000E+00  -1.231944E-03 -6.184375E-04
  9.302928E-04  2.354537E-06  0.000000E+00  -6.197858E-05 -3.524398E-02
  1.071463E-02  1.739549E-02  1.667981E-04  -1.666520E-02 -6.500865E-02
[PERSENT]....................................................................
[PERSENT]...Problem RATIO_P39F_U38C  is a reaction rate ratio sensitivity
[PERSENT]....................................................................
[PERSENT]...Calling the inhomogeneous fixed source driver for the adjoint Gamma
[PERSENT]...|Iter|Outers|Total |pM| Full Error | Target |Flat P0 Err |   Target   | FM removal  initial |
%PERSENT]...|   1|     5|     5|Y | 1.5969E+00 > 1.0E-3 | 1.7321E+00 >  1.0000E-05| 2  1.2E-17  3.5E-02 |
…
%PERSENT]...|   6|     5|    30|Y | 1.1880E-01 > 1.0E-3 | 6.4508E-06 <  1.0000E-05| 2  6.5E-19  4.8E-03 |
%PERSENT]...|   7|     5|    35|N | 1.0193E+00 > 1.0E-3 | 1.9684E-02 >  1.0000E-05| 2  1.9E-17  2.2E-02 |
…
%PERSENT]...|  30|     2|   105|N | 2.5654E-04 < 1.0E-3 | 3.8180E-06 <  1.0000E-05| 2  4.4E-18  1.6E-03 |
[PERSENT]...Sensitivity of the    FISSION         /CAPTURE          macro reaction rate ratio      1.747982 to isotope: U-238S
=PERSENT]...or sensitivity of the FISSION         /CAPTURE          micro reaction rate ratio      6.292736 to isotope: U-238S
[PERSENT]...GROUP   ALPHA->    TOTAL         NU            NUFISSION     FISSION       CAPTURE       GAMMA         SCATTER
[PERSENT]...    1            -6.805380E-02 -2.392720E-03 -2.861094E-03 -2.861094E-03 -3.700099E-02 -3.700099E-02 -2.820518E-02
[PERSENT]...    2            -2.401029E-01 -1.327885E-05  1.088247E-05  1.088247E-05 -2.057973E-01 -2.057973E-01 -3.431557E-02
[PERSENT]...    3            -6.263114E-01 -5.214840E-06  1.915259E-05  1.915259E-05 -6.194722E-01 -6.194722E-01 -6.931312E-03
[PERSENT]...COLUMN SUM       -9.344681E-01 -2.411214E-03 -2.831059E-03 -2.831059E-03 -8.622705E-01 -8.622705E-01 -6.945206E-02
  ELASTIC       INELASTIC     N2N           CHI_FD            ROW SUM
 1.308525E-03 -2.920088E-02 -3.128179E-04  1.643871E-03 -2.049372E-01
-1.094341E-02 -2.337216E-02  0.000000E+00 -5.643560E-03 -7.259636E-01
-6.913813E-03 -1.749861E-05  0.000000E+00 -8.911336E-04 -1.879977E+00
-1.654870E-02 -5.259054E-02 -3.128179E-04 -4.890822E-03 -2.810877E+00
```

Figure 5.7. PERSENT Sensitivity Output for the Power Fraction and Reaction Rate Ratio from Example Problem #14

The “pM” column refers to the partitioned matrix acceleration algorithm of DIF3D-VARIANT which must be disabled in order for the higher order moments to converge. The “Full Error” column gives the iterative error (and its target) in the entire flux vector (all moments of the 6^{th} order P_3 flux in this case) between each call while the “Flat P0 Err” column gives the flat P_0 error (and its target) which is the dominant portion of the solution in the variational nodal method. The “FM removal” column is an assessment of the magnitude of the fundamental mode contamination.

First note that both the “Full” and “Flat P0” errors are relative with respect to each DIF3D call and are not associated with a residual norm (i.e. it is RMS) thus it will not account for the relative importance of the various components. Also note that the full flux vector result will not achieve convergence as fast as the flat P_0 error due to the fixed iteration algorithm used in DIF3D-VARIANT. A code limit of 10^{-3} is placed on the high order moments to ensure some level of accuracy on those moments.

Breaking down the power fraction sensitivity, the “Outers” column can be seen to start at 5 and reduce to 1 at the end of the calculation. The total number of DIF3D outer iterations is 66. The reason for using so few outer iterations per call is due to the fundamental mode contamination which is seen on the right most columns. The first number in the FM section indicates how many iterations were required to completely remove the fundamental mode contamination (only 1 is ever needed, but more are used to make certain it is gone), the second real number indicates the achieved error while the third number represents the fraction of the total solution that was removed in the first iteration. As can be seen, the fundamental mode constitutes 73% of the solution in the first call to DIF3D while at the end it is only 18%. We obviously cannot reduce the number of iterations below 1 and having a fundamental mode contamination greater than 100% indicates that the inhomogeneous solver is likely achieving nothing with regard to getting a solution. The code automatically adjusts the number of outers that can be used either up or down depending upon the amount of fundamental mode contamination it detects. The default lower bound is 10 while the upper bound is 50. In this particular case, we used the input override “LIMIT_OUTERS” to restrict the number of outers to a maximum of 5 based upon the observed fundamental mode contamination.

Another important aspect to note in these two examples is how the error jumps up when the pM acceleration is disabled. In the power fraction case, the sensitivity results were found to be strongly dependent upon the higher order moments while the reaction rate ratio ones were not. In general, the pM acceleration should be disabled when converging the flux solution in VARIANT which is done here after the flat moment error is reduced. For many problems the error goes up slightly and is seen to decrease again. In this case, the problem has a high dominance ratio and is particularly difficult to solve.

Given the default values, we expect all users will at some point restrict the inhomogeneous solver by using the LIMIT_OUTERS input. It is important to note that one can in theory set the maximum and minimum to one and the IFS solver has, and will, obtain the same solution within the reported error as using higher values. The only trick is that the performance goes down dramatically as DIF3D is being called externally (response matrix formation). The error on the full moment solution gives an indication of the expected error in

the sensitivity coefficient hence the minimal convergence specification. The USE_SHIFT option of the sensitivity should always be set to YES, but one can explore the problems that occur with convergence when the shift is not employed as desired by setting it to NO. It is not unusual for users with large problems and little fundamental mode contamination to change the default minimum number of outers from 10 to 30 and the default maximum from 50 to 100.

Because the same isotope set is used in all of the sensitivities, the same reactions are seen to be non-zero where we note that the 1.0E-9 threshold has completely eliminated the alpha and proton sensitivities from these tables. Note that the error in the high order flux moments would likely negate the accuracy of such sensitivities. As a final note, there are two lines of reaction rate ratio outputs for the reaction rate ratio sensitivity. The first is the macroscopic reaction rate ratio while the second is the effective microscopic reaction rate ratio. The macroscopic is explained exactly in the theory section of this document while the microscopic was not. To compute the microscopic value, the atom densities of the numerator and denominator isotopes are summed and the value on the macroscopic line is multiplied by the denominator sum and divided by the numerator sum. If only a single isotope is selected in both the numerator and denominator (or all isotopes in the numerator and denominator have the same atom densities), then the result will exactly be the microscopic reaction rate ratio. It is important to note that the sensitivities are for the macroscopic reaction rate ratio and that for single isotope reaction rate ratios, the atom density factor cancels out.

5.7 PERSENT Inhomogeneous Fixed Source Solver

One key part of Figure 5.7 to pay attention to is the total number of outer iterations required to solve the inhomogeneous problems. For the power fraction, 66 outer iterations are required, over double that required to solve the base eigenvalue problem. For the reaction rate ratio, 105 outer iterations are required which is over four times as many iterations as the base eigenvalue problem. Unfortunately, DIF3D is a rather old code and did not contain an inhomogeneous solver treatment for any solver options. More problematic is the amount of effort required to include an inhomogeneous solver within DIF3D due to the issues of loading multiple NHFLUX and NAFLUX files within the existing ARC system. As a consequence, we constructed one external to PERSENT which thus suffers the computational expense of having to reform the response matrices with each restart in DIF3D. At this point in time, there is no plan to update the DIF3D code with an inhomogeneous solver, and thus one must suffer through using the inhomogeneous solver we provide.

After using the MAKEINPUTONLY option to generate the DIF3D interface files for a given sensitivity problem one must rename them to the standard DIF3D inputs: GEODST, ISOTXS, LABELS, NDXSRF, ZNATDN, VARSRC. Given that the additional dif3d_ifs.x executable provided with PERSENT has the following command line input

```
dif3d_ifs.x <dif3d.x> <input> <output> <NAFLUX> <NHFLUX> [min] [max] [shift]
dif3d_ifs.x ../dif3d.x dif3d.inp dif3d.out b.NAFLUX b.NHFLUX 0 2 yes
```

Unlike PERSENT, there is no control input file for dif3d_ifs.x as the calculation involved is a simple DIF3D input problem. The location of the dif3d executable is the first input and is done similarly to that done in persent.inp shown earlier. The “dif3d.inp” input specifies the DIF3D input file that should come from the null PERSENT run. While you can specify your own, it is

strongly suggested that you utilize PERSENT to generate this file. The "dif3d.out" file is the output file that you wish to accumulate the standard DIF3D output in. The next two inputs specify the binary forward and adjoint flux files for the conventional DIF3D calculations. The final three inputs are optional and provide the LIMIT_OUTERS and USE_SHIFT functionality.

Note that the number of outer iterations from the PERSENT generated input is normally set as "-3" such that DIF3D will skip the flux solve process. When running dif3d_ifs.x, one does not need to modify this input to a valid number in order to allow the inhomogeneous solve to execute properly. The same is not true for a conventional solution using dif3d.x which would obviously obey the "-3" specification and thus it must be modified appropriately. The output from dif3d_ifs.x is very similar to the section of output from PERSENT for the inhomogeneous problem as seen in the example from Figure 5.8. Ignoring the output that is similar to PERSENT, the most important part is the last line which indicates where the Lagrange multiplier flux solution is stored (NAFLUX in this case).

5.8 PERSENT Sensitivity File Format

The sensitivity vector stored internal to PERSENT has three dimensions: energy groups, reactions, and isotope. The sensitivity vector constitutes a large amount of information even though not all of it might be used in a specific UQ calculation. The usage of the sensitivity vector file in PERSENT is primarily meant to export the sensitivity vector from one reactor problem and use it in combination with another reactor problem to compute the representativity. In this regard, PERSENT can accept sensitivity vectors computed by other codes (DPT [30] and ERANOS [31]) so long as they can be rewritten into the format accepted by PERSENT. To accommodate this easily, a human readable file was constructed with the format shown in Figure 5.9. The type 03 isotope names must match between the base ISOTXS file and any sensitivity vector. The two isotope names are required to distinguish a regional breakdown of a sensitivity vector. The expected input is just the reference library isotope name repeated twice.

The verification problem #16 contains an example sensitivity vector file which is too long to show here. To create a sensitivity file, one should add the "filename.sens" to the "SENSITIVITY_EDITS" input in PERSENT. To import a sensitivity vector, one should use the "SENSITIVITY_FILE" input as shown earlier in this manuscript. It is important to note that the reactions recognized by PERSENT do not contain standard sensitivity moments but are numbered in Table 5.7. One should enter zeros for all sensitivity vector moments that are not clear to the user or defined as unusable.

Table 5.7. PERSENT Sensitivity Vector Reaction Rate Ordering

Number	Name	Number	Name	Number	Name
1	*Total*	9	Tritium	17	P1 inelastic
2	Nu	10	Deuterium	18	P1 N-2N
3	Nu-Fission	11	Scatter	19	*Unusable*
4	Fission	12	Elastic	20	Chi
5	Capture	13	Inelastic	21	Chi FD
6	Gamma	14	N-2N	22	*Unusable*
7	Alpha	15	P1 scatter	23	*Unusable*
8	Proton	16	P1 elastic		

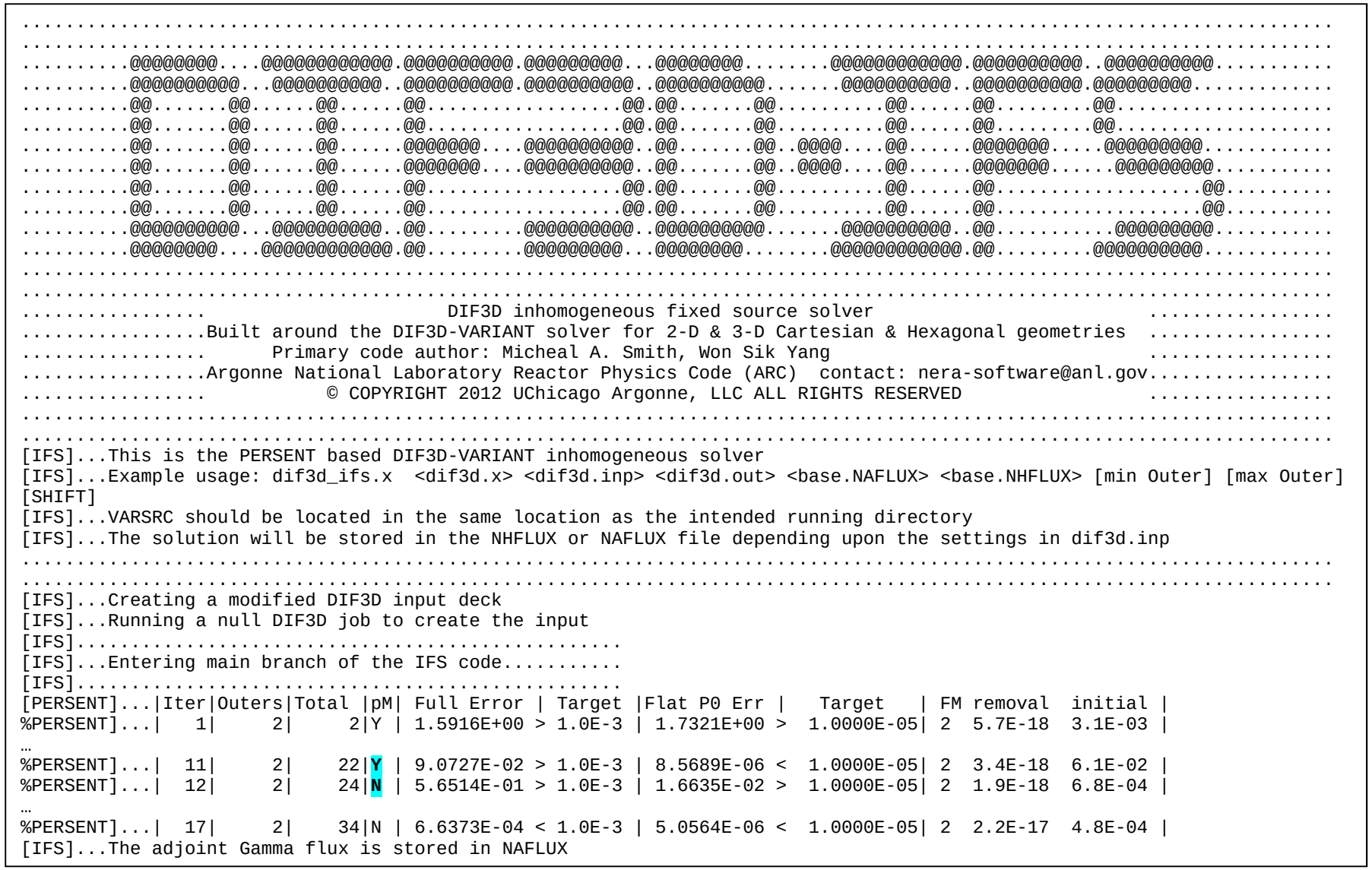

Figure 5.8. PERSENT Example DIF3D-IFS Output from Example Problem #16.

```
------------------------------------------------------------------------------------------------------------------------
- File format description for the PERSENT sensitivity vector
------------------------------------------------------------------------------------------------------------------------
- Type 01     :: file description
- Description :: Ascii string used to help users identify what data the file contains
- Read format :: FORMAT(A120)
------------------------------------------------------------------------------------------------------------------------
- Type 02     :: vector dimensions
- Description :: NumGroups,PERSENT_S_Principles,NumIsotopes
-                NumGroups is the number of neutron energy groups in ISOTXS
-                PERSENT_S_Principles=23 is the number of principle cross sections recognized in version 11.0 of ARC
-                NumIsotopes is the number of isotope data records in the file
- Read format :: FORMAT(10(I8,1X))
------------------------------------------------------------------------------------------------------------------------
- Type 03     :: isotope names
- Description :: These are the origination library name (HABSID) for each isotope followed by either its origination
-                 name (HABSID) or if regionwise unique, its alias isotope name (HISONM).
-                The purpose of a regionwise unique name is to detail the UQ calculation by region/isotope
- Read format :: FORMAT(10(A8,1X))
- Real line   :: (IsotopeName(I),AltIsotopeName(I),I=1,NumIsotopes)
------------------------------------------------------------------------------------------------------------------------
------------------------------------------------------------------------------------------------------------------------
- 1 Start Loop over NumIsotopes
---------------------------------
- Type 04     :: isotope name
- Description :: For reading purposes, this repeats the HABSID name from type 03 cards but is not used
- Read format :: FORMAT(10(A8,1X))
------------------------------------------------------------------------------------------------------------------------
- 2 Start Loop over NumGroups
------------------------------
- Type 05     :: sensitivity data
- Description :: This contains the sensitivity data for each isotope
- Read format :: FORMAT(50(1PE16.9,1X))
- Read line   :: (SensitivityVector(Group,J,Isotope),J=1,PERSENT_S_Principles)
------------------------------
- 2 End Loop over NumGroups
---------------------------------
- 1 End Loop over all NumIsotopes
------------------------------------------------------------------------------------------------------------------------
------------------------------------------------------------------------------------------------------------------------
```

Figure 5.9. PERSENT Sensitivity File Format.

6 Perturbation Theory Examples

The perturbation theory calculations are much easier to check than the sensitivity ones since the reactivity worth can be directly compared against the computed eigenvalue change. There are numerous verification tests provided with PERSENT, but not all are worth discussing in this section. We therefore only focus on two problems as they are used later in the sensitivity verification/validation section.

6.1 Three Group VARI3D verification problem

The first verification problem is a three group test problem created for the VARI3D code and propagated for use in PERSENT. The cross section data includes 15 isotopes and includes P_1 anisotropic scattering data which is impractical to include here as tables. Instead, users can refer to verification problem #5 included with PERSENT for the cross section data, noting that the utility program PrintTables can be used to print the associated ISOTXS file. The geometry for this problem is 120 degree periodic hexagonal where the composition specification is shown in Figure 6.1.

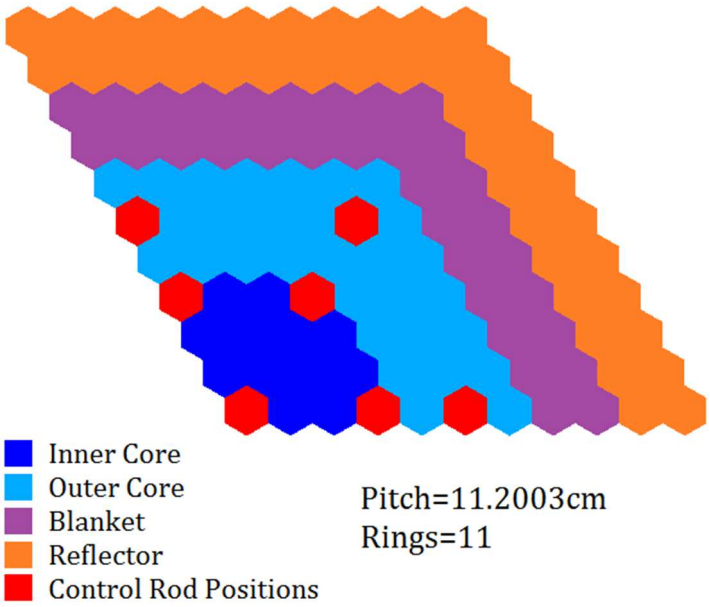

Figure 6.1. Composition Assignment for PERSENT Verification Test #5.

As can be seen in Figure 6.1, there are five major compositions loaded into the problem which have the isotope loadings defined by Table 6.1. As can be seen, the primary purpose of this benchmark is to study a control rod worth which involves switching all control rods in Figure 6.1 from the “Control Rod” to “Empty Control Rod” compositions in Table 6.1. The unrodded eigenvalue was computed with diffusion theory to be 1.14440 while the rodded eigenvalue is 0.90956 leading to a control rod worth of -0.22561. This is obviously the reported result from PERSENT evaluated using the operator. One advantage of using PERSENT is that it can also export the computed results for visualization as shown in Figures 6.2 and 6.3. In

Figure 6.2 we plot the mesh wise contribution (integrated over energy) to the total reactivity worth, and in Figure 6.3 we show the partial contribution from just group 2.

Table 6.1. Isotope Loadings for Verification Test #5

	Inner Core	Outer Core	Blanket	Reflector	Control Rod	Empty Control Rod
Pu-239	0.0011	0.0015				
U-238	0.0064	0.0054	0.0145			
Fe	0.0181	0.0181	0.0173		0.0181	
Na	0.0104	0.0110	0.0066	0.0044	0.0104	0.0220
O	0.0149	0.0138	0.0290	0.0691	0.0149	
B-10					0.0090	
C					0.0412	

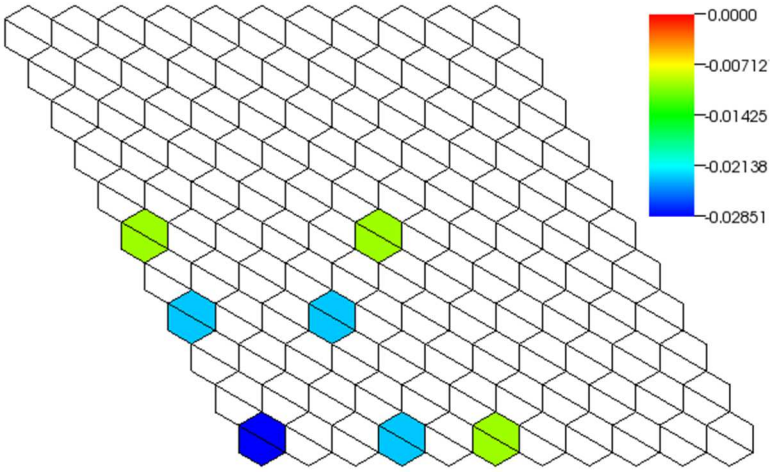

Figure 6.2. Control Rod Reactivity Worth Distribution for Verification Test #5.

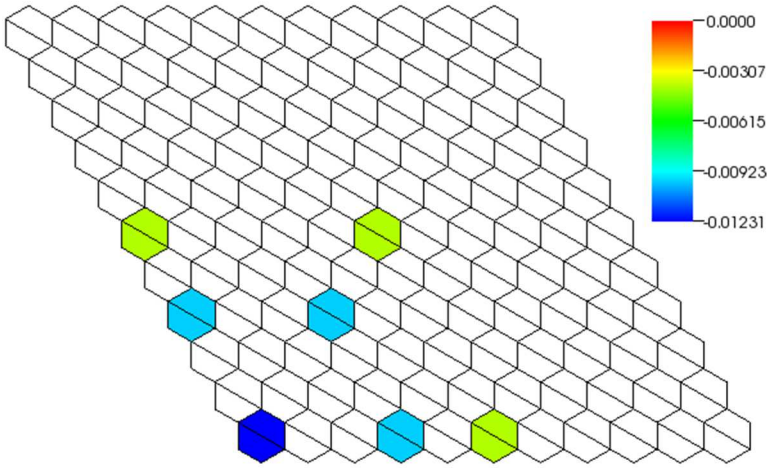

Figure 6.3. Group 2 Control Rod Reactivity Worth Distribution for Verification Test #5.

From the visualization results, one can see that the central control rod is clearly worth more than the other control rods. We can use the utility program provided with DIF3D to plot the forward and adjoint flux distributions as shown in Figure 6.4 to understand the reactivity

worth distribution. Note that we use a common scale for all energy groups such that the spatial gradients in the flux solution in each energy group are sacrificed in favor of showing the gradient in energy. The forward flux plots clearly show the peak of the flux solution is in the second energy group (below 800 keV and above 8 keV) with a substantial amount of neutrons present in the third energy group (below 8 keV) and about an order of magnitude less neutrons are present in the first energy group. The radial distribution in all three plots indicates the expected central peak. From the adjoint plots, one can see that the first energy group is the most important for the adjoint while the third is the least important both of which are the intuitive solutions given that neutrons are produced in the fast group and scattered into the thermal ones. Given the strong central peaking seen in all of the flux plots, it should be no surprise that the central control rod will have a higher worth than the outer lying control rods.

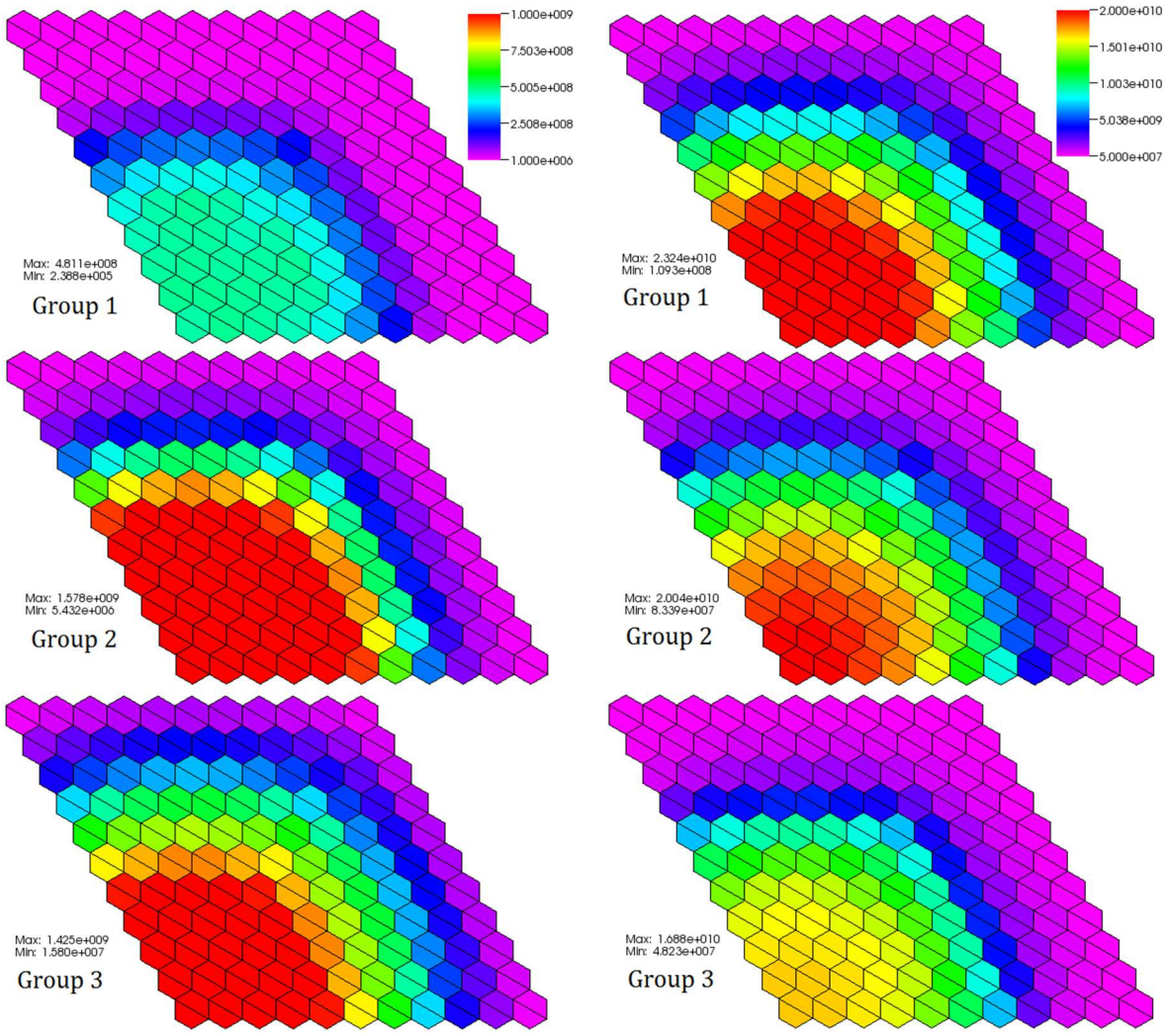

Figure 6.4. Forward and Adjoint Flux Distributions for Verification Test #5.

6.2 Twenty-one Group PERSENT verification problem

In addition to the preceding verification problem, we have also included a more conventional 21 group fast reactor problem with 120 degree periodic boundary conditions. The cross section and material definitions are too large to include as tables. Using the utility program we created the geometry plot shown in the left picture of Figure 6.5 and the forward and adjoint flux distributions for group 6 (the peak of the forward flux). Note that the axial meshing used in the calculation is visible where the pitch is 16.2471cm, the axial height is 480.2 cm, and the active core height is ~114.94 cm.

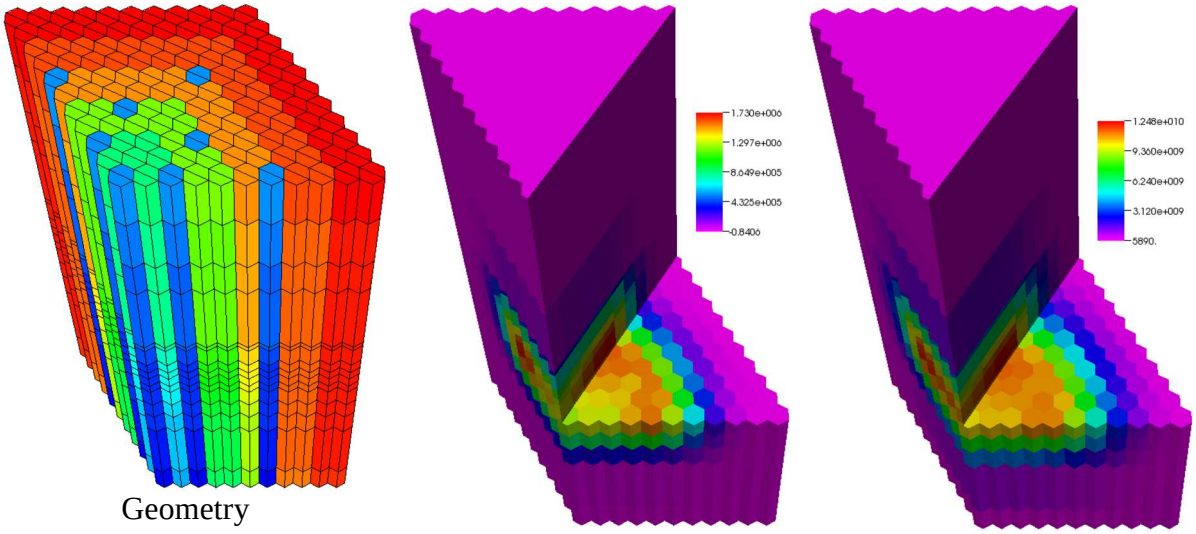

Geometry Forward Group 6 Adjoint Group 6

Figure 6.5. The Geometry and Group 6 Flux Distributions for Verification Test #8.

The base configuration yielded an eigenvalue of 1.04196 in ~11 seconds on a modern workstation using diffusion theory (1665 nodes with 6^{th} order flux and linear leakage approximations). As is typical for fast spectrum systems, we are interested in various reactivity worths for use in a point kinetics model. In the verification study, we compute the Doppler feedback and sodium density reactivity worths along with the kinetics parameters Λ and β. The Doppler reactivity worth calculations was run using generalized perturbation theory while the sodium density was done using first order perturbation theory. Both were verified to match comparable VARI3D results noting that significant mesh refinement was necessary in VARI3D. The entire PERSENT calculation takes ~40 seconds on a modern workstation to perform the 3 flux solves (~33 seconds) followed by the various integrations.

The reactivity worth of the Doppler coefficient was calculated to be -0.002800 (1.03892 was the perturbed eigenvalue) which is slightly different from the result of -0.002805 computed just using the two eigenvalues. This outcome is not unusual and occurs because of the iterative error remaining in the flux solution solver of DIF3D. If one drives the iterative error below the current settings of 10^{-6} on the eigenvalue and 10^{-5} on the flux, this discrepancy vanishes. Similar to the previous benchmark, we can inspect the spatial distribution of the Doppler reactivity worth as shown in Figure 6.6.

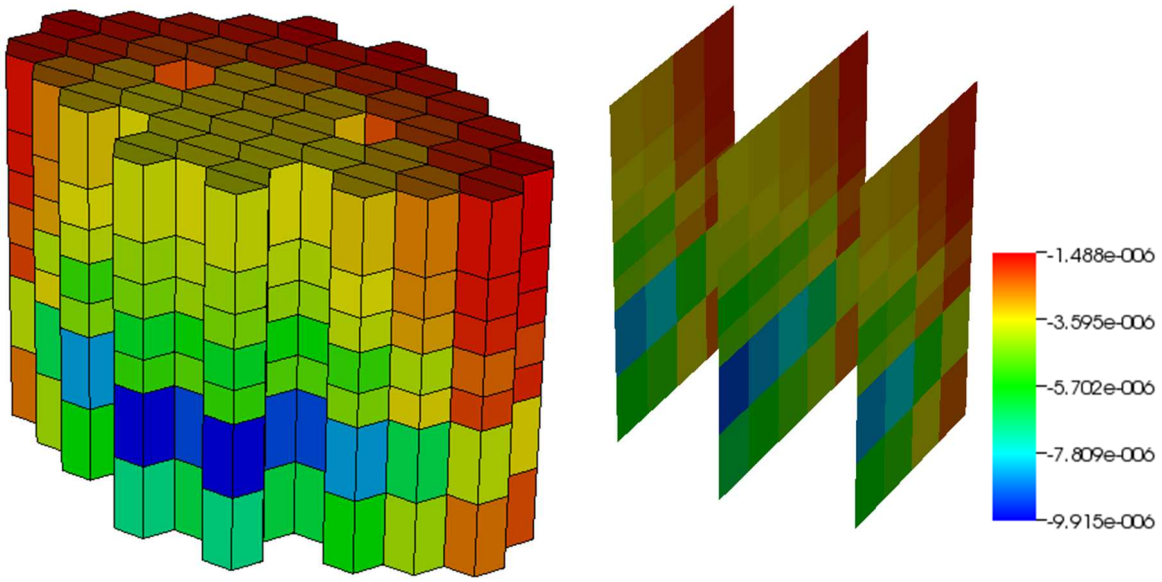

Figure 6.6. Doppler Reactivity Worth Distribution for Verification Test #8.

As was observed in the previous benchmark results (Figures 6.2 and 6.3), the only portion of the domain that displays a reactivity contribution is the part of the domain that is affected by the perturbation. In the case of the Doppler feedback, only the active core regions were modified and thus Figure 6.6 only displays the active core regions (axial holes are control rod positions). From Figure 6.6, one can see the most negative contributions (dark blue) appear at the lower central portion of the core. The slices give a better sense of the radial distribution showing that the lower worth regions are on the outer edge of the core.

We can generate a similar plot for the sodium density as shown in Figure 6.7 where the left hand picture is the mesh-wise contribution to the total worth and the right hand picture is the left hand picture divided by the (sodium) mass change that caused the reactivity change.

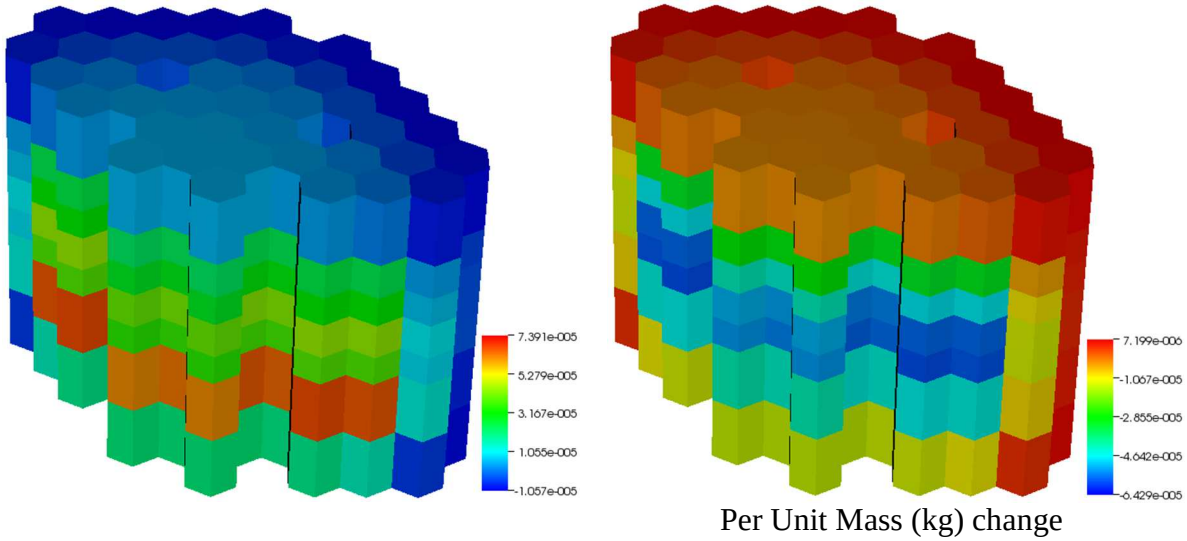

Per Unit Mass (kg) change

Figure 6.7. Sodium Density Reactivity Worth Distributions for Verification Test #8.

Note that in this particular calculation, the sodium density in the plenum region was not modified and thus only the active core is affected. While the left hand picture clearly shows the portion of the geometry responsible for altering the eigenvalue most, users have found worth/unit mass plot to be more understandable. The primary reason is because the right hand picture is not affected by the size of the mesh (i.e. volume) and thus gives a more balanced perspective on the actual amount of reactivity being inserted given a uniform change in the material (sodium density). It is important to note that PERSENT provides the change in mass (kg) on either a mesh wise, region wise, and area wise basis which was found to be an 815 kg change in this calculation.

The final calculation we consider involves the kinetics parameters Λ and β computed to be $4.2 \cdot 10^{-7}$ and 0.00301 (Pu dominated system). Much like VARI3D and other perturbation theory codes, PERSENT provides detailed isotopic and family breakdowns of β in addition to the domain coalesced parameters provided in Table 6.2. The spatial distributions of the delay parameters are plotted in Figure 6.8.

Table 6.2. Domain Coalesced Kinetics Parameters for Verification Test #8

Precursor Group	β_m	λ_m
1	7.356E-05	0.0134
2	5.940E-04	0.0307
3	4.503E-04	0.1170
4	1.068E-03	0.3067
5	6.082E-04	0.8779
6	2.199E-04	2.9418

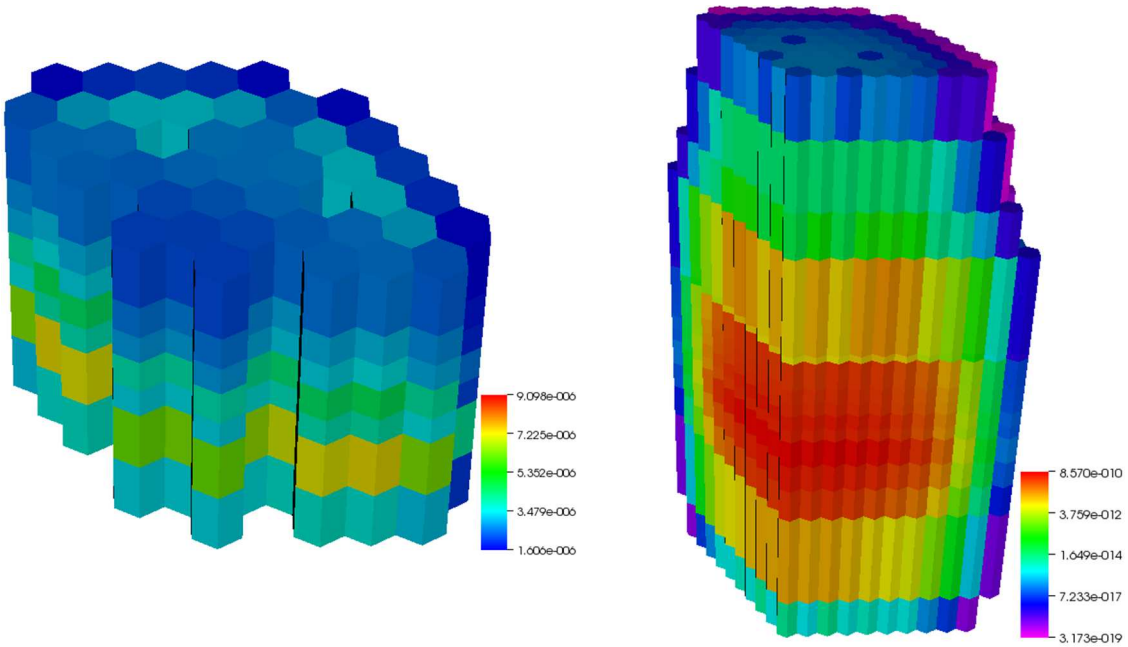

Figure 6.8. β (left) and Λ (right) Distributions for Verification Test #8.

In Figure 6.8, one can see that the β contributions come only from the active core region. Paying close attention to the scale, one can see that the contribution from any given mesh varies by at most an order of magnitude. Unlike the other coefficients, the Λ clearly impacts the entire core where a threshold operation within PERSENT zeros out the components of the solution near the outer domain boundary. From Figure 6.8, one can clearly see that the active core dominates the contribution to Λ much like the flux distribution shown earlier in Figure 6.5.

7 Sensitivity and Uncertainty Computation Examples

The sensitivity code is particularly painful to understand and verify/validate due to the solution of the Lagrange multipliers. In this section we provide several example problems, all of which are part of the verification test suite to demonstrate the methodology. In all cases, the results are compared against finite difference solutions which are considered the reference.

7.1 Infinite Homogeneous One Group Fixed Source Example

The easiest problem to validate is an infinite homogeneous problem which is an extension from the earlier infinite homogeneous example problem. In this case, we consider a fixed source example where the multi-group transport equation is reduced to

$$\Sigma_{t,g}\phi_g = \sum_{g'} \Sigma_{s,g,g'}\phi_{g'} + Q_g \,. \tag{7.1}$$

Writing in a matrix-vector form, we have:

$$\left(\underline{\underline{\Sigma}}_t - \underline{\underline{\Sigma}}_s\right)\underline{\phi} = \underline{\underline{\Sigma}}_a\underline{\phi} = \underline{Q} \quad \rightarrow \quad \underline{\phi} = \underline{\underline{\Sigma}}_a^{-1}\underline{Q} \tag{7.2}$$

and its adjoint

$$\underline{\underline{\Sigma}}_a^T\underline{\phi}^* = \underline{Q}^* \quad \rightarrow \quad \underline{\phi}^* = \underline{\underline{\Sigma}}_a^{-T}\underline{Q}^* \,. \tag{7.3}$$

Similarly, the solutions of Γ and Γ^* are found to be

$$\begin{aligned} \underline{\underline{\Sigma}}_a\underline{\Gamma} &= \underline{S} \quad \rightarrow \quad \underline{\Gamma} = \underline{\underline{\Sigma}}_a^{-1}\underline{S} \\ \underline{\underline{\Sigma}}_a^T\underline{\Gamma}^* &= \underline{S}^* \quad \rightarrow \quad \underline{\Gamma}^* = \underline{\underline{\Sigma}}_a^{-T}\underline{S}^* \end{aligned} \tag{7.4}$$

Starting with the reaction rate sensitivity, we write the parameter of interest in the same form as equation 3.29 as

$$R = \underline{\underline{\Sigma}}_x^T\underline{\phi} = \underline{\phi}^T\underline{\Sigma}_x \,. \tag{7.5}$$

Obtaining the source for Γ^* we can write

$$S^* = \frac{\partial R(\alpha,\psi,\psi^*)}{\partial \psi} = \frac{\partial\left(\underline{\phi}^T\underline{\Sigma}_x\right)}{\partial \underline{\phi}} = \underline{\Sigma}_x \tag{7.6}$$

which has the solution

$$\underline{\Gamma}^* = \underline{\underline{\Sigma}}_a^{-T}\underline{\Sigma}_x \,. \tag{7.7}$$

Defining the alpha to correspond to a single energy group of a given cross section σ_z, we can write the derivative of the response as

$$\frac{\partial R(\alpha,\psi,\psi^*)}{\partial \alpha} = \frac{\partial \underline{\Sigma}_x^T}{\partial \sigma_z}\underline{\phi} = \underline{N}_{z\in x}^T\underline{\phi} \tag{7.8}$$

where $\underline{N}_{z\in x}^T$ is a vector whose only non-zero element is the targeted energy group position of Σ_x that contains σ_z. One example is the capture response (Σ_x) to a change in the group 2 (n,alpha) cross section (σ_z). In this example the non-zero number would be the atom density associated with σ_z noting that this definition can select a single isotope from a mixture of isotopes. In addition, we can write the derivative of the operators in equation 7.2 and 7.3 as

$$\frac{\partial B(\alpha,\lambda)}{\partial \alpha}=\frac{\partial \underline{\underline{\Sigma}}_a}{\partial \sigma_z}=\underline{\underline{N}}_{z\in a} \quad \& \quad \frac{\partial B^*(\alpha,\lambda)}{\partial \alpha}=\frac{\partial \underline{\underline{\Sigma}}_a^T}{\partial \sigma_z}=\underline{\underline{N}}_{z\in a}^T, \tag{7.9}$$

where $\underline{\underline{N}}_{z\in a}$ is a matrix whose only non-zero element is the targeted energy group transfer position of σ_z.

With these definitions, we can write the sensitivity functional in equation 3.16 as

$$\begin{aligned} s_z &= \frac{\sigma_z}{\underline{\underline{\Sigma}}_x^T \underline{\underline{\Sigma}}_a^{-1} \underline{Q}} \left[\underline{\underline{N}}_{z\in x}^T \underline{\underline{\Sigma}}_a^{-1} \underline{Q} - \left(\underline{\underline{\Sigma}}_a^{-T} \underline{\underline{\Sigma}}_x \right)^T \left(\underline{\underline{N}}_{z\in a} \right) \underline{\underline{\Sigma}}_a^{-1} \underline{Q} \right] \\ &= \frac{\sigma_z}{\underline{\underline{\Sigma}}_x^T \underline{\underline{\Sigma}}_a^{-1} \underline{Q}} \left[\underline{\underline{N}}_{z\in x}^T \underline{\underline{\Sigma}}_a^{-1} \underline{Q} - \underline{\underline{\Sigma}}_x^T \underline{\underline{\Sigma}}_a^{-1} \underline{\underline{N}}_{z\in a} \underline{\underline{\Sigma}}_a^{-1} \underline{Q} \right] \end{aligned}. \tag{7.10}$$

For a one-group problem we can simplify this to

$$s_z = \frac{\sigma_z}{\Sigma_x \Sigma_a^{-1} Q} \left[N_{z\in x} \Sigma_a^{-1} Q - \Sigma_x \Sigma_a^{-1} N_{z\in a} \Sigma_a^{-1} Q \right] = \frac{\sigma_z N_{z\in x}}{\Sigma_x} - \frac{\sigma_z N_{z\in a}}{\Sigma_a}. \tag{7.11}$$

We can also obtain a finite difference relationship for the sensitivity equation 3.26 as

$$s_z = \frac{\sigma_z}{R} \frac{R(\sigma_z + c\cdot\sigma_z) - R(\sigma_z)}{c\cdot\sigma_z}. \tag{7.12}$$

Noting that the response is given as $R = \Sigma_x \phi$ with the associated flux solution $\phi = \Sigma_a^{-1} Q$, we can simplify equation 7.12 as

$$s_z = \frac{\left(\Sigma_x + c\cdot\Sigma_z \delta_{z\in x}\right)\left(\Sigma_a + c\cdot\Sigma_z \delta_{z\in a}\right)^{-1} Q - \Sigma_x \Sigma_a^{-1} Q}{c\cdot\Sigma_x \Sigma_a^{-1} Q} = \frac{1}{c}\left[\frac{\left(\Sigma_x + c\cdot\Sigma_z \delta_{z\in x}\right)\Sigma_a}{\Sigma_x\left(\Sigma_a + c\cdot\Sigma_z \delta_{z\in a}\right)} - 1 \right]. \tag{7.13}$$

Using the one-group, one isotope cross section data in Table 7.1, we produced the sensitivity results using both approaches ($c = 0.001$) for two different responses noting that the sensitivity of $\Sigma_{capture}\phi$ and sensitivity to Σ_s are always zero as it is a one group, infinite homogeneous problem. As seen in Table 7.1, both approaches give a physically meaningful answer. For example, a positive increase in Σ_α will result in a negative change in the reaction rate $\Sigma_\gamma \phi$. In this case, the resulting sensitivity is linked to the relative magnitude of Σ_α to Σ_z. Also note that a positive, say 100%, increase in Σ_z will result in a 50% increase in the reaction rate $\Sigma_\gamma \phi$ (50/100=0.5), due to the absorption occurring in other reactions in the system. In a similar sense, the sensitivity of $\Sigma_{tritium}\phi$ to a positive change in $\Sigma_{tritium}$ is nearly unity (or a 100% change will yield a 100% change in the reaction rate) as the overall change in absorption (1.0) in the problem will be minor, but the impact on the reaction rate is substantial. Or more clearly, a change of $\Sigma_{tritium}$ from 0.03 to 0.06 will yield a 97% change in the reaction rate $\Sigma_{tritium}\phi$.

Table 7.1. One Group, One Isotope Reaction Rate Sensitivity Results

$Q = 1.0$	$\Sigma_\gamma \phi$		$\Sigma_{tritium} \phi$	
	PERSENT	Finite Difference	PERSENT	Finite Difference
$\Sigma_\gamma = 0.5$	0.5	0.4998	-0.5	-0.4998
$\Sigma_\alpha = 0.45$	-0.45	-0.4508	-0.45	-0.4498
$\Sigma_{proton} = 0.01$	-0.01	-0.01	-0.01	-0.01
$\Sigma_{deuteron} = 0.01$	-0.01	-0.01	-0.01	-0.01
$\Sigma_{tritium} = 0.03$	-0.03	-0.03	0.97	0.9703

Using the same problem, we also consider the reaction rate ratio response

$$R = \frac{\underline{\Sigma}_x^T \underline{\phi}}{\underline{\Sigma}_y^T \underline{\phi}} = \frac{\underline{\phi}^T \underline{\Sigma}_x}{\underline{\phi}^T \underline{\Sigma}_y} \tag{7.14}$$

which has a solution for Γ^* of

$$\underline{\Gamma}^* = \underline{\underline{\Sigma}}_a^{-T} \left[\frac{\underline{\Sigma}_x}{\underline{\phi}^T \underline{\Sigma}_y} - \frac{\left(\underline{\phi}^T \underline{\Sigma}_x\right) \underline{\Sigma}_y}{\left(\underline{\phi}^T \underline{\Sigma}_y\right)^2} \right] = \frac{\underline{\underline{\Sigma}}_a^{-T} \underline{\Sigma}_x}{\underline{\Sigma}_y^T \underline{\underline{\Sigma}}_a^{-1} \underline{Q}} - \frac{\left(\underline{\Sigma}_x^T \underline{\underline{\Sigma}}_a^{-1} \underline{Q}\right) \underline{\underline{\Sigma}}_a^{-T} \underline{\Sigma}_y}{\left(\underline{\Sigma}_y^T \underline{\underline{\Sigma}}_a^{-1} \underline{Q}\right)^2}. \tag{7.15}$$

given the source

$$S^* = \frac{\underline{\Sigma}_x}{\underline{\phi}^T \underline{\Sigma}_y} - \frac{\left(\underline{\phi}^T \underline{\Sigma}_x\right) \underline{\Sigma}_y}{\left(\underline{\phi}^T \underline{\Sigma}_y\right)^2}. \tag{7.16}$$

Defining the alpha to be a single energy group of a given cross section σ_z, we can write the derivative of the response as

$$\frac{\partial R(\alpha, \psi, \psi^*)}{\partial \alpha} = \frac{\partial}{\partial \sigma_z} \left\{ \frac{\underline{\Sigma}_x^T \underline{\phi}}{\underline{\Sigma}_y^T \underline{\phi}} \right\} = \frac{1}{\underline{\Sigma}_y^T \underline{\phi}} \frac{\partial \underline{\Sigma}_x^T}{\partial \sigma_z} \underline{\phi} - \frac{\underline{\Sigma}_x^T \underline{\phi}}{\left(\underline{\Sigma}_y^T \underline{\phi}\right)^2} \frac{\partial \underline{\Sigma}_y^T}{\partial \sigma_z} \underline{\phi} = \frac{\underline{N}_{z \in x}^T \underline{\phi}}{\underline{\Sigma}_y^T \underline{\phi}} - \frac{\underline{\Sigma}_x^T \underline{\phi} \; \underline{N}_{z \in y}^T \underline{\phi}}{\left(\underline{\Sigma}_y^T \underline{\phi}\right)^2}. \tag{7.17}$$

where $\underline{N}_{z \in x}^T$ and $\underline{N}_{z \in y}^T$ is a vector whose only non-zero moment is the targeted energy group position of Σ_x and Σ_y that contains σ_z. One example is the capture response (Σ_x) to a change in the group 2 (n,alpha) cross section (σ_z) where the non-zero number would be the atom density associated with σ_z noting that this definition can select a single isotope from a mixture of isotopes.

Given that the derivative of the operators is identical to those in equation 7.9, we can write the sensitivity functional as

$$s_z = \frac{\sigma_z \cdot \underline{\Sigma}_y^T \underline{\underline{\Sigma}}_a^{-1} \underline{Q}}{\underline{\Sigma}_x^T \underline{\underline{\Sigma}}_a^{-1} \underline{Q}} \left[\begin{array}{l} \dfrac{\underline{N}_{z\in x}^T \underline{\underline{\Sigma}}_a^{-1} \underline{Q}}{\underline{\Sigma}_y^T \underline{\underline{\Sigma}}_a^{-1} \underline{Q}} - \dfrac{\underline{\Sigma}_x^T \underline{\underline{\Sigma}}_a^{-1} \underline{Q} \underline{N}_{z\in y}^T \underline{\underline{\Sigma}}_a^{-1} \underline{Q}}{\left(\underline{\Sigma}_y^T \underline{\underline{\Sigma}}_a^{-1} \underline{Q} \right)^2} \\ - \left[\dfrac{\underline{\underline{\Sigma}}_a^{-T} \underline{\Sigma}_x}{\underline{\Sigma}_y^T \underline{\underline{\Sigma}}_a^{-1} \underline{Q}} - \dfrac{\left(\underline{\Sigma}_x^T \underline{\underline{\Sigma}}_a^{-1} \underline{Q} \right) \underline{\underline{\Sigma}}_a^{-T} \underline{\Sigma}_y}{\left(\underline{\Sigma}_y^T \underline{\underline{\Sigma}}_a^{-1} \underline{Q} \right)^2} \right]^T \left(\underline{\underline{N}}_{z\in a} \right) \underline{\underline{\Sigma}}_a^{-1} \underline{Q} \end{array} \right], \tag{7.18}$$

which simplifies to

$$s_z = \sigma_z \left[\frac{\underline{N}_{z\in x}^T \underline{\underline{\Sigma}}_a^{-1} \underline{Q}}{\underline{\Sigma}_x^T \underline{\underline{\Sigma}}_a^{-1} \underline{Q}} - \frac{\underline{N}_{z\in y}^T \underline{\underline{\Sigma}}_a^{-1} \underline{Q}}{\underline{\Sigma}_y^T \underline{\underline{\Sigma}}_a^{-1} \underline{Q}} - \frac{\underline{\Sigma}_x^T \underline{\underline{\Sigma}}_a^{-1} \left(\underline{\underline{N}}_{z\in a} \right) \underline{\underline{\Sigma}}_a^{-1} \underline{Q}}{\underline{\Sigma}_x^T \underline{\underline{\Sigma}}_a^{-1} \underline{Q}} + \frac{\underline{\Sigma}_y \underline{\underline{\Sigma}}_a^{-1} \left(\underline{\underline{N}}_{z\in a} \right) \underline{\underline{\Sigma}}_a^{-1} \underline{Q}}{\underline{\Sigma}_y^T \underline{\underline{\Sigma}}_a^{-1} \underline{Q}} \right]. \tag{7.19}$$

For a one-group problem we can simplify this further to

$$s_z = \frac{\sigma_z N_{z\in x}}{\Sigma_x} - \frac{\sigma_z N_{z\in y}}{\Sigma_y} - \frac{\sigma_z N_{z\in a}}{\Sigma_a} + \frac{\sigma_z N_{z\in a}}{\Sigma_a} = \frac{\sigma_z N_{z\in x}}{\Sigma_x} - \frac{\sigma_z N_{z\in y}}{\Sigma_y}. \tag{7.20}$$

The response reduces to $R = \Sigma_x \Sigma_y^{-1}$ and the finite difference relationship for the sensitivity equation is found to be

$$s_z = \frac{\Sigma_y}{c \cdot \Sigma_x} \left[\frac{\Sigma_x + c \cdot \Sigma_z \delta_{z\in x}}{\Sigma_y + c \cdot \Sigma_z \delta_{z\in y}} - \frac{\Sigma_x}{\Sigma_y} \right] = \frac{1}{c} \left[\frac{\Sigma_y}{\Sigma_x} \frac{\Sigma_x + c \cdot \Sigma_z \delta_{z\in x}}{\Sigma_y + c \cdot \Sigma_z \delta_{z\in y}} - 1 \right]. \tag{7.21}$$

Using the one-group, one isotope cross section data in Table 7.2, we produced the sensitivity results using both approaches ($c = 0.001$) for three different responses. As can be seen in Table 7.2, both approaches give a physically meaningful result. In the first two responses, the presence of the capture cross section in the denominator and only one of its components in the numerator yields a meaningful sensitivity value for each result. In both cases, the result is positive when the numerator reaction changes and negative in the other cases due to the increase in capture by another reaction. The final sensitivity is not necessarily meaningful, but it clearly shows that the reaction rate ratio is only dependent upon the two reactions appearing in the response and non-zero as they are both equally affected by the other absorptive reactions in the infinite domain.

Table 7.2. One Group, One Isotope Reaction Rate Ratio Sensitivity Results

$Q = 1.0$	$\Sigma_\gamma \phi / \Sigma_{capture} \phi$		$\Sigma_{tritium} \phi / \Sigma_{capture} \phi$		$\Sigma_{tritium} \phi / \Sigma_{proton} \phi$	
	PERSENT	Finite Difference	PERSENT	Finite Difference	PERSENT	Finite Difference
$\Sigma_\gamma = 0.5$	0.5	0.4998	-0.5	-0.4998	0.0	0.0
$\Sigma_\alpha = 0.45$	-0.45	-0.4508	-0.45	-0.448	0.0	0.0
$\Sigma_{proton} = 0.01$	-0.01	-0.01	-0.01	-0.01	-1.0	-1.0
$\Sigma_{deuteron} = 0.01$	-0.01	-0.01	-0.01	-0.01	0.0	0.0
$\Sigma_{tritium} = 0.03$	-0.03	-0.03	0.97	0.970	1.0	1.0

7.2 Infinite Homogeneous One Group Eigenvalue Example

To verify the remaining responses, an eigenvalue problem is necessary. Focusing on an infinite homogeneous example again, the multi-group transport equation reduces to

$$\Sigma_{t,g}\phi_g = \sum_{g'}\Sigma_{s,g,g'}\phi_{g'} + \frac{1}{k}\sum_{g'}\chi_g\nu_{g'}\Sigma_{f,g'}\phi_{g'}\,. \tag{7.22}$$

Writing in a matrix-vector form, we have:

$$\left(\underline{\underline{\Sigma}}_t - \underline{\underline{\Sigma}}_s\right)\underline{\phi} = \underline{\underline{\Sigma}}_a\underline{\phi} = \tfrac{1}{k}\underline{\underline{F}}\underline{\phi} \quad \rightarrow \quad \underline{\phi} = \tfrac{1}{k}\underline{\underline{\Sigma}}_a^{-1}\underline{\underline{F}}\underline{\phi} \tag{7.23}$$

and its adjoint

$$\underline{\underline{\Sigma}}_a^T\underline{\phi}^* = \tfrac{1}{k}\underline{\underline{F}}^T\underline{\phi}^* \quad \rightarrow \quad \underline{\phi}^* = \tfrac{1}{k}\underline{\underline{\Sigma}}_a^{-T}\underline{\underline{F}}^T\underline{\phi}^*\,. \tag{7.24}$$

We also have the solutions of Γ and Γ^* with the stated restrictions discussed earlier

$$\begin{aligned}\left(\underline{\underline{\Sigma}}_a - \tfrac{1}{k}\underline{\underline{F}}\right)\underline{\Gamma} = \underline{S} \qquad &\rightarrow \quad \underline{\Gamma} = \left(\underline{\underline{\Sigma}}_a - \tfrac{1}{k}\underline{\underline{F}}\right)^{-1}\underline{S} \\ \left(\underline{\underline{\Sigma}}_a - \tfrac{1}{k}\underline{\underline{F}}\right)^T\underline{\Gamma}^* = \underline{S}^* \quad &\rightarrow \quad \underline{\Gamma}^* = \left(\underline{\underline{\Sigma}}_a - \tfrac{1}{k}\underline{\underline{F}}\right)^{-T}\underline{S}^*\end{aligned} \tag{7.25}$$

We need to remove the homogeneous component and thus use equation 3.21 to define

$$a^* = \frac{\underline{\Gamma}^{*T}\underline{\underline{F}}\,\underline{\phi}}{\underline{\phi}^{*T}\underline{\underline{F}}\,\underline{\phi}} \quad \& \quad a = \frac{\underline{\Gamma}\,\underline{\underline{F}}^T\underline{\phi}^*}{\underline{\phi}^{*T}\underline{\underline{F}}\,\underline{\phi}} \tag{7.26}$$

and thus

$$\tilde{\underline{\Gamma}} = \underline{\Gamma} - a\underline{\phi} \quad \& \quad \tilde{\underline{\Gamma}}^* = \underline{\Gamma}^* - a^*\underline{\phi}^*\,. \tag{7.27}$$

The sensitivity functional is given as

$$s_\alpha(x) = \frac{\alpha(x)}{R}\left[\frac{\partial R(\alpha,\psi,\psi^*)}{\partial\alpha} - \left\langle\tilde{\Gamma}^*, \frac{\partial B(\alpha,\lambda)}{\partial\alpha}\psi\right\rangle - \left\langle\tilde{\Gamma}, \frac{\partial B^*(\alpha,\lambda)}{\partial\alpha}\psi^*\right\rangle\right]. \tag{7.28}$$

Instead of doing the derivation for a single response at a time, we do it for all responses of interest and note the common setup for each.

Since a reaction rate sensitivity is not valid in an eigenvalue problem (see sensitivity section), we start with the reaction rate ratio

$$R = \frac{\underline{\underline{\Sigma}}_x^T\underline{\phi}}{\underline{\underline{\Sigma}}_y^T\underline{\phi}} = \frac{\underline{\phi}^T\underline{\underline{\Sigma}}_x}{\underline{\phi}^T\underline{\underline{\Sigma}}_y} \tag{7.29}$$

which has the Lagrange multiplier source

$$\underline{S}^* = \frac{\underline{\underline{\Sigma}}_x}{\underline{\phi}^T\underline{\underline{\Sigma}}_y} - \frac{\left(\underline{\phi}^T\underline{\underline{\Sigma}}_x\right)\underline{\underline{\Sigma}}_y}{\left(\underline{\phi}^T\underline{\underline{\Sigma}}_y\right)^2}\,. \tag{7.30}$$

and a solution for $\tilde{\underline{\Gamma}}^*$ given by

$$\left(\underline{\underline{\Sigma}}_a - \tfrac{1}{k}\underline{\underline{F}}\right)^T\underline{\Gamma}^* = \left[\frac{\underline{\underline{\Sigma}}_x}{\underline{\phi}^T\underline{\underline{\Sigma}}_y} - \frac{\left(\underline{\phi}^T\underline{\underline{\Sigma}}_x\right)\underline{\underline{\Sigma}}_y}{\left(\underline{\phi}^T\underline{\underline{\Sigma}}_y\right)^2}\right] \tag{7.31}$$

and equations 7.26 and 7.27.

Again defining alpha to be a single energy group of a given cross section σ_z, the derivative of the response is found to be

$$\frac{\partial R(\alpha,\psi,\psi^*)}{\partial\alpha}=\frac{\partial}{\partial\sigma_z}\left\{\frac{\underline{\Sigma}_x^T\underline{\phi}}{\underline{\Sigma}_y^T\underline{\phi}}\right\}=\frac{1}{\underline{\Sigma}_y^T\underline{\phi}}\frac{\partial\underline{\underline{\Sigma}}_x^T}{\partial\sigma_z}\underline{\phi}-\frac{\underline{\Sigma}_x^T\underline{\phi}}{\left(\underline{\Sigma}_y^T\underline{\phi}\right)^2}\frac{\partial\underline{\underline{\Sigma}}_y^T}{\partial\sigma_z}\underline{\phi}=\frac{\underline{N}_{z\in x}^T\underline{\phi}}{\underline{\Sigma}_y^T\underline{\phi}}-\frac{\underline{\Sigma}_x^T\underline{\phi}\;\underline{N}_{z\in y}^T\underline{\phi}}{\left(\underline{\Sigma}_y^T\underline{\phi}\right)^2}. \quad (7.32)$$

The derivative of the operator is written using a finite difference formula

$$\frac{\partial B(\alpha,k)}{\partial\alpha}=\frac{B(\sigma_z+c\cdot\sigma_z,k)-B(\sigma_z,k)}{c\cdot\sigma_z}=\frac{\left(\underline{\underline{\Sigma}}_a-\frac{1}{k}\underline{\underline{F}}\right)+c\left(\underline{\underline{\Sigma}}_{z\in a}-\frac{1}{k}\underline{\underline{F}}_{z\in f}\right)-\left(\underline{\underline{\Sigma}}_a-\frac{1}{k}\underline{\underline{F}}\right)}{c\cdot\sigma_z}. \quad (7.33)$$

This approach does not introduce any error, and the new matrices only have non-zero terms if they correspond to the targeted σ_z.

Plugging these into the sensitivity functional we can write

$$s_z=\frac{\sigma_z\underline{\Sigma}_y^T\underline{\phi}}{\underline{\Sigma}_x^T\underline{\phi}}\left[\frac{\underline{N}_{z\in x}^T\underline{\phi}}{\underline{\Sigma}_y^T\underline{\phi}}-\frac{\underline{\Sigma}_x^T\underline{\phi}\;\underline{N}_{z\in y}^T\underline{\phi}}{\left(\underline{\Sigma}_y^T\underline{\phi}\right)^2}-\frac{\tilde{\underline{\Gamma}}^{*T}\left(\underline{\underline{\Sigma}}_{z\in a}-\frac{1}{k}\underline{\underline{F}}_{z\in f}\right)\underline{\phi}}{\sigma_z}\right]. \quad (7.34)$$

Reducing this to a one-group, infinite homogeneous problem, we have the eigenvalue and arbitrary flux solution

$$k=\frac{\chi\nu\Sigma_f}{\Sigma_t-\Sigma_s}=\frac{\nu\Sigma_f}{\Sigma_a}\quad\&\quad\phi=1\quad\&\quad\phi^*=1. \quad (7.35)$$

The source for Γ^* is found to be zero, and thus we know Γ^* is zero as is $\tilde{\Gamma}^*$ for this problem:

$$S^*=\frac{\Sigma_x}{\phi\Sigma_y}-\frac{\phi\Sigma_x\Sigma_y}{\left(\phi\Sigma_y\right)^2}=\frac{\phi\Sigma_y\Sigma_x}{\left(\phi\Sigma_y\right)^2}-\frac{\phi\Sigma_x\Sigma_y}{\left(\phi\Sigma_y\right)^2}=0. \quad (7.36)$$

Plugging these results into the functional we see that it collapses to

$$s_{RR}=\frac{\sigma_z N_{z\in x}}{\Sigma_x}-\frac{\sigma_z N_{z\in y}}{\Sigma_y}. \quad (7.37)$$

The power fraction sensitivity functional has an identical form to equation 7.37 noting that $\Sigma_x=\Sigma_y$ in this special case and thus all sensitivities are zero.

The next response of interest is the reactivity worth using generalized perturbation theory of the form in equation 3.42. Given that the equations of interest have already been shown (starts at equation 3.59), we do not revisit them here and instead focus on the eigenvalue sensitivity given by equation 3.48:

$$s_\alpha=\frac{1}{c\cdot\lambda}\frac{\underline{\psi}^{*T}\left\{\underline{\underline{B}}(\alpha+c\cdot\alpha,\lambda)-\underline{\underline{B}}(\alpha,\lambda)\right\}\underline{\psi}}{\underline{\psi}^{*T}\underline{\underline{F}}\underline{\psi}}. \quad (7.38)$$

Inserting the definitions from equation 7.23 we have

$$s_\alpha=\frac{1}{\lambda}\frac{\underline{\phi}^{*T}\left\{\underline{\underline{\Sigma}}_{z\in a}-\lambda\underline{\underline{F}}_{z\in f}\right\}\underline{\phi}}{\underline{\phi}^{*T}\underline{\underline{F}}\underline{\phi}}. \quad (7.39)$$

The prompt neutron lifetime and beta effective sensitivity functional have similar forms to the reactivity worth where the derivative of the response is found to be

$$\frac{\partial R(\alpha,\psi,\psi^*)}{\partial\alpha}=\frac{\underline{\psi}^{*T}\frac{\partial\underline{\underline{H}}}{\partial\alpha}\underline{\psi}}{\underline{\psi}^{*T}\underline{\underline{F}}\underline{\psi}}-\frac{\left\{\underline{\psi}^{*T}\underline{\underline{H}}\underline{\psi}\right\}\underline{\psi}^{*T}\underline{\underline{N}}_{z\in f}\underline{\psi}}{\left(\underline{\psi}^{*T}\underline{\underline{F}}\underline{\psi}\right)^2}=-\frac{\underline{\psi}^{*T}\underline{\underline{H}}\underline{\psi}}{\underline{\psi}^{*T}\underline{\underline{F}}\underline{\psi}}\frac{\underline{\psi}^{*T}\underline{\underline{N}}_{z\in f}\underline{\psi}}{\underline{\psi}^{*T}\underline{\underline{F}}\underline{\psi}}, \tag{7.40}$$

and

$$\frac{\partial R(\alpha,\psi,\psi^*)}{\partial\alpha}=\frac{\underline{\psi}^{*T}\frac{\partial\underline{\underline{F}}_{i,m}}{\partial\alpha}\underline{\psi}}{\underline{\psi}^{*T}\underline{\underline{F}}\underline{\psi}}-\frac{\left\{\underline{\psi}^{*T}\underline{\underline{F}}_{i,m}\underline{\psi}\right\}\underline{\psi}^{*T}\underline{\underline{N}}_{z\in f}\underline{\psi}}{\left(\underline{\psi}^{*T}\underline{\underline{F}}\underline{\psi}\right)^2}=\frac{\underline{\psi}^{*T}\underline{\underline{M}}_{z\in f}\underline{\psi}}{\underline{\psi}^{*T}\underline{\underline{F}}\underline{\psi}}-\frac{\underline{\psi}^{*T}\underline{\underline{F}}_{i,m}\underline{\psi}}{\underline{\psi}^{*T}\underline{\underline{F}}\underline{\psi}}\frac{\underline{\psi}^{*T}\underline{\underline{N}}_{z\in f}\underline{\psi}}{\underline{\psi}^{*T}\underline{\underline{F}}\underline{\psi}} \tag{7.41}$$

for the prompt neutron and beta effective terms. Note that neither the neutron velocity nor the delay neutron family generation is permitted to be the targeted sensitivity variable. Once again the Lagrange multipliers are zero for the one-group case, and the sensitivity functionals are found to be

$$s_\Lambda=-\frac{\sigma_z N_{z\in f}}{\nu\Sigma_f}\quad\&\quad s_\beta=\frac{\nu}{\nu_{i,m}}\frac{\sigma_z M_{z\in f}}{\nu\Sigma_f}-\frac{\sigma_z N_{z\in f}}{\nu\Sigma_f}. \tag{7.42}$$

The finite difference approach for the reactivity worth sensitivity is given as

$$\begin{aligned}s_{RW}&=\frac{\sigma_z}{R(\sigma_z)}\frac{R(\sigma_z+c\cdot\sigma_z)-R(\sigma_z)}{c\cdot\sigma_z}\\&=\frac{1}{c}\left\{\frac{1}{\left(1+c\delta_{z\in f}\right)}+\frac{c\left(\delta_{z\in a}\left(\Sigma_z-\hat{\Sigma}_z\right)-\frac{1}{k}\delta_{z\in f}\left(\nu\Sigma_f-\nu\hat{\Sigma}_f\right)\right)}{\left(\Sigma_a-\frac{1}{k}\nu\Sigma_f\right)\left(1+c\delta_{z\in f}\right)}-1\right\}.\end{aligned} \tag{7.43}$$

With the one-group cross section data in Table 7.3, the sensitivity results for a typical reaction rate ratio and two reactivity coefficients were done. In this case, the finite difference results (shaded values) were obtained using DIF3D and c=0.0001 and thus are less accurate than the ones from the above formulas.

Table 7.3. One Group, One Isotope Sensitivity Results

	$\Sigma_{capture}\phi \big/ \Sigma_{fission}\phi$		K		$\hat{\Sigma}_\gamma=0.11$ $RW=-0.1$		$\hat{\Sigma}_f$=0.04, $\hat{\Sigma}_\gamma$=0.11 $\hat{\Sigma}_{proton}$=0.006, RW=-0.42		
c		0.0001		0.0001		0.0001		0.0001	0.001
Σ_γ=0.1	0.885	0.885	-0.613	-0.613	1.0	1.01	0.8929	0.9048	0.8929
Σ_α=0.006	0.0531	0.0531	-0.0368	-0.0367	0.0	0.0	0.0357	0.0476	0.0357
Σ_{prot}=0.005	0.0442	0.0442	-0.0307	-0.0306	0.0	0.0	0.0595	0.0476	0.0595
Σ_{deut}=0.001	0.0089	0.0089	-0.0061	-0.0060	0.0	0.0	0.0595	0.0	0.0071
Σ_{trit}=0.001	0.0089	0.0089	-0.0061	-0.0060	0.0	0.0	0.0595	0.0	0.071
Σ_f=0.05	-1.0	-0.999	0.693	0.693	-1.0	-1.0	-1.0	-1.0	-0.998
$\nu=2.0$	0.0	0.0	1.0	1.0	-1.0	-1.0	-1.0	-1.0	-1.0

Note that these results strongly depend upon the definition of the microscopic cross sections and atom densities. In this case, we assume each cross section (ν and Σ_f are together) comes from a different isotope with an atom density of unity. For reactivity worths, the atom density is modified. Focusing on the reaction rate ratio, one can see that all perturbations are significant noting again that scattering is always zero as the problem is infinite.

From Table 7.3, one can see that the finite difference and PERSENT based results are generally similar, if not identical, although there are notable problems with some of the sensitivities. For the reaction rate sensitivities, PERSENT produces a nearly perfect match with the finite difference results where the primary errors stem from round off in the printed values of the reaction rates from DIF3D (i.e. DIF3D only prints the result with so many significant digits). The eigenvalue sensitivity is nearly identical with the errors in the finite difference (FD) primarily due to round off error. For the first reactivity worth, the two codes produce nearly identical results except for Σ_γ whose difference is traceable to the number of significant digits printed by PERSENT. This latter problem is the primary source of troubles for the FD error in the second reactivity worth in Table 7.3. In this case we also provide the FD sensitivities for c=0.001 to show how the small cross section values appear to be zero. Note that with the larger factor, the small cross section values still have significant error. This problem is difficult to compensate for in a real problem as the magnitude of the cross section is highly variable.

7.3 Infinite Homogeneous Three Group Eigenvalue Example

Extending the infinite homogeneous problem to a three-group one, we find the preceding equations are the same. For this example we use the isotopic cross section data and composition definitions in Tables 7.5 and 7.6.

Table 7.4. Three Group Cross Sections

	X			*Y*			*Z*		
$N_{base,i}$:	0.001			0.001			0.01		
$N_{perturbed,i}$:	0.001			0.001			0.00001		
Group	1	2	3	1	2	3	1	2	3
σ_γ	1.0	2.0	3.0	1.0	2.0	2.0	1.0	2.0	2.0
σ_α							0.5	0.5	0.5
σ_{proton}							0.5	0.5	0.5
σ_f	1.0	1.0	1.0	1.0	1.0	1.0			
ν	3.0	3.0	3.0	2.0	3.0	3.0			
χ	0.8	0.2		0.8	0.2				
$\sigma_{s,1\leftarrow g}$	4.0			4.0			4.0		
$\sigma_{s,2\leftarrow g}$	1.0	5.0		1.0	4.0		1.0	4.0	
$\sigma_{s,3\leftarrow g}$		1.0	10.0	0.0	1.0	10.0	0.0	1.0	10.0

Table 7.5. Delay Data for Both Isotope X and Y

	λ	ν_d			χ_d		
Group		1	2	3	1	2	3
Family 1	0.03	0.0031	0.0032	0.0033	0.6	0.4	0.0
Family 2	1.0	0.0027	0.0028	0.0029	0.8	0.2	0.0

We first focus on the sensitivity of the eigenvalue (0.18836338) with respect to three scenarios: 1) isotope Z, 2) isotope Y, and 3) isotope X and Y. Tables 7.6, 7.7, and 7.8 provide the eigenvalue sensitivity results using PERSENT and FD (finite difference) DIF3D calculations for all three scenarios using a fixed c=0.0001 factor.

Table 7.6. Sensitivity Results of *k*-effective to Isotope Z

	PERSENT			FD		
Group	1	2	3	1	2	3
σ_γ	-0.2290	-0.1709	-0.0543	-0.2293	-0.1709	-0.0547
σ_α	-0.1145	-0.0427	-0.0136	-0.1147	-0.0430	-0.0138
σ_{proton}	-0.1145	-0.0427	-0.0136	-0.1147	-0.0430	-0.0138
$\sigma_{s,*\leftarrow g}$	-0.0337	-0.0017	0.0000	-0.0340	-0.0021	0.0000

Table 7.7. Sensitivity Results of *k*-effective to Isotope Y

	PERSENT			FD		
Group	1	2	3	1	2	3
σ_γ	-0.0229	-0.0171	-0.0054	-0.0228	-0.0170	-0.0058
σ_f	0.2131	0.1463	0.0475	0.2129	0.1460	0.0472
ν	0.2360	0.1548	0.0502	0.2357	0.1545	0.0499
$\sigma_{s,*\leftarrow g}$	-0.0034	-0.0002	-0.0000	-0.0037	-0.0005	0.0000

Table 7.8. Sensitivity Results of *k*-effective to Isotopes X and Y

	PERSENT			FD		
Group	1	2	3	1	2	3
σ_γ	-0.0458	-0.0342	-0.0136	-0.0462	-0.0345	-0.0138
σ_f	0.5441	0.2926	0.0950	0.5442	0.2925	0.0950
ν	0.5899	0.3097	0.1004	0.5898	0.3095	0.1003
$\sigma_{s,*\leftarrow g}$	-0.0067	-0.0003	0.0000	-0.0069	-0.0005	0.0000

Starting with Table 7.6, one can see the PERSENT and FD results are very similar. In all cases, the FD solution accuracy is compromised when the magnitude of the cross section data is small. The same is true for Tables 7.7 and 7.8, but overall these results are acceptable for this study.

The next response to consider is the reactivity worth (4.40894) resulting from the perturbation defined in Table 7.4. Similar to the previous case, we consider the sensitivities

with respect to 1) isotope Y and 2) isotopes X and Y. Tables 7.9 and 7.10 give the sensitivity results for the reactivity worth noting that c=0.01 was necessary to produce a reasonable set of values. Once again, the results from PERSENT and FD are very similar in all cases except for those reactions with small cross sections.

Table 7.9. Sensitivity Results for ρ to isotope Y

	PERSENT			FD		
Group	1	2	3	1	2	3
σ_γ	-0.0004	0.0001	0.0013	-0.0002	0.0002	0.0014
σ_f	-0.2358	-0.1544	-0.0507	-0.2352	-0.1540	-0.0506
ν	-0.2354	-0.1545	-0.0513	-0.2348	-0.1540	-0.0513
$\sigma_{s,*\leftarrow g}$	-0.0006	-0.0009	0.0000	-0.0005	-0.0009	0.0000

Table 7.10. Sensitivity Results for ρ to isotopes X and Y

	PERSENT			FD		
Group	1	2	3	1	2	3
σ_γ	-0.0009	0.0002	0.0033	-0.0007	0.0005	0.0034
σ_f	-0.5893	-0.3088	-0.1013	-0.5856	-0.3078	-0.1012
ν	-0.5884	-0.3089	-0.1026	-0.5849	-0.3078	-0.1025
$\sigma_{s,*\leftarrow g}$	-0.0011	-0.0018	0.0000	-0.0009	-0.0018	0.0000

The remaining sensitivities of interest are Λ_G, Λ and β for which we only consider sensitivities to isotopes Y and Z. Starting with Λ_G and Λ, Tables 7.11 and 7.12 give the sensitivities computed using PERSENT and FD with c=0.01. Following equation 3.53, we also compute the sensitivities for Λ provided in Table 7.13 noting that we use the FD relation to compute the FD sensitivities (i.e. not equation 3.53).

Table 7.11. Sensitivity Results for Λ_G to isotope Z

	PERSENT			FD		
Group	1	2	3	1	2	3
σ_γ	0.1896	-0.1090	-0.4190	0.1898	-0.1087	-0.4160
σ_α	0.0948	-0.0273	-0.1048	0.0949	-0.0273	-0.1044
σ_{proton}	0.0948	-0.0273	-0.1048	0.0949	-0.0273	-0.1044
$\sigma_{s,*\leftarrow g}$	0.2091	0.2214	0.0000	0.2088	0.2210	0.0000

Table 7.12. Sensitivity Results for Λ_G to isotope Y

	PERSENT			FD		
Group	1	2	3	1	2	3
σ_γ	0.0190	-0.0109	-0.0419	0.0190	-0.0107	-0.0419
σ_f	-0.3739	-0.1799	0.1446	-0.3725	-0.1795	0.1443
ν	-0.3928	-0.1745	0.1655	-0.3915	-0.1740	0.1653
$\sigma_{s,*\leftarrow g}$	0.0209	0.0221	0.0000	0.0210	0.0221	0.0000

Table 7.13. Sensitivity Results for Λ to isotope Y

	PERSENT			FD		
Group	1	2	3	1	2	3
σ_γ	-0.0039	-0.0280	-0.0473	-0.0040	-0.0281	-0.0474
σ_f	-0.1608	-0.0336	0.1921	-0.1606	-0.0338	0.1919
ν	-0.1569	-0.0196	0.2157	-0.1566	-0.0197	0.2156
$\sigma_{s,*\leftarrow g}$	0.0175	0.0220	0.0000	0.0174	0.0218	0.0000

The sensitivities for Λ and Λ_G from PERSENT match the FD results very closely where the errors are attributable to the selection of the parameter *c*. Continuing with β, we only consider the sensitivity to the total value rather than the isotopic component cases given that PERSENT will not identically give the exact values (see approximation made in equation 3.57). Table 7.14 gives the sensitivity with respect to isotope Z, while Table 7.15 gives the sensitivities with respect to isotope Y. The PERSENT results are again consistent with the FD result where the remaining error is attributable to the *c* factor used in FD.

Table 7.14. Sensitivity Results for β to isotope Z

	PERSENT			FD		
Group	1	2	3	1	2	3
σ_γ	0.0233	-0.0154	-0.0061	0.0241	-0.0148	-0.0056
σ_α	0.0117	-0.0038	-0.0015	0.0120	-0.0037	-0.0009
σ_{proton}	0.0117	-0.0038	-0.0015	0.0120	-0.0037	-0.0009
$\sigma_{s,*\leftarrow g}$	-0.0159	0.0018	0.0000	-0.0157	0.0019	0.0000

Table 7.15. Sensitivity Results for β to isotope Y

	PERSENT			FD		
Group	1	2	3	1	2	3
σ_γ	0.0023	-0.0015	-0.0006	0.0028	-0.0009	0.0000
σ_f	-0.2618	-0.1291	-0.0419	-0.2611	-0.1287	-0.0417
ν	-0.2641	-0.1283	-0.0416	-0.2630	-0.1278	-0.0417
$\sigma_{s,*\leftarrow g}$	-0.0016	0.0002	0.0000	-0.0009	0.0009	0.0000

7.4 One Group Reactivity Worth for Bare Reactor Problem

The preceding problems are somewhat trivial to understand and solve. A slightly more complicated problem is a single-node, one group problem with vacuum boundary conditions which is the verification problem #11. The cross sections are given in Table 7.16, and the geometry is taken to be a 2D cell with 1 cm side lengths.

Table 7.16. Single Node, One Group Cross Section Data

Isotope	Σ_γ	Σ_f	ν	χ	Σ_s
1	6	1	2	1	0
2	12	2	2	1	0
3	0.5	0	0	0	0.5

With DIF3D-VARIANT, only a single node is required to get spatial mesh convergence in diffusion theory. Table 7.17 shows the eigenvalue convergence with respect to mesh when the geometry is filled with either composition 1 or 2. The eigenvalue converges rapidly with respect to the spatial flux and leakage approximations in DIF3D-VARIANT such that a 10^{th} order flux and 4^{th} order leakage approximation are sufficient for convergence.

Table 7.17. Single Node, One Group Diffusion Theory Eigenvalue Convergence

Nodal Flux	Nodal Leakage	Eigenvalue		Worth
		Just Isotope 1	Just Isotope 2	
4	1	0.251897	0.277931	0.371861
5	1	0.256935	0.277931	0.294020
6	1	0.256938	0.277932	0.293987
6	2	0.251892	0.276435	0.352468
7	2	0.251892	0.276435	0.352468
8	3	0.251897	0.276436	0.352403
10	4	0.251890	0.276434	0.352487
13	5	0.251890	0.276434	0.352487

We constructed 5 compositions composed of these three “isotopes” as outlined in Table 7.18. Notice that the base composition includes all isotopes which is a requirement for the sensitivity routine to ensure that there will be a non-zero sensitivity result. The final sequence of compositions is chosen to show how the sensitivity result changes with a reduction in the perturbation magnitude.

Table 7.18. Composition Definitions for the Single Node, One Group Diffusion Problem

Composition	Base	C2	C3	C4	C5	C6
Isotope 1	1.0			0.9	0.99	0.999
Isotope 2	10^{-12}	1.0	1.0	0.1	0.01	0.001
Isotope 3	10^{-12}		1.0			

Starting with the eigenvalue sensitivity of the base configuration, Table 7.19 gives the sensitivities with respect to each isotope using PERSENT and finite difference. As can be seen,

the PERSENT and FD results are nearly identical. The value c=0.01 was used for the FD calculations, and the sensitivities for the other isotopes are zero as expected.

The remaining sensitivities of interest are for the reactivity worths associated with replacing the base composition with each of the other compositions in Table 7.18. Starting with the C2 and C3 perturbations, Tables 7.20 and 7.21 show the sensitivity results for each reactivity worth, respectively. As can be seen, the finite difference and PERSENT results are very similar for both reactivity worths.

Table 7.19. Eigenvalue Sensitivity Results for Single Node, One Group Problem

	PERSENT	FD
σ_γ	-0.66	-0.65
σ_f	0.89	0.89
ν	1.00	1.00

Table 7.20. C2 Reactivity Worth Sensitivities for Single Node, One Group Problem

	PERSENT		FD	
Isotope →	1	2	1	2
σ_γ	7.37	-8.2	7.38	-8.2
σ_f	-10.0	8.9	-9.94	8.8
ν	-11.3	10.3	-11.2	10.2

Table 7.21. C3 Reactivity Worth Sensitivities for Single Node, One Group Problem

	PERSENT			FD		
Isotope →	1	2	3	1	2	3
σ_γ	11.1	-12.38	-0.52	11.1	-12.4	-0.52
σ_f	-15.0	13.81	0.00	-14.9	13.67	0.0
ν	-16.9	15.87	0.00	-16.7	15.71	0.0
σ_s	0.00	0.00	0.016	0	0.0	0.015

Lastly, the sensitivities were calculated for the C4, C5, and C6 reactivity worths which were found to be -0.128954, -0.0113768, and -0.00112428, respectively. The computed sensitivities for PERSENT and FD are shown in Table 7.22 for isotope 1 and Table 7.23 for isotope 3. As seen in the tables, even though the reactivity worth progressively reduces, both PERSENT and FD yield consistent results.

Table 7.22. Isotope 1, C4-C6 Sensitivities for Single Node, One Group Problem

	PERSENT			FD		
	C4	C5	C6	C4	C5	C6
σ_γ	-0.62	-0.62	-0.61	-0.61	-0.61	-0.61
σ_f	-1.10	-1.10	-1.10	-1.09	-1.09	-1.09
ν	-1.00	-1.00	-1.00	-0.99	-0.99	-0.99

Table 7.23. Isotope 3, C4-C6 Sensitivities for Single Node, One Group Problem

	PERSENT			FD		
	C4	C5	C6	C4	C5	C6
σ_γ	0.181	0.192	0.193	0.182	0.192	0.193
σ_s	-0.035	-0.030	-0.030	-0.034	-0.030	-0.030

Note that a c=0.01 factor was used in all of the FD calculations for this section. Overall, the single node, one group benchmark test is not very rigorous, but it allows easy checks with semi-analytical calculations. Such calculations are complicated to reproduce because of the presence of the inhomogeneous eigenvalue solver.

7.5 Three Group Single Node Example

The next example is a 200 cm x 200 cm problem with vacuum boundary conditions that uses the data from Tables 7.4 and Table 7.5 and can be found as verification problem #12. With the introduction of vacuum boundary conditions, we can see the difference in using diffusion and transport theory, and we also incrementally increase the difficulty of the verification problems. We again use FD diffusion theory for the comparison. Table 7.24 shows the eigenvalue convergence with respect to space and angular approximations for diffusion and transport theory.

Table 7.24. Single Node, One Group Diffusion Theory Eigenvalue Convergence

Nodal Flux	Nodal Leakage	Diffusion	P3	P5	P7
4	1	0.177310	0.178895	0.178898	0.178899
5	1	0.177312	0.178898	0.178904	0.178905
6	1	0.177312	0.178898	0.178905	0.178907
6	2	0.177306	0.178892	0.178898	0.178899
7	2	0.177306	0.178892	0.178898	0.178900
8	3	0.177306	0.178892	0.178898	0.178900
10	4	0.177306	0.178892	0.178898	0.178900
13	5	0.177306	0.178892	0.178898	0.178900

From Table 7.24, one can see that the eigenvalue is significantly different between diffusion and transport (~150 pcm). Convergence with respect to angle is achieved near P7 while spatial convergence is observed at an 8^{th} order nodal flux and 3^{rd} order leakage approximation in both cases. As a consequence, all of the diffusion theory calculations are done using these spatial settings and compared against P7 transport in the remainder of this section.

Starting with the eigenvalue, the sensitivities were computed with respect to Isotope Y and tabulated in Table 7.25. Whether using diffusion or transport, the eigenvalue sensitivities compare very well against the finite difference results. The reactivity worth sensitivities are tabulated in Table 7.26. Much like the eigenvalue sensitivities, the PERSENT and finite difference results are very similar. It is important to note that there are considerable differences between diffusion theory and transport in these tables. Most importantly, diffusion theory overpredicts the sensitivity to the scattering cross section by nearly an order of magnitude for

this problem. While the problem uses made-up cross section data rather than actual cross section data, this overprediction highlights the fact that transport can have an impact on the sensitivity calculation and thus PERSENT can be a valuable tool.

Table 7.25. Three Group Sensitivity Results of *k*-effective to Isotope Y

	PERSENT			FD		
Diffusion						
Group	1	2	3	1	2	3
σ_{γ}	-0.0211	-0.0160	-0.0051	-0.0209	-0.0158	-0.0051
σ_{f}	0.2166	0.1462	0.0461	0.2171	0.1466	0.0462
ν	0.2377	0.1542	0.0486	0.2380	0.1545	0.0491
$\sigma_{s,*\leftarrow g}$	-0.0002	0.0007	0.0002	0.0000	0.0011	0.0006
Transport						
σ_{γ}	-0.0215	-0.0162	-0.0051	-0.0212	-0.0157	-0.0050
σ_{f}	0.2161	0.1462	0.0462	0.2163	0.1464	0.0464
ν	0.2376	0.1543	0.0488	0.2381	0.1543	0.0492
$\sigma_{s,*\leftarrow g}$	-0.0011	0.0004	0.0001	-0.0006	0.0006	0.0006

Table 7.26. Three Group Sensitivity Results of ρ to Isotope Y

	PERSENT			FD		
Diffusion						
Group	1	2	3	1	2	3
σ_{γ}	0.0361	0.0155	0.0048	0.0360	0.0152	0.0048
σ_{f}	-0.1708	-0.1561	-0.0750	-0.1707	-0.1558	-0.0749
ν	-0.2070	-0.1639	-0.0774	-0.2067	-0.1636	-0.0775
$\sigma_{s,*\leftarrow g}$	0.2063	0.0604	0.0079	0.2063	0.0605	0.0078
Transport						
σ_{γ}	0.0016	0.0007	0.0030	0.0016	0.0008	0.0029
σ_{f}	-0.2254	-0.1573	-0.0571	-0.2249	-0.1570	-0.0572
ν	-0.2270	-0.1576	-0.0586	-0.2265	-0.1573	-0.0585
$\sigma_{s,*\leftarrow g}$	0.0229	0.0062	0.0015	0.0231	0.0063	0.0016

Continuing with the delay parameters, Tables 7.27 and 7.28 provide the sensitivities for Λ_G and β. The results between PERSENT and FD are very similar with the exception of some very low sensitivity values of Beta corresponding to the scattering. In this last case, the actual change in Beta is below the printed accuracy reported by PERSENT and thus the FD calculation yields zeros. We also note that there is relatively little difference between diffusion theory and transport with regard to either kinetics parameter. This is consistent with other observations that the kinetics parameters are themselves relatively insensitive to using diffusion or transport. Note that this does not mean the distribution is insensitive, but only the total parameter.

Table 7.27. Three Group Sensitivity Results of Λ_G to Isotope Y

	PERSENT			FD		
Diffusion						
Group	1	2	3	1	2	3
σ_γ	0.0176	-0.0107	-0.0405	0.0177	-0.0106	-0.0401
σ_f	-0.3780	-0.1776	0.1465	-0.3764	-0.1770	0.1463
ν	-0.3956	-0.1722	0.1667	-0.3941	-0.1719	0.1668
$\sigma_{s,*\leftarrow g}$	0.0183	0.0228	0.0014	0.0185	0.0228	0.0016
Transport						
σ_γ	0.0179	-0.0108	-0.0406	0.0177	-0.0110	-0.0406
σ_f	-0.3773	-0.1777	0.1460	-0.3762	-0.1775	0.1455
ν	-0.3952	-0.1723	0.1663	-0.3940	-0.1719	0.1660
$\sigma_{s,*\leftarrow g}$	0.0190	0.0226	0.0011	0.0189	0.0225	0.0012

Table 7.28. Three Group Sensitivity Results of β to Isotope Y

	PERSENT			FD		
Diffusion						
Group	1	2	3	1	2	3
σ_γ	0.0022	-0.0015	-0.0006	0.0018	-0.0018	-0.0009
σ_f	0.0494	0.0128	0.0055	0.0489	0.0125	0.0051
ν	-0.2666	-0.1268	-0.0400	-0.2659	-0.1270	-0.0402
$\sigma_{s,*\leftarrow g}$	-0.0019	0.0002	0.0000	-0.0023	0.0000	0.0000
Transport						
σ_γ	0.0022	-0.0015	-0.0006	0.0023	-0.0014	-0.0005
σ_f	0.0496	0.0127	0.0054	0.0494	0.0129	0.0055
ν	-0.2663	-0.1270	-0.0401	-0.2656	-0.1270	-0.0402
$\sigma_{s,*\leftarrow g}$	-0.0018	0.0002	0.0000	-0.0018	0.0005	0.0000

7.6 Three Group Hex Core Verification Problem

Next, we provide results for an extension of the earlier PERSENT perturbation example shown in Figure 6.1. In that example, we focused on the distribution of the reactivity worth for a control rod insertion. In this case, we consider two perturbations that were not previously discussed: a cross section perturbation and a zone density perturbation. A P_3 angular flux approximation is used with a P_3 scattering kernel (only P_1 data was provided) which was combined with a 6^{th} order flux and linear leakage spatial approximations.

The cross section perturbation we consider is an increase in the third group of the sodium gamma cross section by 5%. The base eigenvalue for this calculation was 1.14440 while the perturbed eigenvalue is 1.14430. Clearly this is a very small perturbation. The second

perturbation is a 5% density increase in the reflector assembly which yielded an eigenvalue of 1.14458. This particular perturbation option was added to make some desired user reactivity worths easier to implement. With respect to the sensitivity test, we choose to consider sensitivities to U238, noting that we switch from diffusion theory to P_3 flux with a P_3 scattering kernel combined with a 6^{th} order flux and linear leakage approximation. Table 7.29 gives the computed sensitivities for U-238 for both perturbations

Table 7.29. Three Group Sensitivities of Verification Problem #4 to U-238.

	PERSENT			FD		
Na Cross Section Perturbation						
Group	1	2	3	1	2	3
σ_{γ}	0.0103	0.0355	-0.4725	0.0104	0.0356	-0.4708
σ_{f}	-0.1489	-0.0005	-0.0001	-0.1481	-0.0005	0.0000
ν	-0.1939	-0.0006	0.0000	-0.1931	-0.0005	0.0001
$\sigma_{elast,*\leftarrow g}$	-0.0062	0.0075	0.0301	-0.0060	0.0081	0.0291
$\sigma_{inelast,*\leftarrow g}$	0.0852	0.0512	0.0001	0.0852	0.0512	0.0001
$\sigma_{n-2n,*\leftarrow g}$	0.0009			0.0009		
Reflector Density Perturbation						
σ_{γ}	0.0003	-0.1096	-1.1716	0.0004	-0.1095	-1.1596
σ_{f}	-0.1165	0.0001	0.0007	-0.1163	0.0002	0.0007
ν	-0.1178	0.0004	0.0009	-0.1174	0.0005	0.0010
$\sigma_{elast,*\leftarrow g}$	-0.0711	-0.3590	-0.4619	-0.0716	-0.3628	-0.4692
$\sigma_{inelast,*\leftarrow g}$	-0.0834	-0.1332	-0.0012	-0.0833	-0.1331	-0.0011
$\sigma_{n-2n,*\leftarrow g}$	-0.0007			-0.0005		

As seen in Table 7.29, the PERSENT and FD results are very similar noting that *c*=0.01 was used for all of the FD calculations.

The only sensitivities of interest not well-tested in the previous benchmarks are the power fraction and the reaction rate ratio sensitivities. Referring to back to Figure 6.1, we first computed the sensitivity of the power fraction of the outer core (0.6895) which is tabulated in Table 7.30 and the sensitivity of the ratio of Pu239 fission to U238 capture reaction rates (1.747984) in the outer core region (see Figure 6.1) are provided in Table 7.31. A c=0.01 setting was used for all of the FD calculations.

Much like the previous tables, the PERSENT and FD difference results are again seen to be very similar. It is important to note that those results with large errors are directly attributable to the inability to get enough precision on the output of DIF3D. As an example, the σ_{f} sensitivity for the power fraction in Table 7.30 of -0.0003, depends upon the sixth significant digit change in the power fraction from 0.692957 to 0.692955 which is at the limit of the precision provided by the DIF3D standard output. From PERSENT, one can see this sensitivity is similar (actually reported as -0.00019), but not identical in Table 7.30.

Table 7.30. Three Group Sensitivities of Outer Core Power Fraction to U-238.

	PERSENT			FD		
Group	1	2	3	1	2	3
σ_{γ}	0.0005	-0.0027	-0.0098	0.0004	-0.0027	-0.0102
σ_{f}	-0.0272	-0.0002	-0.0001	-0.0270	-0.0003	-0.0001
ν	-0.0049	0.0000	0.0000	-0.0045	0.0000	0.0000
$\sigma_{elast,*\leftarrow g}$	0.0047	0.0039	0.0009	0.0040	0.0032	0.0007
$\sigma_{inelast,*\leftarrow g}$	0.0152	-0.0009	0.0000	0.0143	-0.0007	0.0000
$\sigma_{n-2n,*\leftarrow g}$	0.0001	0.0000	0.0000	0.0001	0.0000	0.0000

Table 7.31. Three Group Sensitivities of Reaction Rate Ratio to U-238.

	PERSENT			FD		
Group	1	2	3	1	2	3
σ_{γ}	-0.0370	-0.2058	-0.6193	-0.0368	-0.2056	-0.6228
σ_{f}	-0.0029	0.0000	0.0000	-0.0032	-0.0005	-0.0005
ν	-0.0024	0.0000	0.0000	-0.0027	-0.0005	0.0000
$\sigma_{elast,*\leftarrow g}$	0.0014	-0.0110	-0.0072	0.0014	-0.0112	-0.0062
$\sigma_{inelast,*\leftarrow g}$	-0.0293	-0.0234	0.0000	-0.0271	-0.0218	0.0000
$\sigma_{n-2n,*\leftarrow g}$	-0.0003	0.0000	0.0000	-0.0009	0.0000	0.0000

Overall, the above power fraction and reaction rate ratio tests are more prone to numerical roundoff (convergence error especially) with finite difference and thus we consider the comparison provided by Tables 7.30 and 7.31 to be sufficient proof that PERSENT can obtain the sensitivities.

We now make a note on computational effort. The PERSENT calculations for this benchmark problem required a total computational effort of 53 seconds (three forward and three adjoint eigenvalue problems and two inhomogeneous ones) on a modern workstation. A considerable portion of this effort is spent on the inhomogeneous solve where a total of 90 fission source iterations are used for the two inhomogeneous problems compared with a total of 111 for the six eigenvalue calculations (201 fission source iterations for entire PERSENT calculation). The finite difference calculations needed to complete Tables 7.29 through 7.31 obviously required a larger amount of time (~1296 total fission source iterations) for Table 7.29, but that time is comparable to PERSENT given the time spent on the inhomogeneous solves and various integral operations done in PERSENT to build the tables of data. As the number of energy groups increases, the PERSENT methodology will require less computational effort than finite difference by a much wider margin.

7.7 Twenty-one Group Sensitivity

The last sensitivity problem we consider is the calculation of sensitivities for the sodium density worth of the 21 group problem defined earlier in Section 6.2. In this case, we increase

the flux approximation to P_5 and use a P_3 scattering kernel and compare it against the diffusion theory result. Noting that each diffusion theory calculation takes ~23 seconds and each P_5 calculation takes 40 minutes, the sensitivities are much more expensive than any of the previous problems. PERSENT will compute 16 total reaction rates when specifying the "everything" option for alpha.

Noting that each application of the coefficient matrix is approximately equivalent to a single outer iteration (0.5 seconds in diffusion theory and 48 seconds in P_5 transport), this calculation will require 16×21=336 applications (168 seconds in diffusion theory and 4.5 hours in P_5 transport), it is strongly advised that users use caution. In the 33 group problem, we have 29 unique isotope labels of interest including structure, fuel, and coolant. Computing the transport sensitivities of just the eigenvalue for all reactions of all isotopes will require 29×16×21=9744 applications which translate to 130 hours of computational effort. We performed these calculations by precomputing and storing the NHFLUX and NAFLUX files and simultaneously carrying out the sensitivities for each reaction of each isotope. This requires at most 168 input problems per sensitivity but only requires ~30 minutes of computational effort per reaction of any given isotope. Note that performing the finite difference sensitivities is considerably more expensive as each of the 9744 applications would require a flux solution.

While the generation of all of these sensitivities is straightforward, the purpose of this manuscript is to demonstrate the significance of having a transport versus diffusion theory capability. Therefore, rather than generate sensitivities for all isotopes, we only consider the sensitivities for Na, Fe, and Pu239. One especially important aspect to note is the ability to compute the sensitivities to anisotropic scattering. Of all of the sensitivities to compute, we choose to study the behavior of the eigenvalue given in Tables 7.32 through 7.36, a sodium density perturbation given in Tables 7.37 through 7.41, and the point kinetics parameter Λ given in Tables 7.42 through 7.46. The diffusion theory eigenvalue was computed as 1.041997 while the P_5 transport eigenvalue was 1.054364 (P_3 scattering kernel). The sodium density reactivity worth in diffusion theory was computed as 0.0170233 while the P_5 transport worth was 0.0179385. Finally, Λ was computed in diffusion theory to be $3.999 \cdot 10^{-7}$ while the P_5 transport value is $3.967 \cdot 10^{-7}$.

Starting with the eigenvalue sensitivity, Tables 7.32 through 7.34 give the sensitivities for the σ_γ, $\sigma_{elastic}$, and $\sigma_{inelastic}$ cross sections for isotopes Na, Fe, and Pu-239. Table 7.35 gives the sensitivities of the $\sigma_{fission}$ and ν cross sections for Pu-239 while Table 7.36 gives the P_1 anisotropic $\sigma_{elastic}$ scattering cross section of all three targeted isotopes. Note that in all of these tables and Tables 7.37 through 7.46, the sensitivities are multiplied by 10^3 to improve the readability of the data. In Table 7.32, one can see that the σ_γ sensitivities for Pu-239 and Fe are more than an order of magnitude greater than the corresponding sensitivities for Na. The peak of the sensitivities for each isotope occurs at different energies due to the different resonance characteristics of each isotope. Comparison of the diffusion theory result to the transport shows very little impact for this cross section for any of the targeted isotopes. This is expected as the σ_γ cross section is not the dominant portion of the total cross section in these isotopes and thus does not dramatically change the flux solution (either spectrum or leakage) whether it be diffusion or transport theory.

The sensitivities for $\sigma_{elastic}$ given in Table 7.33 show a considerable increase in magnitude relative to the σ_γ sensitivities in Table 7.32. Most interesting is the change in Na sensitivities in Table 7.33 for transport. Upon closer inspection, the sensitivities for nearly all energy groups are substantially reduced when using transport, with the exception being the large negative sensitivities for the resonance range which increase when using transport. The Fe sensitivities are also observed to decrease like those of Na while the Pu239 sensitivities are much more like those in Table 7.33. The behavior of Na is expected as it accounts for a bulk of the elastic scattering in the core region followed closely by Fe. One interesting thing to note is that there is a significant amount of change in the Fe sensitivity from diffusion to transport in the higher energy groups, but the bulk of the total change still comes from a few key energy groups again associated with resonances in the problem.

The $\sigma_{inelastic}$ scattering results shown in Table 7.34 are very similar to the σ_γ sensitivities in both magnitude and transport/diffusion behavior. Note that because this is a threshold reaction, there is an energy below which no inelastic scattering occurs. As a consequence, the bulk of the sensitivities come from those groups with a large inelastic scattering probability.

Of all the sensitivities listed in Tables 7.32 through 7.36, the sensitivities to the $\sigma_{fission}$ and ν cross sections are certainly the most important as they dominate the fission neutron production. As a consequence, the sensitivities are at least an order of magnitude larger than those observed with the other cross sections as seen in Table 7.35. Close inspection shows that the magnitude of the sensitivities almost follows the shape of the flux spectrum for the system. Interestingly, there is little if any difference between the diffusion and transport results which indicates that changing these cross sections does not fundamentally change the shape of the solution.

One of the main advantages of having a transport (versus a diffusion-only) sensitivity capability is that the impact of the anisotropic scattering cross sections can be assessed. In the current version, we only allow sensitivities for the P_1 scattering kernel noting that it would be quite trivial to modify the code to target higher order moments. Table 7.36 gives the P_1 scattering sensitivities for each targeted isotope. These values are smaller than the sensitivities observed for the isotropic scattering moments. In general, this is the expected result as the magnitude of the higher order moments should be less than the isotropic component. The size of the core also reduces the impact that the anisotropic scattering kernel has on the overall solution and thus sensitivities.

From Tables 7.32 through 7.36, it should be clear that the cross sections associated with the fission neutron production are by far the most important with regard to sensitivities while those that have a minor impact on the flux solution are the least important. Unlike the previous calculations, we did not expend any additional effort to verify the sensitivities by performing FD calculations. This is primarily because of the overwhelming computational expense associated with that effort as evident from the expense of the PERSENT work.

Table 7.32. Twenty-one Group Sensitivities·10^3 of the Eigenvalue for σ_γ.

	Diffusion			Transport			Error of Diffusion		
Upper Energy	Na	Fe	Pu239	Na	Fe	Pu239	Na	Fe	Pu239
14,190,700	0.00	-0.01	0.00	0.00	-0.01	0.00	0.50%	-0.10%	-2.70%
6,065,310	0.00	-0.03	0.00	0.00	-0.03	0.00	0.70%	0.20%	-2.10%
3,678,790	-0.01	-0.11	-0.02	-0.01	-0.11	-0.02	0.70%	0.30%	-2.00%
2,231,300	-0.01	-0.24	-0.06	-0.01	-0.23	-0.06	0.70%	0.70%	-1.40%
1,353,350	-0.02	-0.59	-0.16	-0.02	-0.59	-0.17	0.80%	0.70%	-1.20%
820,850	-0.04	-1.86	-0.85	-0.04	-1.85	-0.86	0.70%	0.40%	-1.00%
497,871	-0.05	-1.24	-1.25	-0.05	-1.24	-1.26	0.30%	-0.10%	-1.10%
301,974	-0.11	-1.70	-1.88	-0.11	-1.70	-1.90	0.30%	-0.10%	-0.90%
183,156	-0.12	-1.86	-2.19	-0.12	-1.86	-2.20	0.10%	-0.20%	-0.90%
111,090	0.00	-2.39	-2.38	0.00	-2.39	-2.40	0.30%	-0.10%	-0.80%
67,380	-0.08	-1.13	-2.66	-0.08	-1.13	-2.69	0.10%	-0.20%	-0.80%
40,868	-0.14	-2.26	-2.24	-0.14	-2.28	-2.28	-0.60%	-1.30%	-1.50%
24,788	0.00	-0.92	-3.54	0.00	-0.93	-3.57	-0.10%	-0.90%	-0.70%
15,034	0.00	-0.80	-3.06	0.00	-0.81	-3.08	0.00%	-0.50%	-0.50%
9,119	-0.02	-0.99	-2.45	-0.02	-0.99	-2.46	0.10%	-0.40%	-0.40%
5,531	-0.08	-0.22	-2.32	-0.08	-0.22	-2.33	0.10%	-0.90%	-0.60%
3,355	-0.42	-0.06	-1.34	-0.41	-0.06	-1.34	0.20%	-1.00%	-0.50%
2,035	-0.21	-0.29	-3.62	-0.21	-0.29	-3.63	-0.10%	-0.70%	-0.10%
1,234	-0.10	-4.35	-5.00	-0.10	-4.38	-5.01	-0.70%	-0.80%	-0.20%
454	-0.04	-0.72	-2.24	-0.05	-0.74	-2.26	-1.20%	-2.30%	-1.00%
61	-0.02	-0.43	-0.19	-0.02	-0.44	-0.20	-0.80%	-2.40%	-2.70%
Total	**-1.48**	**-22.18**	**-37.46**	**-1.48**	**-22.29**	**-37.71**			

Table 7.33. Twenty-one Group Sensitivities·10^3 of the Eigenvalue for $\sigma_{elastic}$.

	Diffusion			Transport			Error of Diffusion		
Upper Energy	Na	Fe	Pu239	Na	Fe	Pu239	Na	Fe	Pu239
14,190,700	0.10	0.86	0.04	0.06	0.75	0.04	73.50%	14.60%	14.70%
6,065,310	0.73	2.85	0.15	0.55	2.56	0.13	31.90%	11.00%	11.80%
3,678,790	1.57	6.28	0.30	1.04	5.61	0.27	50.90%	11.90%	11.20%
2,231,300	1.35	5.99	0.24	0.67	5.38	0.22	103.20%	11.30%	8.20%
1,353,350	1.52	5.99	0.19	0.89	5.51	0.17	69.90%	8.80%	7.00%
820,850	1.96	8.06	0.34	1.23	7.36	0.32	60.00%	9.60%	4.50%
497,871	-1.25	6.54	0.15	-1.86	5.29	0.12	-32.70%	23.60%	17.70%
301,974	-0.27	4.18	0.22	-0.86	3.26	0.21	-68.30%	28.20%	5.40%
183,156	-0.79	4.78	0.25	-1.33	4.04	0.23	-40.50%	18.40%	7.50%
111,090	-1.79	2.83	0.13	-1.93	2.73	0.13	-6.90%	3.60%	1.00%
67,380	-1.09	0.52	0.09	-1.16	0.48	0.09	-6.30%	8.80%	2.70%
40,868	-0.29	4.58	0.05	-0.99	1.56	0.02	-70.70%	193.80%	190.80%
24,788	1.64	2.21	0.13	1.40	2.09	0.12	17.10%	5.60%	2.10%
15,034	0.72	1.13	0.06	0.65	1.07	0.06	10.60%	6.40%	0.60%
9,119	0.20	0.48	0.01	0.18	0.46	0.01	8.70%	4.00%	3.10%
5,531	0.15	0.05	0.01	0.15	0.05	0.01	3.70%	-0.70%	9.70%
3,355	0.51	0.12	0.00	0.48	0.13	0.00	6.10%	-4.70%	15.80%
2,035	-0.01	-0.14	0.00	-0.02	-0.14	0.00	-15.70%	6.40%	-193.60%
1,234	0.08	-0.01	0.01	0.09	0.00	-0.01	-7.30%	321.80%	-193.10%
454	-0.19	-1.32	0.02	-0.17	-1.35	-0.02	10.80%	-1.60%	-192.30%
61	-0.06	-0.47	0.00	-0.05	-0.47	0.00	13.90%	-1.40%	-191.70%
Total	**4.77**	**55.52**	**2.39**	**-0.99**	**46.39**	**2.13**			

Table 7.34. Twenty-one Group Sensitivities·10^3 of the Eigenvalue for $\sigma_{inelastic}$.

	Diffusion			Transport			Error of Diffusion		
Upper Energy	Na	Fe	Pu239	Na	Fe	Pu239	Na	Fe	Pu239
14,190,700	-0.34	-1.65	-0.04	-0.38	-1.73	-0.04	-10.20%	-4.10%	-6.10%
6,065,310	-0.36	-4.40	-0.27	-0.47	-4.54	-0.29	-23.40%	-3.10%	-4.40%
3,678,790	-2.19	-7.17	-0.89	-2.35	-7.37	-0.92	-6.80%	-2.80%	-3.60%
2,231,300	-1.50	-11.03	-0.92	-1.61	-11.02	-0.94	-7.10%	0.10%	-2.50%
1,353,350	-2.17	-7.70	-0.53	-2.20	-7.64	-0.55	-1.50%	0.80%	-2.30%
820,850	-3.09	-0.24	-0.69	-3.10	-0.24	-0.70	-0.30%	-0.80%	-1.90%
497,871	-0.04	-0.13	-0.18	-0.04	-0.14	-0.19	-0.40%	-5.00%	-6.50%
301,974	0.00	-0.06	-0.07	0.00	-0.06	-0.08	0.00%	-7.80%	-4.80%
183,156	0.00	-0.07	-0.12	0.00	-0.08	-0.12	0.00%	-5.20%	-3.50%
111,090	0.00	-0.10	-0.08	0.00	-0.10	-0.08	0.00%	1.20%	0.40%
67,380	0.00	-0.11	-0.04	0.00	-0.11	-0.04	0.00%	2.00%	2.40%
40,868	0.00	-0.09	-0.01	0.00	-0.12	-0.02	0.00%	-23.50%	-36.90%
24,788	0.00	-0.19	0.03	0.00	-0.19	0.03	0.00%	0.10%	12.20%
15,034	0.00	0.00	0.02	0.00	0.00	0.02	0.00%	2.60%	0.20%
9,119	0.00	0.00	0.00	0.00	0.00	0.00	0.00%	0.00%	1.40%
5,531	0.00	0.00	0.00	0.00	0.00	0.00	0.00%	0.00%	0.00%
3,355	0.00	0.00	0.00	0.00	0.00	0.00	0.00%	0.00%	0.00%
2,035	0.00	0.00	0.00	0.00	0.00	0.00	0.00%	0.00%	0.00%
1,234	0.00	0.00	0.00	0.00	0.00	0.00	0.00%	0.00%	0.00%
454	0.00	0.00	0.00	0.00	0.00	0.00	0.00%	0.00%	0.00%
61	0.00	0.00	0.00	0.00	0.00	0.00	0.00%	0.00%	0.00%
Total	**-9.69**	**-32.94**	**-3.79**	**-10.15**	**-33.33**	**-3.92**			

Table 7.35. Twenty-one Group Sensitivities·10^3 of the Eigenvalue for Pu-239 $\sigma_{fission}$ and ν.

	Diffusion		Transport		Error of Diffusion	
Upper Energy	Nu	Fission	Nu	Fission	Nu	Fission
14,190,700	2.58	1.77	2.61	1.77	-1.00%	-0.20%
6,065,310	8.25	5.61	8.31	5.61	-0.70%	0.00%
3,678,790	21.66	14.08	21.79	14.05	-0.60%	0.20%
2,231,300	31.91	21.00	31.94	20.88	-0.10%	0.60%
1,353,350	35.52	24.21	35.49	24.05	0.10%	0.70%
820,850	58.48	40.65	58.39	40.37	0.20%	0.70%
497,871	47.86	34.17	47.76	33.92	0.20%	0.70%
301,974	54.22	39.32	54.14	39.09	0.20%	0.60%
183,156	58.27	42.86	58.19	42.65	0.10%	0.50%
111,090	50.04	37.35	49.96	37.17	0.20%	0.50%
67,380	42.33	32.06	42.24	31.89	0.20%	0.50%
40,868	31.52	24.18	31.61	24.16	-0.30%	0.10%
24,788	37.82	29.17	37.88	29.17	-0.20%	0.00%
15,034	25.49	19.58	25.53	19.60	-0.20%	-0.10%
9,119	15.40	11.77	15.43	11.78	-0.20%	-0.10%
5,531	11.81	9.01	11.85	9.03	-0.30%	-0.20%
3,355	5.45	4.15	5.46	4.16	-0.20%	-0.10%
2,035	17.47	13.27	17.46	13.25	0.10%	0.20%
1,234	25.83	19.61	25.82	19.59	0.10%	0.10%
454	10.09	7.43	10.16	7.48	-0.70%	-0.60%
61	0.86	0.64	0.88	0.65	-2.20%	-2.00%
Total	**592.87**	**431.91**	**592.89**	**430.32**		

Table 7.36. Twenty-one Group Sensitivities·10^3 of the Eigenvalue for P_1 $\sigma_{elastic}$.

	Na	Fe	Pu239
14,190,700	-0.07	-0.70	-0.03
6,065,310	-0.28	-1.80	-0.12
3,678,790	-0.96	-3.06	-0.22
2,231,300	-1.13	-2.66	-0.16
1,353,350	-1.29	-1.70	-0.11
820,850	-1.67	-2.46	-0.17
497,871	-0.21	-0.64	-0.06
301,974	-0.20	-0.67	-0.07
183,156	-0.11	-0.36	-0.05
111,090	-0.06	-0.19	-0.02
67,380	-0.05	-0.23	-0.01
40,868	0.00	-0.03	0.00
24,788	-0.07	-0.12	0.00
15,034	-0.03	-0.06	0.00
9,119	0.00	-0.01	0.00
5,531	-0.01	0.00	0.00
3,355	0.00	0.00	0.00
2,035	0.00	0.00	0.00
1,234	0.00	0.00	0.00
454	0.00	0.01	0.00
61	0.00	0.01	0.00
Total	**-6.15**	**-14.69**	**-1.02**

Table 7.37. Twenty-one Group Sensitivities·10^3 of the Na Density Perturbation for σ_γ.

	Diffusion			Transport			Error of Diffusion		
Upper Energy	Na	Fe	Pu239	Na	Fe	Pu239	Na	Fe	Pu239
14,190,700	0.03	-0.03	0.00	0.03	-0.03	0.00	4.00%	5.70%	0.00%
6,065,310	0.11	-0.10	-0.01	0.10	-0.09	-0.01	4.70%	7.90%	1.60%
3,678,790	0.31	-0.46	-0.06	0.29	-0.43	-0.06	4.80%	7.70%	1.90%
2,231,300	0.49	-0.48	-0.07	0.47	-0.42	-0.06	5.60%	13.80%	6.30%
1,353,350	0.64	-2.79	-0.61	0.60	-2.54	-0.58	5.60%	9.60%	5.20%
820,850	1.51	-9.70	-3.41	1.43	-8.91	-3.23	5.70%	8.90%	5.60%
497,871	1.62	-5.90	-4.26	1.53	-5.45	-4.04	5.80%	8.30%	5.40%
301,974	4.03	-5.57	-3.75	3.80	-5.12	-3.50	6.10%	8.70%	7.20%
183,156	4.28	-3.27	-0.64	4.03	-2.97	-0.55	6.20%	10.00%	15.10%
111,090	0.07	-4.02	-0.82	0.06	-3.65	-0.72	6.30%	10.20%	13.90%
67,380	2.69	0.00	4.00	2.53	0.03	3.81	6.30%	-110.1%	5.00%
40,868	5.08	-1.33	1.84	4.81	-1.38	1.51	5.70%	-4.10%	21.90%
24,788	0.07	1.80	15.79	0.06	1.71	15.00	6.60%	5.30%	5.30%
15,034	0.14	4.06	22.67	0.13	3.83	21.47	6.80%	6.20%	5.60%
9,119	0.79	5.53	18.87	0.74	5.20	17.86	6.80%	6.40%	5.60%
5,531	2.96	-1.88	-25.11	2.78	-1.77	-23.76	6.40%	6.20%	5.70%
3,355	14.28	0.19	9.68	13.39	0.18	9.18	6.60%	5.60%	5.50%
2,035	7.24	4.11	78.45	6.73	3.86	74.06	7.50%	6.50%	5.90%
1,234	3.45	70.83	113.08	3.22	66.23	106.12	7.20%	6.90%	6.60%
454	0.86	2.70	40.78	0.81	2.59	38.13	6.20%	4.30%	7.00%
61	0.04	-0.30	0.44	0.04	-0.23	0.43	0.10%	33.80%	2.30%
Total	**50.67**	**53.41**	**266.86**	**47.58**	**50.63**	**251.04**			

Table 7.38. Twenty-one Group Sensitivities·10^3 of the Na Density Perturbation for $\sigma_{elastic}$.

	Diffusion			Transport			Error of Diffusion		
Upper Energy	Na	Fe	Pu239	Na	Fe	Pu239	Na	Fe	Pu239
14,190,700	-0.48	8.77	0.49	-0.11	6.94	0.37	321.10%	26.30%	32.00%
6,065,310	-14.29	22.92	1.36	-12.31	18.94	1.05	16.10%	21.00%	29.50%
3,678,790	-13.59	60.97	3.34	-8.63	49.43	2.58	57.50%	23.30%	29.50%
2,231,300	14.68	43.59	1.73	18.23	36.33	1.35	-19.50%	20.00%	27.80%
1,353,350	34.24	61.47	2.33	35.27	51.84	1.86	-2.90%	18.60%	24.90%
820,850	45.47	96.12	5.85	46.92	83.88	5.04	-3.10%	14.60%	16.10%
497,871	86.87	48.63	1.39	89.76	35.24	0.94	-3.20%	38.00%	48.50%
301,974	68.86	29.75	2.49	68.16	23.40	2.18	1.00%	27.10%	14.00%
183,156	64.54	15.88	1.27	65.86	11.79	0.94	-2.00%	34.80%	35.20%
111,090	75.89	4.71	0.51	70.66	4.47	0.39	7.40%	5.50%	29.70%
67,380	48.95	-11.13	0.26	45.50	-8.87	0.24	7.60%	25.50%	8.20%
40,868	21.67	6.06	-0.26	34.55	-4.14	-0.53	-37.30%	-246.70%	-50.90%
24,788	-37.19	-3.85	-0.57	-29.88	-3.12	-0.57	24.50%	23.60%	-1.10%
15,034	-26.77	-10.53	-0.46	-23.93	-9.60	-0.48	11.90%	9.70%	-3.40%
9,119	-7.24	-4.51	-0.14	-6.57	-4.26	-0.14	10.20%	5.80%	-1.00%
5,531	-10.32	6.71	0.38	-9.88	6.75	0.37	4.40%	-0.50%	2.60%
3,355	-22.64	-1.07	-0.01	-20.12	-1.61	-0.01	12.50%	-33.70%	-17.50%
2,035	-4.06	-17.60	-0.52	-3.57	-16.44	-0.49	13.90%	7.10%	6.90%
1,234	-6.50	-20.93	-0.36	-5.58	-19.44	-0.35	16.40%	7.70%	4.70%
454	1.17	-3.39	0.00	1.33	-3.04	0.00	-12.10%	11.70%	-384.40%
61	0.24	-0.68	0.00	0.28	-0.58	0.00	-14.70%	17.50%	555.60%
Total	**319.49**	**331.88**	**19.07**	**355.95**	**257.91**	**14.75**			

Table 7.39. Twenty-one Group Sensitivities·10^3 of the Na Density Perturbation for $\sigma_{inelastic}$.

	Diffusion			Transport			Error of Diffusion		
Upper Energy	Na	Fe	Pu239	Na	Fe	Pu239	Na	Fe	Pu239
14,190,700	17.34	-11.64	-0.23	17.19	-11.86	-0.26	0.80%	-1.90%	-9.00%
6,065,310	24.82	-6.63	-0.62	24.70	-7.28	-0.68	0.50%	-8.90%	-9.50%
3,678,790	101.79	-30.26	-3.57	99.09	-30.89	-3.73	2.70%	-2.00%	-4.20%
2,231,300	71.49	-14.69	-1.34	68.54	-12.79	-1.35	4.30%	14.90%	-0.40%
1,353,350	92.86	-59.40	-2.99	88.47	-54.38	-2.99	5.00%	9.20%	0.00%
820,850	107.69	-2.17	-4.75	103.31	-2.00	-4.54	4.20%	8.70%	4.60%
497,871	1.19	-1.09	-1.22	1.14	-1.06	-1.31	4.30%	3.10%	-6.80%
301,974	0.00	-0.40	-0.23	0.00	-0.39	-0.22	0.00%	2.70%	2.60%
183,156	0.00	-0.50	-0.47	0.00	-0.47	-0.46	0.00%	6.10%	1.60%
111,090	0.00	-0.76	-0.58	0.00	-0.66	-0.52	0.00%	14.10%	11.10%
67,380	0.00	-0.75	-0.23	0.00	-0.63	-0.18	0.00%	18.10%	28.60%
40,868	0.00	-0.79	-0.26	0.00	-1.00	-0.33	0.00%	-20.80%	-22.10%
24,788	0.00	-0.64	0.13	0.00	-0.58	0.09	0.00%	10.20%	52.60%
15,034	0.00	-0.01	-0.06	0.00	-0.01	-0.08	0.00%	5.90%	-18.20%
9,119	0.00	0.00	0.00	0.00	0.00	0.00	0.00%	0.00%	-225.70%
5,531	0.00	0.00	0.00	0.00	0.00	0.00	0.00%	0.00%	0.00%
3,355	0.00	0.00	0.00	0.00	0.00	0.00	0.00%	0.00%	0.00%
2,035	0.00	0.00	0.00	0.00	0.00	0.00	0.00%	0.00%	0.00%
1,234	0.00	0.00	0.00	0.00	0.00	0.00	0.00%	0.00%	0.00%
454	0.00	0.00	0.00	0.00	0.00	0.00	0.00%	0.00%	0.00%
61	0.00	0.00	0.00	0.00	0.00	0.00	0.00%	0.00%	0.00%
Total	**417.17**	**-129.74**	**-16.43**	**402.43**	**-124.01**	**-16.56**			

Table 7.40. Twenty-one Group Sensitivities·10^3 of the Na Density Perturbation for Pu239 $\sigma_{fission}$ and ν.

	Diffusion		Transport		Error of Diffusion	
Upper Energy	Nu	Fission	Nu	Fission	Nu	Fission
14,190,700	7.44	3.87	7.10	3.53	4.70%	9.50%
6,065,310	16.18	8.65	15.12	7.72	7.00%	12.10%
3,678,790	52.04	25.58	48.85	22.88	6.50%	11.80%
2,231,300	3.63	-8.03	0.77	-10.21	369.90%	-21.30%
1,353,350	96.22	53.98	87.44	47.27	10.00%	14.20%
820,850	181.79	110.32	166.01	98.31	9.50%	12.20%
497,871	134.49	87.77	121.46	77.14	10.70%	13.80%
301,974	86.16	56.42	75.80	48.05	13.70%	17.40%
183,156	1.33	-3.16	-4.12	-8.02	-132.40%	-60.60%
111,090	11.13	6.79	6.03	2.22	84.60%	205.80%
67,380	-56.70	-41.29	-56.91	-42.24	-0.40%	-2.30%
40,868	-11.13	-5.10	-11.19	-6.24	-0.50%	-18.30%
24,788	-140.96	-102.41	-134.66	-98.04	4.70%	4.50%
15,034	-174.61	-130.91	-165.12	-123.73	5.80%	5.80%
9,119	-111.37	-83.49	-105.04	-78.64	6.00%	6.20%
5,531	136.56	106.28	129.27	100.62	5.60%	5.60%
3,355	-37.41	-28.02	-35.40	-26.50	5.70%	5.70%
2,035	-376.53	-285.55	-354.84	-268.96	6.10%	6.20%
1,234	-581.55	-441.02	-544.68	-412.81	6.80%	6.80%
454	-185.07	-136.65	-172.69	-127.42	7.20%	7.20%
61	-1.89	-1.39	-1.86	-1.36	2.10%	2.10%
Total	**-950.26**	**-807.36**	**-928.64**	**-796.42**		

Table 7.41. Twenty-one Group Sensitivities·10^3 of the Na Density Perturbation for P_1 $\sigma_{elastic}$.

	Na	Fe	Pu239
14,190,700	1.50	-6.57	-0.34
6,065,310	5.99	-13.03	-0.91
3,678,790	19.81	-26.09	-2.09
2,231,300	22.67	-14.27	-0.92
1,353,350	20.13	-14.16	-1.12
820,850	29.40	-26.63	-2.55
497,871	2.54	-4.39	-0.45
301,974	3.28	-4.67	-0.62
183,156	1.59	-1.40	-0.18
111,090	0.95	-0.69	-0.07
67,380	0.99	-0.62	-0.03
40,868	0.04	0.03	0.00
24,788	0.80	0.05	0.02
15,034	0.57	0.30	0.01
9,119	0.08	0.08	0.00
5,531	0.02	-0.11	0.00
3,355	0.00	-0.01	0.00
2,035	0.05	0.19	0.00
1,234	0.00	0.17	0.00
454	-0.04	0.04	0.00
61	-0.01	0.01	0.00
Total	**110.34**	**-111.78**	**-9.24**

Table 7.42. Twenty-one Group Sensitivities·10^3 of Λ for σ_γ.

	Diffusion			Transport			Error of Diffusion		
Upper Energy	Na	Fe	Pu239	Na	Fe	Pu239	Na	Fe	Pu239
14,190,700	0.00	0.00	0.00	0.00	0.00	0.00	295.5%	275.9%	111.2%
6,065,310	0.00	0.01	0.00	0.00	0.00	0.00	8563.1%	4009.6%	170.7%
3,678,790	0.00	0.05	0.01	0.00	0.00	0.00	-2648.8%	-1564.1%	180.2%
2,231,300	0.00	0.05	0.03	0.00	-0.06	0.01	-225.7%	-179.7%	424.1%
1,353,350	0.00	-0.08	0.05	-0.01	-0.34	-0.02	-97.2%	-77.5%	-380.5%
820,850	-0.01	-0.67	0.09	-0.03	-1.51	-0.29	-65.1%	-56.0%	-132.4%
497,871	-0.03	-1.05	-0.25	-0.05	-1.63	-0.81	-40.2%	-35.5%	-69.4%
301,974	-0.10	-1.77	-0.85	-0.16	-2.56	-1.70	-33.6%	-30.9%	-50.2%
183,156	-0.16	-2.78	-1.70	-0.22	-3.66	-2.69	-25.8%	-24.0%	-36.8%
111,090	0.00	-4.82	-2.74	0.00	-5.95	-3.82	-20.5%	-19.1%	-28.2%
67,380	-0.17	-2.85	-4.22	-0.21	-3.39	-5.42	-16.9%	-15.9%	-22.1%
40,868	-0.39	-7.20	-4.58	-0.46	-8.40	-5.60	-14.9%	-14.2%	-18.3%
24,788	-0.01	-4.14	-9.78	-0.01	-4.63	-11.35	-11.2%	-10.7%	-13.8%
15,034	-0.02	-4.28	-10.41	-0.02	-4.68	-11.77	-9.30%	-8.60%	-11.5%
9,119	-0.11	-5.86	-9.46	-0.12	-6.34	-10.54	-8.10%	-7.60%	-10.30%
5,531	-0.50	-1.61	-10.05	-0.54	-1.73	-11.08	-7.00%	-7.00%	-9.30%
3,355	-2.80	-0.46	-6.17	-3.00	-0.50	-6.75	-6.40%	-6.40%	-8.60%
2,035	-1.76	-2.80	-21.25	-1.87	-2.96	-22.78	-5.70%	-5.30%	-6.70%
1,234	-1.26	-54.92	-41.84	-1.32	-57.35	-43.98	-4.70%	-4.20%	-4.90%
454	-1.39	-24.93	-35.10	-1.42	-25.56	-36.41	-2.10%	-2.50%	-3.60%
61	-1.35	-33.75	-9.80	-1.35	-34.18	-10.04	0.10%	-1.30%	-2.40%
Total	**-10.06**	**-153.86**	**-168.00**	**-10.77**	**-165.44**	**-185.06**			

Table 7.43. Twenty-one Group Sensitivities·10^3 of Λ for $\sigma_{elastic}$.

	Diffusion			Transport			Error of Diffusion		
Upper Energy	Na	Fe	Pu239	Na	Fe	Pu239	Na	Fe	Pu239
14,190,700	-0.16	-1.24	-0.11	-0.07	-0.72	-0.08	121.80%	73.50%	39.10%
6,065,310	-1.23	-4.13	-0.39	-0.71	-2.46	-0.29	72.10%	67.70%	35.10%
3,678,790	-2.33	-8.37	-0.76	-1.07	-4.65	-0.56	118.20%	79.90%	34.70%
2,231,300	-0.86	-5.03	-0.60	0.41	-1.52	-0.46	-311.70%	230.70%	31.90%
1,353,350	0.26	-2.02	-0.43	1.55	1.31	-0.33	-83.50%	-254.10%	30.50%
820,850	5.75	7.39	-0.60	6.85	11.28	-0.45	-16.10%	-34.50%	33.40%
497,871	9.19	6.81	-0.24	8.65	9.28	-0.16	6.20%	-26.60%	44.80%
301,974	8.38	13.55	-0.26	7.97	14.61	-0.18	5.20%	-7.20%	45.40%
183,156	10.01	13.83	-0.26	9.41	15.33	-0.17	6.40%	-9.80%	55.60%
111,090	9.33	11.86	-0.08	8.56	13.39	-0.05	9.10%	-11.40%	63.80%
67,380	7.77	13.92	-0.01	7.18	14.41	0.01	8.10%	-3.40%	-175.40%
40,868	9.52	17.33	0.13	7.16	8.59	0.13	33.00%	101.60%	5.00%
24,788	19.58	23.28	0.08	19.27	23.09	0.12	1.60%	0.80%	-33.40%
15,034	9.01	14.07	0.04	9.13	14.16	0.06	-1.30%	-0.70%	-30.10%
9,119	4.33	3.91	0.02	4.53	4.10	0.03	-4.40%	-4.60%	-8.30%
5,531	2.21	1.55	-0.01	2.41	1.75	-0.01	-8.20%	-11.40%	20.60%
3,355	2.78	1.31	0.02	2.63	1.28	0.02	5.90%	2.50%	-5.00%
2,035	3.57	7.86	0.07	3.49	7.78	0.06	2.30%	1.00%	24.30%
1,234	5.67	24.86	0.07	5.74	25.03	0.05	-1.20%	-0.70%	51.90%
454	-2.62	-10.11	-0.16	-2.23	-10.59	-0.20	17.40%	-4.60%	-19.30%
61	-3.29	-17.78	-0.10	-2.78	-18.08	-0.12	18.20%	-1.70%	-14.70%
Total	**96.88**	**112.84**	**-3.57**	**98.07**	**127.34**	**-2.60**			

Table 7.44. Twenty-one Group Sensitivities·10^3 of Λ for $\sigma_{inelastic}$.

	Diffusion			Transport			Error of Diffusion		
Upper Energy	Na	Fe	Pu239	Na	Fe	Pu239	Na	Fe	Pu239
14,190,700	0.76	4.10	0.10	0.64	3.43	0.08	17.80%	19.30%	17.80%
6,065,310	1.29	12.81	0.70	1.22	11.01	0.60	5.40%	16.30%	17.20%
3,678,790	5.49	18.73	2.19	4.61	15.78	1.84	18.90%	18.70%	19.10%
2,231,300	3.81	27.88	2.33	3.22	23.03	1.95	18.60%	21.10%	19.60%
1,353,350	5.88	23.66	1.45	4.93	20.10	1.23	19.20%	17.70%	18.00%
820,850	9.23	0.92	2.12	7.71	0.81	1.80	19.70%	13.30%	17.80%
497,871	0.13	0.55	0.55	0.11	0.49	0.47	17.20%	11.80%	17.20%
301,974	0.00	0.30	0.25	0.00	0.27	0.21	0.00%	11.40%	19.20%
183,156	0.00	0.41	0.35	0.00	0.38	0.29	0.00%	9.20%	22.10%
111,090	0.00	0.40	0.23	0.00	0.38	0.18	0.00%	7.10%	26.00%
67,380	0.00	0.37	0.11	0.00	0.34	0.09	0.00%	9.20%	28.70%
40,868	0.00	1.33	0.10	0.00	1.12	0.08	0.00%	19.20%	19.60%
24,788	0.00	3.84	0.24	0.00	3.73	0.24	0.00%	2.80%	-2.50%
15,034	0.00	0.04	0.10	0.00	0.04	0.10	0.00%	-2.50%	-5.20%
9,119	0.00	0.00	0.01	0.00	0.00	0.01	0.00%	0.00%	-6.00%
5,531	0.00	0.00	0.00	0.00	0.00	0.00	0.00%	0.00%	0.00%
3,355	0.00	0.00	0.00	0.00	0.00	0.00	0.00%	0.00%	0.00%
2,035	0.00	0.00	0.00	0.00	0.00	0.00	0.00%	0.00%	0.00%
1,234	0.00	0.00	0.00	0.00	0.00	0.00	0.00%	0.00%	0.00%
454	0.00	0.00	0.00	0.00	0.00	0.00	0.00%	0.00%	0.00%
61	0.00	0.00	0.00	0.00	0.00	0.00	0.00%	0.00%	0.00%
Total	**26.58**	**95.33**	**10.83**	**22.45**	**80.90**	**9.17**			

Table 7.45. Twenty-one Group Sensitivities·10^3 of Λ for Pu-239 $\sigma_{fission}$ and ν.

	Diffusion		Transport		Error of Diffusion	
Upper Energy	Nu	Fission	Nu	Fission	Nu	Fission
14,190,700	-4.05	-3.37	-2.89	-2.56	40.40%	31.40%
6,065,310	-12.89	-10.99	-9.14	-8.44	41.00%	30.20%
3,678,790	-33.43	-28.11	-23.63	-21.73	41.50%	29.40%
2,231,300	-48.23	-42.14	-33.75	-32.59	42.90%	29.30%
1,353,350	-52.51	-48.73	-36.41	-37.76	44.20%	29.10%
820,850	-81.31	-79.32	-54.90	-61.01	48.10%	30.00%
497,871	-62.47	-65.20	-40.90	-49.82	52.70%	30.90%
301,974	-65.05	-71.76	-40.64	-54.14	60.00%	32.50%
183,156	-59.35	-71.35	-33.21	-52.20	78.70%	36.70%
111,090	-40.24	-54.87	-17.80	-38.18	126.00%	43.70%
67,380	-22.81	-39.06	-3.87	-24.75	489.30%	57.80%
40,868	-8.17	-23.15	5.91	-12.44	-238.20%	86.20%
24,788	11.03	-12.84	27.88	0.17	-60.40%	-7444.30%
15,034	21.09	1.02	32.47	9.78	-35.00%	-89.60%
9,119	19.68	5.70	26.55	10.97	-25.90%	-48.00%
5,531	20.48	8.37	25.79	12.42	-20.60%	-32.60%
3,355	11.05	5.06	13.47	6.92	-18.00%	-26.90%
2,035	56.13	31.47	63.73	37.31	-11.90%	-15.60%
1,234	147.35	95.35	158.73	104.06	-7.20%	-8.40%
454	126.38	84.69	132.13	88.88	-4.40%	-4.70%
61	39.67	28.30	40.58	28.91	-2.20%	-2.10%
Total	**-37.63**	**-290.94**	**230.07**	**-96.19**		

Table 7.46. Twenty-one Group Sensitivities·10^3 of Λ for P_1 $\sigma_{elastic}$.

Upper Energy	Na	Fe	Pu239
14,190,700	0.10	0.70	0.07
6,065,310	0.39	1.78	0.25
3,678,790	1.30	2.97	0.46
2,231,300	1.35	1.95	0.33
1,353,350	1.15	0.52	0.21
820,850	1.31	0.37	0.27
497,871	0.07	-0.30	0.10
301,974	0.05	-0.29	0.08
183,156	-0.03	-0.39	0.05
111,090	-0.02	-0.25	0.02
67,380	-0.04	-0.39	0.00
40,868	0.03	0.04	0.00
24,788	-0.27	-0.55	0.00
15,034	-0.08	-0.26	0.00
9,119	-0.01	-0.02	0.00
5,531	0.03	-0.02	0.00
3,355	0.00	0.01	0.00
2,035	-0.04	-0.07	0.00
1,234	-0.01	-0.09	0.00
454	0.06	0.09	0.00
61	0.08	0.22	0.00
Total	**5.42**	**6.00**	**1.84**

Continuing with the sensitivities of the sodium density perturbation, as can be inferred from a reactivity worth of 0.017, this is a considerable change in the sodium content of the reactor (it is a sodium void worth) and we can expect rather large sensitivities. Starting with the σ_γ sensitivities given in Table 7.37, one observes a dramatic change relative to the eigenvalue sensitivities of Table 7.32 for all three isotopes. A bulk of this change occurs in the lower energy groups for all isotopes not because the lower energy range is more important, but actually because it is less important in the perturbed case. The large positive number is an artifact of the way the reactivity worth is defined. It is quite obvious that the sodium density perturbation would be affected by changes in the capture cross section of sodium and one can understand that the subsequent hardening of the spectrum will alter the importance of the resonances for all of the isotopes. As a final note, there is again relatively little difference between diffusion and transport theory when estimating the sensitivities of this cross section data.

The $\sigma_{elastic}$ and $\sigma_{inelastic}$ sensitivities for the sodium density perturbation are given in Tables 7.38 and 7.39. As was the case with the σ_γ sensitivity, these sensitivities are considerably larger than the eigenvalue sensitivities for the same cross sections. As an example, for inelastic Na scattering, we see a total sensitivity of 0.417 while the eigenvalue was merely 0.009. Looking at the elastic scattering sensitivities, one can see significant changes in the Fe values between diffusion and transport mostly attributable to the higher energy groups. The same behavior is seen in the inelastic scattering sensitivities, but the threshold reaction precludes any contribution from lower energy groups. Of the two results, we note the extremely high importance of the fourth through sixth energy group sodium inelastic scattering cross section, as all of the sensitivities are considerably higher than those for the elastic scattering cross sections. This highlights the fact that when the sodium is voided, the spectrum is hardened, and thus cross sections that result in softening of the spectrum become far more important.

Looking at the Pu239 $\sigma_{fission}$ and ν sensitivities in Table 7.40, one can see that they are of the same magnitude as the eigenvalue sensitivity but increased by about a factor of two for the sodium density perturbation problem. Much like the eigenvalue sensitivities, no real difference is observed between diffusion and transport in this case and the sensitivity distribution matches the actual flux profile. What is important to note in this case is that the sensitivities of the other reactions are no longer an order of magnitude smaller than those for $\sigma_{fission}$ and ν, but they are now on par with them. This is evidence of the importance of the spectrum change on those cross sections.

Table 7.41 is the last table of sodium density perturbation results and displays the higher order inelastic scattering cross section sensitivities. Once again, the sensitivities are about an order of magnitude larger than the eigenvalue sensitivities and one can see that the upper energy regimes are clearly the dominant components due to the spectrum change.

To complete the scope of the sensitivity calculations, we computed the sensitivities of Λ with respect to the same reactions of the same isotopes. Starting with σ_γ in Table 7.42, one can see that the sensitivity values are distinctly different from the reactivity worth and eigenvalue sensitivities. Specifically looking at the Pu-239 result, the lower energy groups are most important as the parasitic capture removes neutrons that would otherwise be available for potential fissions in the lower energy groups. As was the case with the eigenvalue and sodium

density, the use of diffusion theory or transport did not make a significant difference in computing the Λ sensitivities.

Continuing with the $\sigma_{elastic}$ and $\sigma_{inelastic}$ reactions in Tables 7.43 and 7.44, one can see that the higher energy ranges typically have positive sensitivities while the lower energy ones have negative sensitivities. The positive values can easily be explained in that as more collisions are required to slow the neutrons down in energy will increase the net lifetime. Increasing the scattering rate in the lower energy regimes will decrease the lifetime due to more leakage and parasitic absorption rather than fission. The net value would seem to indicate that increasing the elastic scattering off of Na and Pu-239 will increase the lifetime while Pu-239 has little to no effect. As was the case with the other sensitivities, there is little difference between diffusion and transport.

Looking at the Pu-239 $\sigma_{fission}$ and ν sensitivities for Λ in Table 7.45, one observes a notable difference from the eigenvalue and reactivity worth cases. In Table 7.45, the sensitivities clearly have a negative upper energy and positive lower energy tilt for all three isotopes. None of them show any real similarities to the underlying flux spectrum and there is a considerable change in the sensitivity when switching from diffusion to transport. Much like the reactivity worth and eigenvalue sensitivities, the distribution can be explained by the impact on the net production and destruction of neutrons in the system.

To conclude the example, we look at the P_1 $\sigma_{elastic}$ sensitivities for Λ in Table 7.46. Unlike the other reactions, changes to the anisotropic scattering kernel are much less important, as they merely pose a change in the shape of the scattering rather than its magnitude. This tends to highlight the importance of anisotropic scattering for the sodium density reactivity worth rather than stating anything about Λ.

7.8 Uncertainty Calculation Example

For completeness, we provide an example output for verification benchmark problem #17. This benchmark is based upon a manufactured 2D box problem the details of which are not important as it is merely meant to test the functionality of the uncertainty calculation process. The sensitivity input is focused on computing the eigenvalue uncertainty due to cross section uncertainties associated with a few isotopes. As was the case with the preceding sensitivity data, the amount of information produced by PERSENT is overwhelming and difficult to present succinctly. The output example in Figure 7.1 therefore only shows a truncated part of each primary output section from the uncertainty calculation.

Each table of data in Figure 7.1 is separated by a table header in PERSENT which are compactly described by

```
UQ TABLE 1: Detailed Table of Data for Isotope/Reaction from Isotope/Reaction to Follow
UQ TABLE 2: Summary Table of Data for Isotope from Reaction to Follow
UQ TABLE 3: Summary Table of Data for Isotope from Isotope to Follow
UQ TABLE 4: Summary Table of Uncertainty Quantification Calculation to Follow
```

These were removed from the figure for brevity. The first table in Figure 7.1 labeled “UQ TABLE 1” is the output from equation 3.81 for U-235 and is triggered by the first “YES” command on the SENSITIVITY_DOUQ input seen in Figure 5.2.

```
 [COMMARA]...Importing data from bnl.1.apr.2011.commara.with.chi.mubar.matrix
 [PERSENT]...WARNING::: Only using     70 of the available    416 COMMARA matrix lines?
…  ||| UQ TABLE 1 |||
[PERSENT]...    Summary of uncertainty computation for isotope U235_7   reaction ELASTIC
[PERSENT]...        U235_7          U235_7       U235_7       U235_7        U235_7
[PERSENT]...Group  FISSION          CAPTURE      ELASTIC     INELASTIC      N2N          Column Sum
[PERSENT]... 1  3.268502E-08*i  0.000000E+00  1.357524E-08  1.321570E-08  1.235091E-08  2.359711E-08*i
[PERSENT]... 2  1.221131E-07*i  3.552299E-09  7.892027E-08  1.614073E-07  1.850529E-08  1.331322E-07
…
[PERSENT]... 32  0.000000E+00   0.000000E+00  0.000000E+00  0.000000E+00  0.000000E+00  0.000000E+00
[PERSENT]... 33  0.000000E+00   0.000000E+00  0.000000E+00  0.000000E+00  0.000000E+00  0.000000E+00
[PERSENT]...Row  6.570422E-07*i 3.851723E-06  7.834997E-07  1.958203E-06  2.224839E-08  4.342003E-06
…  ||| UQ TABLE 2 |||
[PERSENT]...    Summary of reaction-wise uncertainty computation for isotope         U235_7
[PERSENT]...Group    NU          FISSION       CAPTURE       ELASTIC         INELASTIC       N2N          Total
[PERSENT]... 1  4.036672E-08  3.000962E-07  0.000000E+00   2.359711E-08*i 2.587349E-08  8.419280E-08 3.144650E-07
[PERSENT]... 2  1.817562E-07  1.087754E-06  5.247196E-07*i 1.331322E-07   4.488999E-07  8.733878E-08 1.080637E-06
[PERSENT]... 3  3.481064E-07  1.844531E-06  1.208068E-06*i 6.001583E-07   1.746748E-06  2.017965E-08 2.340036E-06
…
…  ||| UQ TABLE 3 |||
[PERSENT]...Summary of overall uncertainty data by isotope
[PERSENT]...Isotope  O16__7     U235_7       U238_7       PU2397       PU2407       PU2417       FE56_7       NA23_7       Total
[PERSENT]...O16__7 1.766917E-03 0.000000E+00 0.000000E+00 0.000000E+00 0.000000E+00 0.000000E+00 0.000000E+00 0.000000E+00 1.766917E-03
[PERSENT]...U235_7 0.000000E+00 9.934133E-05 0.000000E+00 0.000000E+00 0.000000E+00 0.000000E+00 0.000000E+00 0.000000E+00 9.934133E-05
[PERSENT]...U238_7 0.000000E+00 0.000000E+00 1.283190E-02 0.000000E+00 0.000000E+00 0.000000E+00 0.000000E+00 0.000000E+00 1.283190E-02
[PERSENT]...PU2397 0.000000E+00 0.000000E+00 0.000000E+00 3.905468E-03 0.000000E+00 0.000000E+00 0.000000E+00 0.000000E+00 3.905468E-03
[PERSENT]...PU2407 0.000000E+00 0.000000E+00 0.000000E+00 0.000000E+00 3.122052E-03 0.000000E+00 0.000000E+00 0.000000E+00 3.122052E-03
[PERSENT]...PU2417 0.000000E+00 0.000000E+00 0.000000E+00 0.000000E+00 0.000000E+00 7.575845E-04 0.000000E+00 0.000000E+00 7.575845E-04
[PERSENT]...FE56_7 0.000000E+00 0.000000E+00 0.000000E+00 0.000000E+00 0.000000E+00 0.000000E+00 6.895036E-03 0.000000E+00 6.895036E-03
[PERSENT]...NA23_7 0.000000E+00 0.000000E+00 0.000000E+00 0.000000E+00 0.000000E+00 0.000000E+00 0.000000E+00 2.052539E-03 2.052539E-03
[PERSENT]...Total  1.766917E-03 9.934133E-05 1.283190E-02 3.905468E-03 3.122052E-03 7.575845E-04 6.895036E-03 2.052539E-03 1.565624E-02
…  ||| UQ TABLE 4 |||
[PERSENT]...    Summary of overall uncertainty data by reaction
[PERSENT]... Isotope       NU       FISSION       CAPTURE      ELASTIC     INELASTIC      N2N          CHI          Total
[PERSENT]...  O16__7 0.000000E+00 0.000000E+00 1.696857E-03 4.902903E-04 4.782573E-05 0.000000E+00 0.000000E+00 1.766917E-03
[PERSENT]...  MO92_7 0.000000E+00 0.000000E+00 0.000000E+00 0.000000E+00 0.000000E+00 0.000000E+00 0.000000E+00 0.000000E+00
[PERSENT]...  MO94_7 0.000000E+00 0.000000E+00 0.000000E+00 0.000000E+00 0.000000E+00 0.000000E+00 0.000000E+00 0.000000E+00
[PERSENT]...  MO95_7 0.000000E+00 0.000000E+00 0.000000E+00 0.000000E+00 0.000000E+00 0.000000E+00 0.000000E+00 0.000000E+00
[PERSENT]...  MO96_7 0.000000E+00 0.000000E+00 0.000000E+00 0.000000E+00 0.000000E+00 0.000000E+00 0.000000E+00 0.000000E+00
…
=PERSENT]...Total UQ product for problem REFERENCECORE     S*C*S =  2.451178E-04 square root =  1.565624E-02
```

Figure 7.1. PERSENT Example Uncertainty Computation Output from Example Problem #17.

As can be seen, this isotope has contributions from U-235 capture, fission, elastic scattering, inelastic scattering, and n2n scattering. Several of the components were negative and after applying the square root have the imaginary "*i" applied to them. For each isotope, a row and column-wise sum are provided. While there are only a few isotopes in this test problem, for real problems with 40 or more isotopes, this table can be very large.

The next table in Figure 7.1, titled "UQ TABLE 2" corresponds to equation 3.82 and lists the group-wise breakdown of each reaction contribution for a given isotope. It is triggered by the second "YES" command on the SENSITIVITY_DOUQ input. This table was substantially truncated to remove reactions which had zero contributions. Much like the previous table, both row and column sums are provided for this table of data. Because this table is also summarized by isotope, there can be a considerable amount of data in the output.

The third table in Figure 7.1, titled "UQ TABLE 3" corresponds to equation 3.83 and thus is the non-standard input triggered by the third YES command on the SENSITIVITY_DOUQ input. This output simply summarizes the co-variance contributions between isotopes which for the co-variance in this problem is seen to be purely diagonal (COMMARA). As was the case for the previous tables, a row and column sum are provided of which the sum of all values yields the total uncertainty.

The last table in Figure 7.1, titled "UQ TABLE 4" corresponds to equation 3.84 and is not optional. It summarizes the reaction contributions for each isotope. Row and column sums are again given such that the sum of all rows or all columns yields the total uncertainty value. This is by far the most reported table result for any uncertainty calculation as it cites which reactions of which isotopes factor most into the total uncertainty.

The last line of the output for an uncertainty calculation is the total product result. For this particular problem the total uncertainty on the eigenvalue is 0.0156 or 1560 pcm due to cross section errors. Because the problem is made up, one should not assume this value has any real physical meaning beyond the mathematics involved in merging the co-variance information. As a final note, the first two lines of output in Figure 7.1 show the co-variance data file that was imported and the total number of isotope-reaction data lines that are actually used from that co-variance data file on the existing reactor problem. Clearly the problem constructed is very simplistic relative to normal reactor problems as evident from the small number of isotopes appearing in "UQ TABLE 3."

8 Conclusions

Overall, PERSENT performed excellently on the perturbation and sensitivity benchmark problems shown in Sections 6 and 7. All of these benchmark problems are included as part of the test suite and normally take less than 20 minutes to complete on a modern workstation (3 GHz Intel Xeon dual core chip with 4 MB L2 Cache and 32 GB aggregate memory at 1333 MHz). For perturbation theory problems, PERSENT provides an ability to generate and view the detailed spatial contributions to any given reactivity worth or kinetics parameter of interest. For sensitivity and uncertainty calculations, PERSENT generates the desired results in a fraction of the computational effort required if using a finite difference method for obtaining the results. While we did not generate a complete list of sensitivities for the last benchmark, as a whole, the preceding set of benchmarks is sufficient to demonstrate that the sensitivity and uncertainty quantification functionality of PERSENT is working correctly and yielding physically meaningful results.

From Section 4, the input and output description of VARI3D is provided for historical reasons as is the code itself. However, because PERSENT can be applied in diffusion theory, it can also obtain identical if not superior solutions for the same problems (Cartesian and hexagonal geometries) as VARI3D and thus should be considered its replacement. The input and output for PERSENT are relatively intuitive and most of it is a follow on to the input and output results observed in DIF3D and generated by VARI3D (its inspiration). Overall, the computational effort required to carry out PERSENT based perturbation and sensitivity calculations is acceptable and there are clearly demonstrated ways in the preceding sections on how to handle slow computational performance by breaking up the PERSENT computation into multiple steps using the “MAKE_INPUT_ONLY” option. For any and all support on PERSENT, feel free to consult nera-software@anl.gov as necessary.

9 References

1. K. L. Derstine, "DIF3D: A Code to Solve One-, Two-, and Three-Dimensional Finite-Difference Diffusion Theory Problems," ANL-82-64, Argonne National Laboratory (1984).
2. G. Palmiotti, E. E. Lewis, and C. B. Carrico, "VARIANT: VARIational Anisotropic Nodal Transport for Multidimensional Cartesian and Hexagonal Geometry Calculations," ANL-95/40, Argonne National Laboratory (1995).
3. I. Dilber and E. E. Lewis, "Variational Nodal Methods for Neutron Transport," Nucl. Sci. Eng., 91, 132 (1985).
4. C. B. Carrico, E. E. Lewis, and G. Palmiotti, "Three-Dimensional Variational Nodal Transport Methods for Cartesian, Triangular, and Hexagonal Criticality Calculations," Nucl. Sci. Eng., 111, 168 (1992).
5. M. A. Smith, N. Tsoulfanidis, E. E. Lewis, G. Palmiotti and T. A. Taiwo, "Higher Order Angular Capabilities of the VARIANT Code," Trans. Am. Nucl. Soc., 86, 321-322, (2002).
6. W. S. Yang, M. A. Smith, G. Palmiotti, and E. E. Lewis, "Interface Conditions for Spherical Harmonics Methods," Nucl. Sci. Eng. 150, 259 (2005).
7. E. P. Wigner, Effects of Small Perturbations on Pile Period, CP-3048, Manhattan Project Report (1945).
8. J. Lewins, Importance: The Adjoint Function, Pergamon Press, Oxford, England (1965).
9. W. M. Stacy, Variational Methods in Nuclear Reactor Physics, Academic Press, New York, N.Y. (1974).
10. E. Greenspan, "Development in Perturbation Theory," Advances in Nuclear Science and Technology, Vol. 9, Academic Press, New York, N.Y. (1976).
11. M. L. Williams, "Perturbation Theory for Nuclear Reactor Analysis," CRC Handbook of Nuclear Reactors Calculations, Vol. III, CRC Press, Inc., Boca Raton, Florida (1986).
12. L. N. Usachev, "Perturbation Theory for the Breeding Ratio and Other Number Ratios Pertaining to Various Reactor Processes," J. Nucl. Energy, Parts A/B, 18, 571 (1964).
13. A. Gandini, "A Generalized Perturbation Method for Bilinear Functionals of the Real and Adjoint Neutron Fluxes," J. Nucl. Energy, 21, 755 (1967).
14. M. Becker, "Perturbation Theory for Ratios in Linear and Nonlinear Problems," Nucl. Sci. Eng. 62, 296 (1977).
15. A. Gandini, G. Palmiotti, and M. Salvatores, "Equivalent Generalized Perturbation Theory (EGPT)," Ann. Nucl. Energy, 13, 109 (1986).
16. G. Palmiotti, M. Salvatores, G. Aliberti, H. Hiruta, R. McKnight, P. Oblozinsky, W. S. Yang, "A Global Approach to the Physics Validation of Simulation Codes for Future Nuclear Systems," Ann. Nucl. Energy, 36, 355 (2009).
17. E. Greenspan, "Sensitivity Functions for Uncertainty Analysis," Advances in Nuclear Science and Technology, Vol. 14, Plenum Press, New York (1982).
18. C. H. Adams, "Specifications for VARI3D – A Multidimensional Reactor Design Sensitivity Code," FRA-TM-74, Argonne National Laboratory (1975).
19. K. F. Laurin-Kovitz and E. E. Lewis, "Variational Nodal Transport Perturbation Theory," Nucl. Sci. Eng., 123, 369 (1996).
20. G. J. Habetler and M. A. Martino, "Existence Theorems and Spectral Theory for the Multigroup Diffusion Model," Proc. Of Symposia in Applied Mathematics, Vol. XI, 127 (1961).

21. G. Birkhoff and R. S. Varga, “Reactor Criticality and Nonnegative Matrices,” J. Soc. Indust. App. Math. Vol. 6, 354 (1958).
22. E. M. Oblow, “Sensitivity Theory from a Differential Viewpoint,” Nucl. Sci. Eng., 59, 187 (1976).
23. C. V. Parks and P. J. Maudlin, “Application of Differential Sensitivity Theory to a Neutronic/Thermal-Hydraulic Reactor Safety Code,” Nucl. Tech. 54, 38 (1981).
24. G.Aliberti, G.Palmiotti, and M.Salvatores, “Sensitivity and Uncertainty Analysis with the ERANOS Code System,” Nuclear Physics and Related Computational Science R&D for the Advanced Fuel Cycle Workshop, August 10-12, Bethesda, Maryland (2006).
25. The visualization toolkit (2013). Retrieved April 22, 2013, from http://www.vtk.org/.
26. VISIT visualization software. Retrieved April 22, 2013, from https://wci.llnl.gov/codes/visit/.
27. G. Aliberti, M.A.Smith, private conversation March 19 (2013).
28. R. M. Lell, J. A. Morman, R. W. Schaefer and R. D. McKnight, “ZPR-6 Assembly 7 High ^{240}Pu Core Experiments: A Fast Reactor Core With Mixed (Pu,U)-Oxide Fuel and a Central High ^{240}Pu Zone,” ZPR-LMFR-EXP-002, International Handbook of Evaluated Reactor Physics Benchmark Experiments, NEA/ NSC/DOC(2006)1, March (2009).
29. M. A. Smith, E. E. Lewis, and E. R. Shemon, “DIF3D-VARIANT 11.0: A Decade of Updates,” ANL/NE-14/1 January (2014).
30. W. S. Yang and T. J. Downer, “Generalized Perturbation Theory for Constant Power Core Depletion,” Nucl. Sci. Eng., 99, 353-366 (1988).
31. G. Rimpault et al. “The ERANOS Code and Data System for Fast Reactor Neutronic Analyses”, Proc. Int. Conf. PHYSOR 2002, Seoul, Korea, October 7-10, (2002).

This page left blank intentionally

Nuclear Engineering Division
Argonne National Laboratory
9700 South Cass Avenue, Bldg. 208
Argonne, IL 60439

www.anl.gov

Argonne National Laboratory is a U.S. Department of Energy laboratory managed by UChicago Argonne, LLC